



UNIVERSITY OF NAIROBI

**GROUNDWATER POTENTIAL ASSESSMENT USING REMOTE SENSING,
GEOGRAPHICAL INFORMATION SYSTEM AND ELECTRICAL RESISTIVITY
METHODS IN CRYSTALLINE TERRAIN IN KAPURI AREA, JUBEK STATE, SOUTH
SUDAN**

BY

MOSES GEORGE NAZARIO

I56/89164/2016

**A Dissertation submitted in partial fulfillment of the requirements for
the degree of Master of Science in Geology (Applied Geophysics) of the
University of Nairobi**

2020

DECLARATION

This MSc. research dissertation is my original work and has not been submitted elsewhere for examination, award of a degree or publication. Where other people’s work or my own has been used, this has properly been acknowledged and referenced in accordance with the University of Nairobi requirements.

Signature.....

Date.....

Moses George Nazario

I56/89164/2016

Department of Geology

School of Physical Sciences

University of Nairobi

The dissertation is submitted for examination with our approval as research supervisors.

Dr. Zacharia N. Kuria

Signature

Date

Department of Geology,
University of Nairobi

.....

.....

Dr. Charles M. Gichaba

Signature

Date

Department of Geology,
University of Nairobi

.....

.....

UNIVERSITY OF NAIROBI

DECLARATION OF ORIGINALITY FORM

This form must be completed and signed for all works submitted to the University for Examination.

Name of student: Moses George Nazario

Registration Number: I56/89164/2016

College: BIOLOGICAL AND PHYSICAL SCIENCES

Faculty/school/institute: SCHOOL OF PHYSICAL SCIENCES

Department: GEOLOGY

Course Name: Masters of sciences in Geology

Title of the work: GROUNDWATER POTENTIAL ASSESSMENT USING REMOTE SENSING, GEOGRAPHICAL INFORMATION SYSTEM AND ELECTRICAL RESISTIVITY METHODS IN CRYSTALLINE TERRAIN IN KAPURI AREA, JUBEK STATE, SOUTH SUDAN

DECLARATION

1. I understand what plagiarism is and I am aware of the university's policy in this regard.
2. I declare that this _____ (Thesis, project, essay, assignment, paper, report etc.) is my original work and has not been submitted elsewhere for examination, award of a degree or publication. Where other people's work or my own has been used, this has properly been acknowledge and referenced in accordance with the University of Nairobi's requirements.
3. I have not sought or used the services of any professional agencies to produce this work.
4. I have not allowed. And shall not allow anyone to copy my work with the intension of passing it off as his/her own work.
5. I understand that any false claim in respect of this work shall result in disciplinary action, in accordance with university plagiarism policy.

Signature: _____

Date: _____

DEDICATION

Dedicated to my wife, Mrs. Evilin George Zakaria and to my lovely daughters, Marlyn Moses George and Marcy Moses George.

ACKNOWLEDGEMENTS

First I thank Almighty God for having been my source of strength and hope and for bringing me this far.

Thanks to Water and Society project (WaSo) for offering me the scholarship to do my MSc studies at the University of Nairobi, Kenya.

I am grateful to my supervisors; Dr. Zacharia N. Kuria, Dr. Charles M. Gichaba for their intellectual guidance, support and encouragement throughout the studies. I also thank Dr. Denis Duku and Dr. John Ariki for all their assistance and invaluable advice they were giving me during my research project.

I wish to acknowledge the work that all the academic and administrative boards of the University of Nairobi for their support during my coursework and my research project. Their closeness and assistance allowed me to move forward with great hope.

I also take this opportunity to thank and appreciate Mr. David Felix, Mr. Samuel Luete and Mr. John Marcello and all my Students who helped me during Data collection and, I sincerely thank University of Juba administration for granting me leave for study.

I would also like to thank all my classmates for their support that they offered to me in one way or another. Also I would like to thank my best friend Simon Ngetich for his constant encouragement and moral support. I would also like to thank my colleague Mr. Thomas Oromo, Mr. Francis Khamis for their standing with me throughout my studies period.

I would like to express my deepest gratitude to my Mother, Father, sisters, brothers, Cousins for their continuous support and prayers. I pray that God bless all those who directly and indirectly enabled me to accomplish this work. Thank you and God bless you all.

ABSTRACT

This research project was carried out in Kapuri area of Lury County, Jubek state South Sudan; an area that is geologically underlain by crystalline basement rocks. Groundwater investigations in the crystalline rocks is quite challenging because the overall permeability of these rocks is usually very low. The groundwater is typically confined within the fractured and weathered zones. Therefore, the yields from wells tapping these formations may not, in most cases, be sufficient for exploitation. The study area is further compounded by additional problems in that no borehole has been drilled in this area, the previous groundwater studies are scanty, and they experiences high water demand due to resettlement of refugees returning from neighbouring countries. The main aim of the investigation was to evaluate earth's subsurface geoelectric properties that might indicate suitable geological and/or structural aspects favourable for groundwater occurrence. This main objective was achieved through use of remote sensing data, application of Geographic Information System (GIS) techniques and ground geophysical survey. As a first step, groundwater potential assessment was carried out using remote sensed data from Landsat ETM+8 and digital elevations from which thematic maps were derived using ArcGIS software. These thematic layers include lithology, geomorphology, Lineament density, DEM, slope, drainage density, Land Use Land Cover map. The individual thematic layer were assigned weights for the purpose of spatial analysis. On geophysical survey, electrical resistivity profiling using weaner configuration was carried out to delineate subsurface geological structures along 3 horizontal profiles each stretching over a distance of 1500 meters. The horizontal separation of the profiles was 500 metres. At each station, resistivity data was collected at three levels namely 15m, 35m and 45m below ground level. These profiles were plotted in Microsoft Excel and fractures along each profiles were identified. In addition, 192 vertical electrical soundings (VES) were performed using schlumberger array. These VES data were analysed using the Interpex IX1D computer software and the resistivity versus depth models for each location was estimated. This followed by construction of 2D profiles and 3D models using leapfrog software.

The GIS and remote sensing results revealed that Kapuri area is characterized by relatively good to moderate groundwater potential confined at the western part of Lury County. The results from geophysical survey indicate that the area is generally underlain by four geologic

section which include top soil (sandy clay), moderately weathered, fractured and fresh basement. Moderately weathered material ranging from less than one meter to several meters in thickness separate the overburden from the underlying weathered and fractured bedrock, while the basal layer is comprised of compact and massive fresh basement. The fractured and the moderately weathered rock make up the aquiferous zone within the study area.

This work recommends that boreholes be drilled in areas that have been identified to have high groundwater potential. Additional works, is recommended using 2D and 3D resistivity tomography, with the aim of establishing highly fractured rock mass and therefore identify more aquifers.

TABLE OF CONTENTS

DECLARATION	ii
DECLARATION OF ORIGINALITY FORM	iii
DEDICATION	iv
ACKNOWLEDGEMENTS	v
ABSTRACT	vi
TABLE OF CONTENTS	viii
LIST OF TABLES	xi
LIST OF FIGURES	xii
LIST OF ABBREVIATION/ACRONYM AND SYMBOLS	xiv
CHAPTER ONE: INTRODUCTION	1
1.1 Background Information.....	1
1.2 Scope of the Research.....	3
1.3 Problem Statement	3
1.4 Aims and Objectives	4
1.5 Justification and Significance of the Research	4
1.6 The study Area.....	5
1.6.1 Location and Description	5
1.6.2 Climate and Vegetation	6
1.6.3 Physiographic and Drainage	6
1.6.4 Geology and Structures.....	6
1.6.5 Hydrogeology	9
CHAPER TWO: LITERATURE REVIEW	10
2.1 Background.....	10
2.2 Groundwater Occurrence.....	10
2.3 Application of remote sensing and GIS techniques.....	11
2.4 Application of Geophysical Survey	16
CHAPTER THREE: MATERIALS AND METHODS	25
3.1 Introduction.....	25
3.1 Development of different thematic map.	25
3.2 Spatial analysis and Integration of thematic maps and modeling.....	27

3.2.1 Weightage Assignment	27
3.3 Basic theory of resistivity method	31
3.3.1 Introductions.....	31
3.3.2 Principle of Resistivity Methods.....	32
3.4 Electrode configuration for resistivity survey.....	36
3.4.1 Wenner Configuration.....	37
3.4.2 Schlumberger configuration	37
3.5. Field procedures for data collection.....	38
3.5.1 Horizontal electrical profiling	41
3.5.2 Vertical Electrical Sounding (VES)	43
3.6 Apparent resistivity.....	44
3.6.1 Inversion and modeling.....	45
3.6.2 Data Analysis and interpretation.....	45
CHAPTER FOUR: RESULTS AND DISCUSSIONS.....	47
4.1 Map lithology and geological structure, lineament, drainage, geomorphology change from remote sensing data	47
4.1.1 Lithology of Kapuri Area	47
4.1.2 Geomorphology of Kapuri Area	49
4.1.3 Lineament Map	52
4.1.4 Drainage Density Map	53
4.1.5 Slope and DEM Map.....	55
4.1.6 Land Use Land Cover	57
4.1.7 Integration of Thematic Layers for modeling groundwater potential zone using GIS: (Weighted Index Overlay Model)	59
4.3 Delineation thickness of aquifer as well as lateral extent from geophysical data	61
4.3.1 Profile I.....	61
4.3.2 Profile II	63
4.3.3 Profile III.....	65
4.4 3D Model showing groundwater potential zone.....	68
4.4.1 3D resistivity Model for subsurface geological structures	70

CHAPTER FIVE: CONCLUSION AND RECOMMENDATION.....	75
5.1 Conclusion	75
5.2 Recommendation	75
REFERENCE.....	76
Appendix I: Horizontal profile survey sheet.	89
Appendix II: VES survey sheet.	93
Appendix III: 3D Model data used for leapfrog software.	104
Appendix IV.: Pictures captured during data collection	124

LIST OF TABLES

Table 3.1 Assigned weight, features and Ranks for different thematic maps.....	29
--	----

LIST OF FIGURES

Figure 1.1: Location map of the study Area	5
Figure 1.2: Geological map of Jubek State (Persits, at el., 2002).....	8
Figure 1.3: Stream flow during wet season, recharging groundwater in the study area.....	9
Figure 3.1: Flowchart of Methodology.....	26
Figure 3.2: The basic definition of resistivity in a homogeneous block.....	33
Figure 3.3: The current flowing from electrode to distribute current uniformly over the shell.....	34
Figure 3.4: The potential distribution from a pair of current electrodes.....	35
Figure 3.5: The generalized form of the electrode configuration used in resistivity measurements	35
Figure 3.6: The Wenner array.....	37
Figure 3.7: Schlumberger array	38
Figure 3.8: VES locations in Kapuri Area.....	40
Figure 3.9: Equipment's used for data collection.....	41
Figure 4.1: Lithology of Kapuri area	48
Figure 4.2: Different types of rock units in Kapuri Area. A) Gneiss, B) Chlorite schist, C) Amphibolite, D) Dolerite Dyke.....	49
Figure 4.3: Geomorphology of Kapuri Area.....	51
Figure 4.4: Lineament Map, with rectangle inside the circle showing the study area.....	53
Figure 4.5: Drainage Density Map.....	54
Figure 4.6: Slope map.....	55
Figure 4.7: Drainage Density Map.....	56
Figure 4.8: Land used Land cover Map	58
Figure 4.9: Groundwater potential map.....	60
Figure 4.10: profile N0.I.....	62
Figure 4.11: Profile N0.II.....	64
Figure 4.12: Profile N0.III	66
Figure 4.13: Cross section profile for all VES.....	67
Figure 4.14: VES logs of Kapuri Area.....	69

Figure 4.15: 3D Resistivity models showing North face of Kapuri Area.....	71
Figure 4.16: 3D Resistivity models showing south face Kapuri Area.....	73
Figure 4.17: 3D Resistivity models showing East face Kapuri Area	74

LIST OF ABBREVIATION/ACRONYM AND SYMBOLS

AHP – Analytic Hierarchy Process
CRM – Computerize Resistivity Meter
CSI – Cumulative Suitability Index
DEM- Digital Elevation Model
E.P- Electrical profile
ETM-Enhance thematic map.
GCP – Ground Control Points
GIS- Geographical information System
GPS – Geographical Positioning System
HP – Horizontal Profile
Km- Kilometer
LULC — Land use land Cover
M- Meters
MCE – Multi-criteria Evaluation
MCDM –Multi- criteria Decision Making
MIR – Middle Infrared
Rho- Resistivity
RS-Remote Sensing
SWIR – Shortwave Infrared
UTM – Universal Transverse Mercator
VES-Vertical Electrical Sounding
WIO – Weighted Index Overlay

CHAPTER ONE

INTRODUCTION

1.1 Background Information

Water is an essential commodity for the survival of every living thing (plants and animals). Most human beings generally require about 2.5 liters of water every day for direct consumption. On average amount of water ,household can used about 200 liters of water daily (Hamil and Bell, 1986). Normally the most efficient means to meet this demand is the surface water resources. Nevertheless, fresh water from lakes, rivers and streams is not readily available to everyone because it is distributed irregularly throughout the world. It is approximated that by 2025 about 1.8 billion of the people who live in the world will not be able to access adequate water. While this is the case, about two-thirds of the population in the world will not have sufficient water for use in their home by this time (UN Water, 2007). Therefore, measures must be taken to investigate the possibilities of providing alternative sources of water to meet the challenges of water scarcity emanating from increased population pressure. Globally, groundwater is the second main source of water representing approximately 30 percent of the fresh water (Subramanya, 2008). As a result, over 1.5 billion people globally rely on groundwater for daily use.

South Sudan water source is transboundary water, it shared with the surrounding country. River Nile is the main water body share by 10 country, in facts this causes extreme water stress, which is when demand for water exceeds the amount available. Water stress is a problem that roughly a quarter of Africa's population suffer from (Islam and Susskind, 2015). 97% of South Sudan's water is used for Agriculture, an industry that employs 80% of the population, whilst only 2% of South Sudan water is for domestic use. South Sudan is suffering from a water crisis due to constant conflicts that left the water system neglected or destroyed. Poor rains combined with the after effect of the 2011 East Africa drought and increasing population has depleted the country's water supply system (Aghakouchak, 2014).

In Kapuri area(Fig 1.1) apart from suffering from insufficient water supply, most of the water sources are polluted, thereby vulnerable to various water-borne diseases such as cholera and guinea worm (UNESCO, 2004). From the time the peace agreement was signed in 2005, access to quality water has been a major issue for majority of the people living in South Sudanese rural areas especially the areas that do not have surface water. Kapuri is a newly demarcated area for settlement of persons who are returning from the neighboring countries like Uganda, Sudan, and Kenya as a refugees. This resettlement has resulted into increasing local industrial scheme and agricultural activities that demand proportionate increase in water demand. Therefore, access to sufficient supply of potable water is becoming increasingly difficult particularly in the face of the fast growing population. This suppresses the adequacy of the water that is not readily available in the area. For this reason, there is need to identify other sources of water that could be reliable.

Groundwater resource is important water supply mostly for domestic used particularly during dry season in areas that not located on the river and no permanent surface water. Throughout Jubek State, groundwater resource is important water source mostly used for domestic water supply and therefore its occurrence and distribution is pivotal to giving the required water demand for household, irrigation and industrial purposes (Anornul *et al.*, 2012). The provision of groundwater through modern hand-dug wells, boreholes, and piped systems has augmented considerably over the past years in the Equatorial region and hence groundwater has now become vital resource of water for urban and rural water source (Nicola, 2005).

Groundwater data are scarce thereby resulted into lacks sufficient knowledge about factors responsible for the storage, movement and occurrence of groundwater that poses a great uncertainty resulting in drilling dry borehole and low yield borehole.

Groundwater exploration will greatly increase the socioeconomic activities in the study area. It was noted by (WHO, 2010) that access of sufficient water for small- scale in such an area is thereby an important aspect because it helps in alleviating poverty. It may also be important in improving the quality of health benefits.

1.2 Scope of the Research

The study was conducted in Kapuri area, Jubek State which is located on the western side of Juba city. It entailed identifying of groundwater potential zones using GIS techniques, Remote Sensing data and geophysical techniques. The use of the remote sensing and GIS data was for the delineation of surface geological features that connote groundwater occurrence in crystalline rocks i.e. faults, fracture zone. Delineated geological features were subjected to geophysical survey, electrical resistivity profiling was carried out to determine lateral variation of the subsurface geological formation while Vertical Electrical Sounding (VES) was performed to determine vertical variation of the formation with depth and determine groundwater bearing zones. In the end a 3D geo-electric model was developed showing ground water potential zones.

1.3 Problem Statement

Kapuri area is geologically underlain by crystalline basement rocks (Hunting., 1980s). Groundwater investigations in the crystalline rocks is quite challenging because the overall permeability of these rocks is usually very low. The groundwater is typically confined within the fractured and weathered zones. Therefore, the yields from wells tapping these formations may not, in most cases, be sufficient for exploitation. Kapuri Area is further compounded by additional problems in that no borehole has been drilled in this area, the previous groundwater studies are scanty, and the area experiences high water demand due to resettlement of refugees returning from neighbouring countries. In addition, the kapuri area is located in a relatively tropical to sub-tropical area having medium groundwater potential due to average rainfall recharging the aquifers within fractured and highly weathered zone of Basement Complex rock.

1.4 Aims and Objectives

The main aim of the investigation was to evaluate subsurface geological structures and geoelectric properties that indicate occurrence and distribution of groundwater will lead to a recommending where drilling should be done in the study area.

The specific objectives of this study were as follows:

1. -To map Lithology and geological structures in the area lineaments, drainage geomorphology change from remote sensing data.
2. -To delineate thickness of aquifer as well as lateral extent from geophysical data.
3. -To develop a 3D model showing ground water potential.

1.5 Justification and Significance of the Research

Groundwater is vital to every human being because it is instrumental in irrigating the land during dry season, for industrial use and domestic use especially in dry parts of the world. The study has ever an increase in demand for water due to population growth, unfortunately the geology of kapuri area shows that it is underlain with crystalline basement of Precambrian rock and dolerite dyke swamps trending along east to west direction. (Hunting, 1980s). Generally these rock do not support largscale aquifer (Clark, 1985). The results accrued from this study will provide the basic data required in groundwater resource evaluation and such information is important for policy makers in the region together with the government, which is responsible for providing local people with clean water. Therefore, a basis for future research work will be laid down. In addition from the result of this study stake holder in water sectors (government and NGO'S) can drill high yielding borehole and ameliorate current acute water shortage.

1.6 The study Area

1.6.1 Location and Description

The study area lies in Kapuri area west of Juba City in Lury County of Jubek State of South Sudan and covers an approximate area of about 15 Km². It lies within the latitude 31°47'47.7"N to 31°49'05.3"N and Longitude 4°86'63.8"E to 4°86'72.7"E. It's surrounded by mountain Kujur to the South East, Lury Mountain to the West, Lado Mountain to the North, and Rajaf Mountain to the far south (figure 1.1). Majority of the people living in the area returned to their places of origin after a peace deal was signed incumbent government with rivals. Because the region is dry there is serious problem of water. As a result, the people living here rely on hand-dug wells, boreholes and seasonal streams.

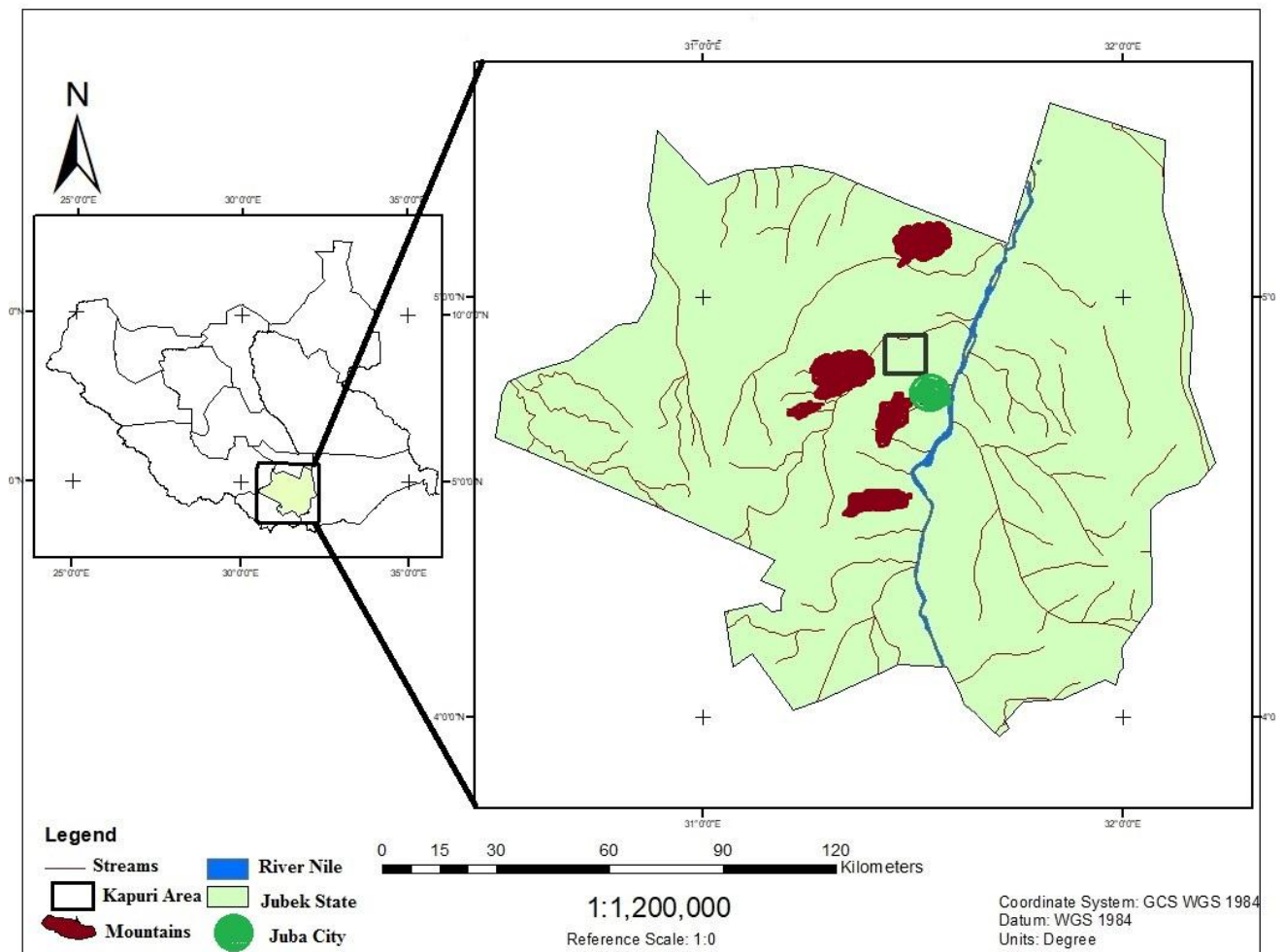


Figure 1.1: Location map of the study Area

1.6.2 Climate and Vegetation

The climate of the kapuri area is largely tropical to sub-tropical meaning that it receives rain with high humidity and sometimes suffers from prolonged dry seasons. The amount of rainfall received in the area annual lies between 800 mm and 1,000 mm (Hunting,1980). Most of this rain start in April and late November with May and October being the months that receive more rainfall. In spite of this, the rain does not have a predictable routine of the way it falls. The temperature is normally high between January and March and it averages at about 35 degrees Celsius. July is the coolest month with a temperature of between 20 and 30 degrees Celsius. Because of this, the study area has less dense vegetation cover that consists of shrubs, grass, and teak and mango trees.

1.6.3 Physiographic and Drainage

The Area is largely mountainous but with rather subdued range in elevation i.e. 400---500 meters that produces a generally monotonous landscape. The ground of the region is largely Precambrian with granitic rocks intrusion contrary to the neighboring area whose basement is terrain with meta-sedimentary formations forms an area of relatively high relief. As a result of the above, dykes are common in the study area and they lie in E-W direction. Juba area lies within Nile basin of generally northerly flowing drainage, the main river is White Nile and its tributaries including Khor lury, khor Rumhla, khor Ladukeji and lobuliate. The drainage pattern is largely dendritic – a typical one in mountainous areas, drainage density and pattern area variable comprise of both are seasonal and perennial streams.

1.6.4 Geology and Structures

The country as a whole lies within Mozambique Belt extends from Mozambique to Eritrea (Holmes, 1951). It form part of the orogenic belt with several tectonic histories (Berhe, 1991). The underlying geology comprises mainly of Precambrian rock of medium to high grade metamorphic rock.

Very little systematic geological work was carried out in the study area until recently, previously known mineral occurrences were recorded by (Deane and Mohammed ,1960) due to the paucity of field data, the subsequent work on Sudan geology by (Whiteman, 1971) and

more by (Vail, 1987) made only relatively brief mention of data relevant to the area, Much information has been therefore derived by extrapolation from the published geology of adjacent countries. The study area has Proterozoic rock with medium to high metamorphic grade and Precambrian Archean (Hunting, 1980's), which are correlated with basement complex from west Nile and Karamojong districts (Uganda)(Figure 1.2). Besides, the basement rock has post-tectonic acid and plutonic bodies whose age is unknown (Hunting, 1980). The Precambrian rock has doleritic dyke probably similar to those found in Ethiopia and Sudan (Hunting, 1980). The Nile Gneiss, Alluvium, Precambrian Granite and Meta-sediments are the most common types of rock in the area (Hunting, 1976).

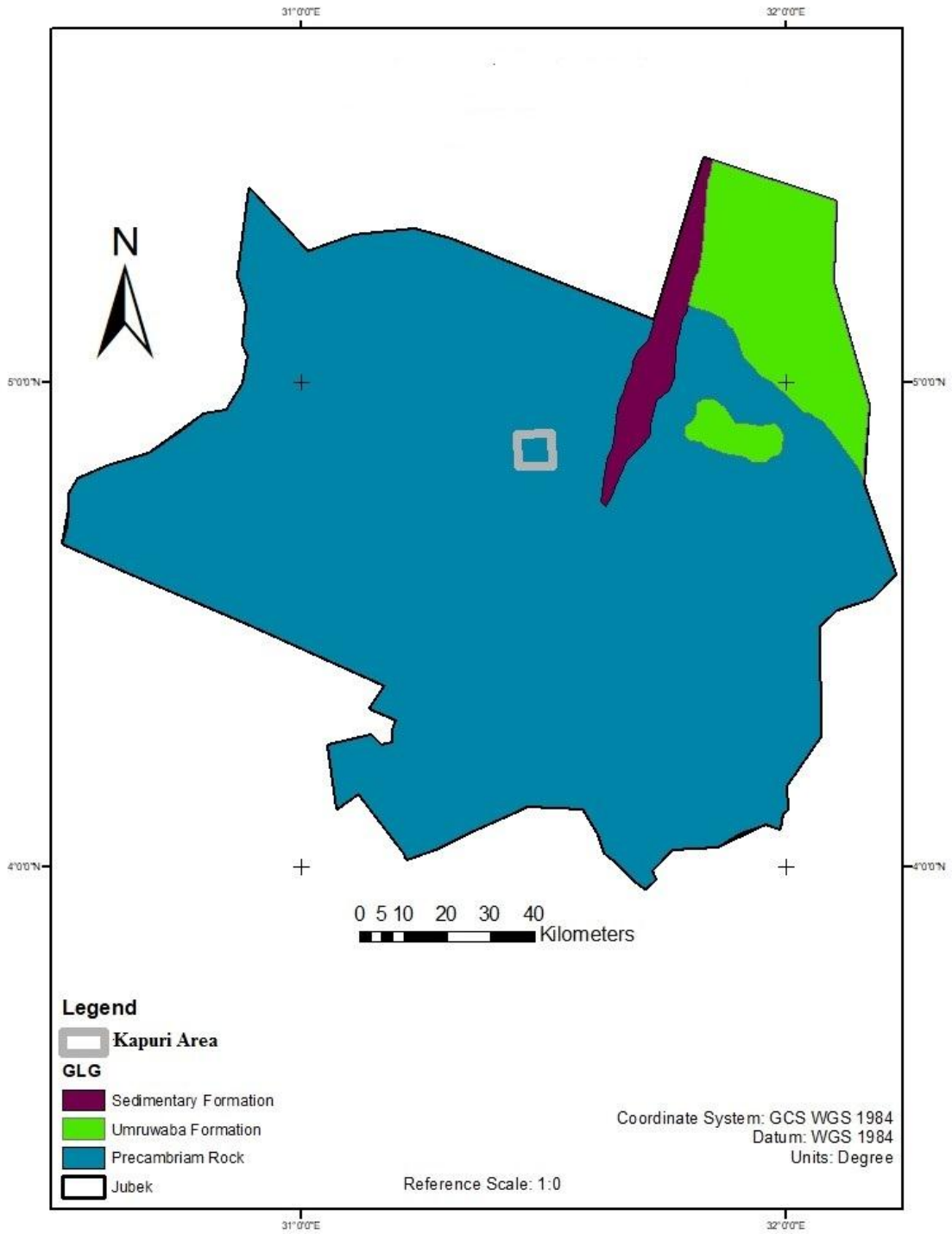


Figure 1.2: Geological map of Jubek State (Persits, *at el.*, 2002)

1.6.5 Hydrogeology

Generally Hydrogeology of south Sudan is not well known. The hydrogeology of this area is dictated by crystalline basement most of which are Precambrian in age, where typically groundwater exist within weathered and fractured rock formation under water table condition. Water table lies at the depth generally less than 20m and the maximum depth of borehole rarely exceed 75m (Upton *et al.*,2018). Surface water is the most important source of water in the Kapuri area, but it faces a lot of challenges from daily and seasonal fluctuations. The area experiences dry season from January to March of every year. The streams depend on rainfall and therefore, they flow only during the wet season and dry up during dry season. The streams mostly arise from the south-western slope of Luri mountain and south-eastern of Kujur mountain and flow to northern direction and finally drain into the river Nile.



Figure 1.3: Stream flow during wet season, recharging groundwater in the study area

CHAPER TWO

LITERATURE REWIEW

2.1 Background

Groundwater is water that located beneath earth surface mostly in fractures and pore spaces of lithologic formations. Aquifer is an unconsolidated deposit that yields usable water (Alabi *et al.*, 2010). Even if most of the countries in the world depend largely on groundwater, its nature is undocumented. As a result, it becomes almost hard for majority of the people to believe that groundwater can be relied upon (Osej *et al.*, 2006). In spite of there, there are several methods that can be utilized to locate and assess the amount of groundwater. Each of these methods has its level of sensitivity and usefulness in the exercise (Kearey *et al.*, 2002). In the light of this, researchers have developed techniques and procedures that can be used to locate places rich in groundwater easily using geophysical methods, remote sensing and GIS method.

2.2 Groundwater Occurrence.

The origin of groundwater is precipitation which is conveyed to aquifers through the mechanical process of infiltration and conductivity through porous media. However, several factors influence infiltration and conductivity of precipitation water in the ground. These factors include lithology, precipitation, land cover/ use, slope and drainage network. The lithology is important in that it defines the porosity and permeability by precipitation water. In addition precipitation is the amount of water reaching land surface. Further, land cover /use influences the amount of precipitation available for infiltration. Slope influences infiltration rates and ground water storage potential. Steep slopes lead to reduced infiltration rate and reduced groundwater storage potential. Flat terrains enhance infiltration rate and lead to increased ground water storage potential (Bruijnzeel, 2004; Mwega, 2016). Vegetation cover and its density have significant influence of the quantity of water that can be dug underground. As a result, forests have more underground water than others because of tree canopies. In addition, vegetation have the ability to regularize runoffs by reducing their severity. For soils that do not have vegetation covers, the capacity of soil to retain water is reduced significantly. This results to high levels of soil erosion that affect underground water indirectly (Barten, 2006; Mwega, 2016).

Groundwater may be classified as water that occurs naturally below the earth's surface. This water occurs in pore spaces and within fractured rocks. Groundwater hydrology is a science branch that applies physical, mathematical and biological principles in the study of quality, movement and occurrence of water below the earth's surface. In this respect, groundwater is part of hydrological cycle, which concerns itself with the occurrence and movement of water among the land, sea and atmosphere. This process is largely complex because it is controlled by sun's energy (Heath, 1987; Mwega, 2016). Groundwater occurs in two zones. The first one occurs just beneath land surface in areas that are unsaturated zones or areas with good air circulation. Most of those areas are underlain by interconnected zones filled with water. Such areas are known as saturated zones (Heath, 1987; Issah, 2015). The presence of such water points depend on geology of surface and climate (Vandas *et al.*, 2002).

2.3 Application of remote sensing and GIS techniques

Remote sensing helps in providing images that contain spectral and spatial information at low cost (Battaglin *et al.*, 1993). Soil, geology, lineaments, geomorphology, slope, land use and drainage are important elements in the process of locating groundwater (Srivastava and Bhattacharya 2006). Remote sensing analyzes indirectly the information of the aforementioned elements (Kuria *et al.*, 2012 , Gopinath *et al.*, 2004). In contrast, GIS stores geo-referenced data obtained from different sources (Lillesand and Keifer, 2000).

Researchers have utilized dissimilar criteria to identify zones with potential groundwater. Kumar *et al.*, (2007) and Sreedevi *et al.*, (2005) have combined geophysical data with geospatial data to delineate groundwater zone they found out that about 50% of the study area can be identified as very good or good potential zones, whereas the remaining area falls under moderate to poor categories, whereas Nag (2005) has utilized lineament and hydro geomorphology-based approach to locate groundwater zone in India, Purlieu District. He found out that groundwater potential zone in this region is confined within the fracture zone and weathered residuum. Hydrogeomorphologically, the entire area is classified into following categories as i) very shallow weathered pediment, ii) Moderately weathered pediment, iii) Valley fills, iv) Erosional gullies, v) Lateritic Upland and vi) Accumulation gullies.. Geomorphology and lineaments are very critical in this process. Other researchers such as

(Singh *et al.*, 2007 and Gustavsson *et al.*, 2006) have utilized satellite imagery to locate lineaments and geomorphic features.

In the current study, both GIS and remote sensing methods were utilized because of their ability to locate relevant elements in the analysis. The information that was sensed remotely from slope layers, drainage and soil were combined with the ones obtained via GIS methods. The analysis was based on the total weight estimates. Higher estimates predicted the potential for groundwater whereas low estimates demonstrated unlikelihood of groundwater (Krishnamurthy *et al.*, 1995).

A multi-criterion approach was utilized to generate maps of regions with groundwater. The approach allowed the researcher to combine linear weights with those from thematic maps with individual capability value. The values were then converted to the right ones using Bayesian statistics. The Capability value were multiplied by relevant probability weights of the potential maps. Afterwards, the classification of groundwater of separated into six units that ranged from excellent to very poor (Sarkar *et al.*, 2001).

Kanta *et al.*, (2018) combines a multi-criteria approach with the geospatial one to prospect for groundwater. They compared and contrasted the GIS-based Multi-Criteria Decision Analysis (MCDA) technique, Catastrophe theory and Analytic Hierarchy Process (AHP) as they located groundwater in India. Thematic layers that evaluated factors that impacted the occurrence of groundwater were evaluated. Some of factors considered included slope, proximity to water bodies, geology and runoff coefficients among others. Themes were assigned weights in line with catastrophe and AHP theories. The GIS method was then applied to identify areas with groundwater.

Saidi *et al.*, (2017) used the multi-criteria approach to locate areas with groundwater. The process of identifying areas with groundwater depends largely on physical parameters as well as groundwater vulnerability. GIS technique can be critical in dealing with data from different disciplines for each of the parameters. In this analysis, weighting coefficients assigned to each parameter using analytic hierarchy process based on local conditions.

Agarwal and Garg (2016) utilized remote sensing method to identify regions with underground water in Rae Bareli district, India. They applied GIS-based technique in their final decision. With the help of multi-criteria and remote sensing methods, (Mandal *et al.*, 2016) determined the availability of groundwater in Balasore district of Odisha, India. This shows that a variety of methods can be utilized to identify areas with groundwater in different parts of the world. So far, Remote Sensing (RS) is the most advanced technology to be used in the exercise (Surajit 2014; Todd, 1980) . The advantage with this technology is that it can be applied even to the most remote areas, which are inaccessible. Because of this RS has been refined to produce hand-held tools that are easy to carry around (Gupta & Srivastava, 2010).

Prafull Singh *et al.*, (2014) used Geospatial techniques in natural sciences to assess, monitor and manage natural resources in their analysis that focused on groundwater. The study was conducted in Deccan Volcanic Province of Maharashtra, India to identify areas with groundwater using multi-criteria analyses. Thematic information from slope, lineaments, drainage, lithology and geomorphology were incorporated in the analysis. This method was helpful in predictive process of managing groundwater. The thematic layers analyzed in the analysis were included in the final analysis using Multi criteria evaluation techniques.

Deepesh *et al.*, (2014) employed multiple linear regressions (MLR), remote sensing, MCDM, and GIS techniques. They utilized maps of 11 hydrological/ hydrogeological factors that included geomorphology, drainage density, land use/cover, transmissivity, net recharge, groundwater depths, proximity to water bodies, slope, elevation and soil in their analysis. Themes with their respective features were allocated apposite weights that were normalized using MCDM technique. Lastly, a map for potential groundwater was developed to identify areas with groundwater.

Muheeb *et al.*, (2013) integrated remote sensing, multi-criteria evaluation techniques and geographic information systems (GIS). They developed 8 thematic layers in GIS and allocated multi-criteria evaluation techniques apposite weights. Slope, elevation, rainfall, soil texture, drainage density, lineament density, geomorphology and lithology were the layers included in

the analysis. The potential for groundwater in the study was produced by GIS and it had five levels ranging from very high to very low.

Gumma and Palevic (2013) delineated the availability of groundwater using GIS and remote sensing method. They obtained their data from satellite, geology and climate. They assigned weights and subjective scores to the seven spatial data layers and demarcated groundwater into five categories that ranged from very good to very poor from the percentage scores they obtained from the analysis.

Olutoyin *et al.*, (2013) utilized the MCDA, GIS and RS techniques in their analysis to delineate groundwater within the Nigerian crystalline basement terrain. Nine thematic layers that included drainage proximity, slope, land use, lineament density, drainage density, soil, rainfall, geomorphology and geology were integrated in the analysis. The Saaty's analytic hierarchy approach was utilized to assign weight whereas thematic maps were introduced into the analysis using ArcGIS 10.0 software. The aim of doing this was to generate a map that depicted the potential of groundwater within the area.

Garhi, (2013) utilized integrated approach consisting of GIS and Remote sensing to identify groundwater within Narava basin in Visakhapatnam region. Thematic maps produced in the analysis included LULC, slope, drainage density, lineament density, geology, and geomorphology. The Weighted index overlay (WIO) technique was applied to evaluate the probable possibilities of choices and determine their suitability in line with weights for various units. The map showed groundwater prospects in the region.

Kumar, (2012) utilized GIS and RS techniques to identify areas with potential groundwater within the district of Tamilnadu. They prepared a variety of thematic maps that included factors that influenced potential for groundwater. Some of those factors included slope, geology, data obtained from government, land use, soil types and rainfall. Weightings and ranks were assigned to different categories that were determined by criterion tables whereas multi-criterion analysis was utilized to obtain the Cumulative Suitability Index (CSI) values.

Gupta and Srivastava, (2010) utilized GIS, remote sensing and field work techniques to identify groundwater in Pavagarh region, which was hilly. Thematic maps consisting of land use/land cover (LULC), slope map, DEM, drainage density, and lineament density were generated in the analysis. The multi-criteria evaluation technique (MCE) was applied to evaluate the probable possibilities and determine their suitability.

For a long time, Remote Sensing images have successfully mapped and extracted geology, land use, recharge and discharge areas, lineaments, soil types, fractures, and geomorphology (Agarwal *et al.*, 2016; Dar *et al.*, 2010). When these layers are integrated, they are able to provide an overview of areas rich in groundwater. In India and elsewhere, different researchers (Elmahdy and Mohamed, 2015; Jaiswal *et al.*, 2003.; Krishnamurthy *et al.*, 1995; Murthy *et al.*, 2000; Rashid *et al.*, 2011; Shahid *et al.*, 2000; Sikdar *et al.*, 2004) have been able to use GIS and Remote Sensing techniques to assess areas with groundwater. The thematic layers utilized in these analyzes vary across studies because their selection processes are normally random. This is largely because the processes of assigning weights to thematic layers tend to be based on personal decisions. In this respect, (Chowdhury *et al.*, 2009; Jha *et al.*, 2010) recently was able to utilize MCDM technique to find the weights for groundwater in their analysis. This technique is accepted worldwide in evaluating complex issues.

The processes of exploring and utilizing groundwater particularly in hard rock terrains need through understanding of lineaments, geomorphology and geology, which in one way or the other depend on terrain characteristics (Pradeep, 1998; Kumar *et al.*, 2007; Ravindran and Jayaram, 1997). When these data are integrated effectively and then they are followed closely with hydrogeological investigation, they provide efficient processes for delineating areas with groundwater in a manner that is cost-effective. Even though it has been possible to combine these data systematically and identify areas with groundwater, the process is normally difficult, time consuming and sometimes marred with a lot of errors. Over the last few years, digital technique has been developed and integrated with various data to identify areas with groundwater and solve other problems. The various data are prepared using thematic maps using GIS software tool. The thematic maps are then combined using “Spatial Analyst” tool that consists of Boolean and mathematical operators. A model that is developed on the basis

of problems at hand like identification of groundwater is developed. Afterwards, the data that is remotely sensed from lineament, geology, drainage and geomorphological characteristics is utilized to identify areas with groundwater. To date, these methods have been utilized in different parts of the world to identify the potential for groundwater.

Over the last few years, satellite data in conjunction with conventional maps as well as rectified data obtained from ground have simplified the process of identifying areas rich in groundwater (Tiwari and Rai,1996; Das *et al.*,1997; Harinarayana *et al.*, 2000; Chowdhury, 2010; Tomas *et al.*,1999). However, with major developments occurring in digital technology, it has been possible for GIS technique to improve the accurateness of results obtained from hydrogeological researches and even identification of areas rich in groundwater. In addition, different authors such as (Fashae *et al.*, 2014; Krishnamurthy *et al.*, 1996; Murthy,2000; Sikdar *et al.*, 2004; Srivastava and Bhattacharya, 2006) among others have been able to apply DGIS and RS techniques in the processes of exploring for groundwater and identifying artificial recharge areas.

2.4 Application of Geophysical Survey

Geophysics is largely utilized to explore hydrocarbon at depths that are beyond 1000 meters. Over the last three decades, notable progresses have been made in this field of study particularly in seismic reflection techniques. Contrary to this, the near-surface geophysics is restricted to depths of up to 250 meters in the process of searching for groundwater. The application of this technique is largely on confining units, mapping thickness and depths of aquifers and locating the preferential fluid migration paths.

Different geophysical techniques have so far been utilized in the processes of investigating the presence of groundwater. Some of them have been successful whereas others have been unsuccessful. Geophysics has in the past been utilized either as a tool for mapping groundwater or discriminating the characteristics of groundwater. During the groundwater mapping, geophysics does not focus its attention on groundwater, but its attention is always on geological situation under which water exists. The electromagnetic and electrical methods tend to be applied widely in groundwater studies because most of the properties in geological formation,

which are vital in hydrogeology, are able to be correlated with signatures from electrical conductivity. General procedures utilized in geophysical techniques of exploring groundwater have been developed so far (Van Dongen and Woodhouse, 1994) but according to (Macdonald *et al.*, 2001), areas with compound hydrogeology and geology rarely comply with generic techniques and they require unique targeting methods. Majority of geophysical methods are utilized in the processes of characterizing groundwater, but the most efficient ones are those that rely on electromagnetic and electrical techniques.

Shanshal, (2018) carried out a study to evaluate the potential for groundwater in Sumel District in the northern part of Iraq using the geophysical Electrical survey method. The study was intended to determine whether it was possible to obtain water for agricultural and drinking purposes, which was not available in the target region. About 16 VES points were identified using the Schlumberger array technique to identify the sub-surface aquifer areas in the region. The depth penetrations went as far as 150 meters below the ground and their electric resistivity were between 10 and 70 Ω .m. A total of three zones were identified at different depths. The first one had electric resistivity of between 20 and 50 Ω .m. This represented deposits of clay. The second one had an electric resistivity of between 11 and 17 Ω .m that represented a sandstone layer with multiple sizes. The third one had electric resistivity of between 22 and 55 Ω .m that represented a layer of clay stone with silt in certain depths. This layer had semi-confined groundwater aquifer with permeable layers of sandstone. The study established that there were traces of groundwater in the area, but the depth of boreholes needed to be deep.

Mukund *et al.*, (2017) utilized Schlumberger and Wenner method to identify groundwater and even compare the application of the method in the process. About 54 VES soundings were conducted in the Dhule district. VES curves were then drawn from the data that was obtained from the study. Upon comparing results from the two methods, both methods were found to have their own merits and demerits. However, upon comparing the merits to demerits, it was determined that Wenner method was better in terms of calculations as well as interpretation of the result, but it required lateral length that was a constrain. Likewise, Schlumberger method was determined to be simple in the application process, but strange in interpretation of the

results. Overall, the study proved that geophysical techniques could be applied in evaluation of water resources.

Salami and Ogbamikhumi, (2017) conducted their study within Ihiebe Ogben community, which is found in Nigeria to evaluate the presence of groundwater within Basement Complex rocks using VES and Schlumberger Array configuration methods. The evaluation of the various aspects included in the study identified hydrogeological parameters of different thickness. The ranking maps that were generated from the analysis were utilized to rank are within VES stations. The results showed that most of potential areas had ranks of as high as 8 values and VES values of up to 6.

Muchiri *et al.*, (2016) conducted a study in Kangonde area in Machakos County Kenya with a view to identify the geophysical structure of the area. They conducted electrical resistivity survey to specify the subsurface layers and their respective characterization. The Schlumberger and Wenner arrays were carried out using VES and horizontal profiling respectively. A terrameter was utilized to determine the apparent resistivity, which was then plotted on log-log graph that was obtained from field data as part of qualitative analysis. In contrast, the IP2Win software was utilized to describe the variation in true resistivity as part of quantitative analysis. The resistivity results identified highly conductive zones at depths that ranged between 70m and 160m. Their respective resistivity values ranged between 10 Ω m and 100 Ω m. Stations within 979900Northing 348000Easting and 980450Northing 349000Easting respectively displayed low resistivity and high measurements. The low values lay along the steep gradient indicating that the study area was somewhat tilted. The basement rock within the area was compact with resistivity values that lay between 1000 Ω m and 5000 Ω m.

Mwega *et al.*, (2016) carried out geo-electrical investigation along Lake Chala Watershed found in Kenya to evaluate the possibility of groundwater in the area. They utilized the Schlumberger VES configuration with a current electrode that varied between 250 and 320m. The electrode was utilized to gather information relating to sub-surface lithology and aquifer. About 50 VES were carried out throughout the study and the data that was obtained from them analyzed using computer iteration process. The results showed that there were about four to

six distinctive sub-layers within the region. The layers consisted of topsoil (composed of gravel, sand, silt, clay and sandy soil with clay), rhyolite that was highly weathered, fractured basalt that was highly weathered, fresh and dry basalt that was slightly fractured, basalt basement rock, weathered basalt, and basalt volcanic ash that was moderately weathered. The results further showed that the auriferous layer in the area consisted of basalt geological materials that were weathered, volcanic and basalt ash that was moderately weathered and fractured basalt that was highly fractured. The resistivity ranged between 40 and 200 whereas thickness ranged between 1.38 and 91 meters. The area was identified as having great potential for groundwater that could be exploited to provide water to the people living in the area.

Abdullahi *et al.*, (2014) carried out geoelectrical method to evaluate the potential for groundwater and aquifer shielding capability of the overburden units in Sabo area in Kaduna State, Northwestern Nigeria. Their results identified three to five geo-electric sections; topsoil, fresh basement and gravel. The fractured rocks in the underground had aquiferous zones with weathered basement. The aquifers had depressions of up to 65 meters and resistivity values of between 10 Ω m and 756 Ω m.

Murasingh, (2014) and Srinivasan *et al.*, (2013) carried out their study along Wellington vault of Vellar bowl to evaluate the availability of groundwater. They surveyed the sub-surface of the region to determine if it had any potential for groundwater. They made effort to determine the lithology of the sub-surface as well as the geo-electrical resistivity of the aquifer zones. The technique was utilized to layout the stations in the area. The Schlumberger framework was utilized to obtain the electrical soundings within an area covering 5 kilometers. The pseudo portions were prepared using Ipi2 WIN ver.3.1 whereas iso-resistivity maps were developed by Mapinfo 8.5 program

Jatau *et al.*, (2013) evaluated the availability of groundwater in Parts of Kaduna South and surrounding areas using Wenner Offset Method of Electrical Resistivity Sounding. Their research revealed a four layer case for Barnawa area with topsoil had sandy clay whose thickness was 1.7m with a resistivity value of 216 Ω m. The second layer composed of lateritic clay whose thickness was 2.4m with resistivity value of 202 Ω m. The third layer, probably a

weathered layer with resistivity value and thickness of $115\Omega\text{m}$ and 14.4m respectively and had fresh basement whose resistivity value was $1931\Omega\text{m}$ underground.

Van-Dycke *et al.*, (2013) carried out a similar study using VES and resistivity profiling within Karaga and Gushiegu Districts, Northern part of Ghana with a view to evaluating the aquifer characteristics of the region and recommend the requisite hydro-geologically sites for drilling boreholes. The analysis was able to identify areas with weathered rocks and three layers were identified. The layers included weathering profile that laid on fractured bedrocks, weathered layer and topsoil. From this analysis, the authors were able to recommend the rights sites for drilling boreholes.

In Abiola *et al.* (2013) conducted a geo-electric evaluation of groundwater in Supare Estate,, Nigeria. This area was underlain by Precambrian Basement Complex rocks that had low porosity and permeability. A total of 14 VES were obtained using the Schlumberger electrode array. They showed that the area had four geo-electric layers along the sub-surface. These included the fresh basement, weathered basement, weathered layer and topsoil. The thickness of the overburden varied between 2 and 18 meters that determined the groundwater for the area.

Coker, (2012) utilized the VES resistivity sounding method to identify areas with groundwater within Akobo area, South western part of Nigeria. The Schlumberger configuration was utilized to conduct 21 VES experiments. The Abaque (master) curve was utilized to interpret the data. The geo-electrical sections in the study included shale/clay, fresh basement, sandy clayey, topsoil and clayey sand. The study established that fractured and weathered horizons occurring along the easternmost part of the study area had water-bearing zones because they had aquifers with thickness that exceeded 20 m.

Okiongbo and Akpofure, (2012) conducted 19 Schlumberger VES within and around Yenagoa city, along the southern part of Nigeria. They utilized maximum current electrode separation that ranged between 300 and 400 meters with a view to determine the possibility of identifying Quaternary sediments in the area as a way of inferring the geological structure of the area. This was intended to determine the possibility of groundwater in the area. The data collected was

interpreted using 1X1D, Interpex, USA, which was a computer-assisted iterative program. The results identified four distinctive geo-electric layers.

Ravindran *et al.*, (2012) conducted a VES study using Wenner electrode configuration method. They utilized equipments with CRM 500 resistivity to locate good sites within Thoothukudi District, India. The area had a rock type whose groundwater is found in secondary porosity that develops out of weathering, fracturing and faulting during the sub-surface formation. The SP logging and apparent resistivity techniques were utilized to carry out the interpretations. The resistivity level ranged between 100 and 120 Ωm and they indicated presence of freshwater zone in the study area.

Dahab *et al.*, (2012) evaluated the availability of groundwater in Abu Habil, northern part of Kordofan and its environs using VES. A total of 20 VES data was obtained from areas within study area. This method is normally utilized in the exploration of groundwater with a focus to issues related to depth and resistivity level of sub-surface layers. The Schlumberger VES measurements are carried out using a portable ABEM SAS1000 instrument. To obtain reliable data, the analysis should cover an area with resistivity values ranging between 3.0 Ωm and 5500 Ωm . This reflects resistivity variation of basement complex and sediments. In line with this, the study established sediments of relative thickness that did not exceed 25 meters along the southwest part of study area.

Innocent *et al.*, (2012) utilized an electrical resistivity surveying method to evaluate the resistivity and thickness of layered media within Zimbabwe. The study focused its attention on assessing the potential for groundwater in the study area that sat within fractured unconfined aquifers. Before this study was carried out, one-dimensional (1D) VES surveys had been utilized to conduct similar studies in the area. The unfortunate thing with this model (1D VES) was that it was able to evaluate layered structures without necessarily providing complete details concerning the interpretation of the structures and depth of hydro-geological features of sub-surface. As a result, it would be necessary to incorporate two-dimensional (2D) geophysical techniques in identification of groundwater so that comprehensive details can be obtained in such analysis. When 2D model is combined with 1D VES it provides better results

because 2D model is efficient in evaluating water availability within fractured and weathered basaltic greenstone rocks. It provides accurate hydro-geophysical results than conventional VES.

Anomohanran, (2011) Carried out geophysical investigation in Oleh, Nigeria. The study sought to evaluate the potential of groundwater. The VES and Schlumberger configuration methods were utilized to conduct the study. A computer iteration process was utilized to interpret that data that was obtained from field study. When the data was compared with lithologic log obtained from existing boreholes, it identified four layers. The resistivity survey that was conducted in this study was intended to identify the horizontal and vertical boundaries. The Schlumberger array utilized in the analysis identified the water-bearing aquifers. This was an efficient process because of its usefulness in mapping and interpreting depths in the exploration of groundwater. It was identified as superior than other methods (Amajor *et al.*, 2007; Egai, 2013). Accordingly, it was selected for the study because of its merits over those other methods. This included its ease in interpretation, cost, its quantitative techniques and non-invasiveness (Mbonu *et al.*, 1994; Egai and Imasuen, 2013; Fronlch, *etal.*, 1994; Egai, 2013; Egai and Douglas, 2015).

Alabi *et al.*, (2010) carried a resistivity survey to establish the availability of groundwater in Lagos State University. The study focused much of its attention on resistivity, sediment, thickness and depth levels of water. The Horizontal profiling and VES methods were utilized in the analysis. The focus of the study was identifying areas with groundwater. The Schlumberger configuration together with Horizontal method was utilized to conduct 4 VES in the area. The VES data was subjected to WIN RESIST software to show the areas with sand, sandy clay, clay and top soil. The data from Horizontal Profiling was subjected to DIPPRO to provide the resistivity variation. The relevant layers were identified with sand of VES1-4 that signified the probability of aquiferous zone whose resistivity was between 206.2_m and 406.6_m whereas thickness ranged between 3.0m and 13.0m. The areas with favorable thickness and resistivity had sand formation. The study concluded that there was no notable difference between horizontal and VES profiling.

Pervaize *et al.*, (2010) conducted a geo-electrical resistivity survey using VES at Chaj Doab. This was in Pakistan within a land that lay between rivers Jhelum and Chenab as well as Rachna Doab that lay between rivers Chenab and Ravi. The study sought to identify the availability of groundwater in the areas. About 90 sites were identified; 43 of them came from Chaj region whereas 47 of them came from Rachna Doabs. A resistivity meter was utilized to obtain VES data. The data was then interpreted using Interpex IX1D together with resistivity model to determine the depth for each location.

Awomeso *et al.*, (2008) carried out 17 offset Wenner electrical sounding experiments relating to ground conductivity profiling using a resistivity meter (Terrameter) along the Osun State, Southwest Nigeria. The study intended to identify areas that were rich in groundwater for the sake of drilling boreholes. The software utilized in the analysis identified high conductivity anomalies, which were thought to result from bedrock fissuring and deep weathering.

Batte *et al.*, (2008) evaluated the availability of groundwater in eastern part of Uganda in an area that had crystalline basement rocks interfaced between bedrock and overburden. The study was conducted with an aim of identifying areas huge potential of groundwater in areas in Kamuli District. The study established that boreholes that were sunk after appropriate geophysical techniques were applied gave sufficient amounts of water whereas those sunk without applying those techniques dried up after a while. The VES and resistivity anomaly techniques were utilized to locate the water-bearing zones. VES focused its attention on geological overview whereas resistivity profiling was utilized to identify hydrogeological parameters. The boreholes that bore water had resistivity values of between 100 and 200 ohm.m. The bedrocks had depths of more than 20 meters.

Srinivas *et al.*, (2008) conducted a geophysical survey near Abhishekapatti, Tirunelveli district, Tamilnadu using electrical resistivity in a study that attempted to determine the possible structural features of the subsurface in the area. A resistivity meter was utilized to conduct the survey. The Wenner configuration and VES were utilized to evaluate the resistivity profiling. The area under investigation was covered largely by thin soil that was underlain by massive crystalline metamorphic rocks that had high resistivity. The inferences made provided notable insights into the manner in which resistivity was distributed in the area. Lateral and vertical

extension of fractures with low resistivity, apparent resistivity and resistivity pseudo section obtained from the analysis showed existence of contact zone along the east west direction.

Gressando, (1999) and Mwege, (2016) utilized resistivity method to investigate groundwater in Lake Naivasha area. The investigation utilized Schlumbergher arrangement for vertical electric resistivity and Wenner arrangement for horizontal profiling. The schlumbergher array involved twenty five vertical electrical resistivity soundings (VES) which were spread out from Lake Naivasha shore (swamp zone) to Suswa in the southeast and Malewa catchment in the northeast of the study area. Horizontal profiling was used to obtain the lateral variations of the subsurface lithology.

.

.

CHAPTER THREE

MATERIALS AND METHODS

3.1 Introduction

This chapter describes various approaches and methodologies adopted for present study which include application of remote sensing data from the imageries, integration of the various data sets in GIS platform and acquisition geophysical data in the field followed by analysis and interpretation. The goal of the study was to determine groundwater potential zones. The detailed methodologies are described below.

3.1 Development of different thematic map.

Thematic maps were developed from reconnaissance survey and remotely sensed data to demarcate areas with groundwater potential. The seven main maps that were developed included Geomorphology map, lineament map, drainage density, slope, LULC, DEM and Lithology. The pan-chromatic bands, middle infrared (MIR), shortwave infrared (SWIR) and visible (1, 2 and 3) were the ETM+ imagery data that were utilized in the analysis. The spatial resolutions for infrared and visible were 30 meters whereas that for pan-chromatic was 15 meters. The geometric and advance image correction was conducted using ground control points (GCP's) that was further collected through GPS method. The DEM at 30 m resolution that was obtained from data that came from an advanced radiometer that was obtained from provider's website ([http:// asterweb.jpl.nasa.gov/gdem.asp](http://asterweb.jpl.nasa.gov/gdem.asp)). The basin's layers of stream network obtained in the analysis were corrected by positional shifts. A line smoothing functions was equally utilized to edit the positional shifts manually. The lineament features were improved through data editing.

A detailed flow chart of the process followed to conduct the study is provided in (Figure 3.1). The information contained in the flowchart depicts the process followed to prepare thematic maps; the process followed to delineate LULC and lineaments, drainage density, slope was generated from DEM with the help of unsupervised classification technique. An accuracy assessment was finally conducted on the entire process.

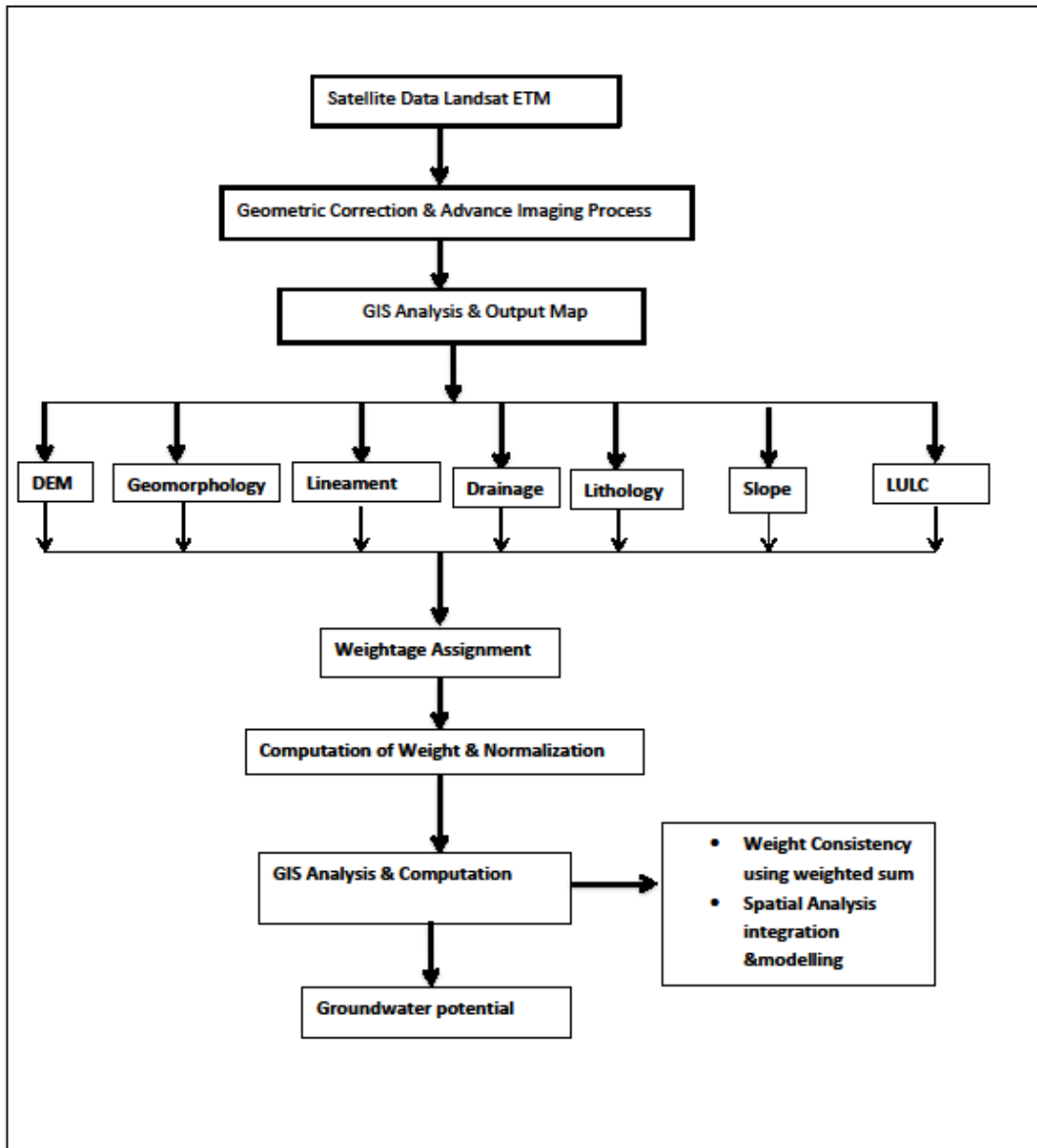


Figure 3.1: Flowchart of Methodology

The ArcGIS (10.3) was utilized to prepare the additional thematic layers. The Landsat images of Jubek state, which was in 1:50,000 scale provided the contour and drainage layers. The contour map generated DEM that was used to obtain the slope of the area, soil and geology and lineament map. The slope's map provided the terrain properties of the region. The World Geographic System 84 (WGS84) was utilized to geo-reference all input datasets. The reclassification, which was conducted by assigning weights to thematic features once relative contribution characteristics were evaluated, was as provided below. The layers considered in the analysis were integrated in GIS environment.

3.2 Spatial analysis and Integration of thematic maps and modeling

To segregate groundwater potential zone from the following thematic layer such as geomorphology, Lineament, drainage density, LULC and slope map and Lithology which were prepared from Landsat image and DEM, all the individual thematic layer are assigned weight in order to assist in spatial analysis as shown in the table (3.1), the integration and analysis of these factors on a GIS platform aided in locating zones with groundwater potential. The layers were converted into raster format using the arc map convert comment under images analysis for integration in GIS environment.

Categorization and reclassified of thematic layers were combined using GIS weighting. They were then assigned scale that ranged from 5 which is very high very to 1 which is very low on the basis of their suitability and capability to store and hold groundwater. Afterwards, the classification of regions with groundwater was then done using polygons that were categorized into 7 groups that ranged from very good to nil.

3.2.1 Weightage Assignment

The factors that govern the movement and occurrence of groundwater in any given area varies greatly, the factors are express in term of thematic layers such as geomorphology, lithology, Lineament, drainage density, slope, land use/land cover and DEM. Parameter estimates for each thematic layer was derived from published sources. Each layer was then divided into ranks and their spatial extent identified (Table 3.1). Weighted index overlay analysis (WIOA) is a simple and effective method for combining analysis of multi-ranks map(Nag, 2005). The

strength of this method lies on personal decision/experiences in groundwater investigation and including previous literature review that were incorporated into the analysis through a weighting system. Weighted index overlay analysis (WIOA) method takes into consideration the relative importance of the parameters and the ranks belonging to each parameter by weighting. As there is no standard scale for WIOA, each criteria where defined and each parameter assigned according to its relative significant in groundwater investigation (Gumma and Pavelic, 2013; Nag, 2005).

Table 3.1 Assigned weight, features and Ranks for different thematic maps

Thematic Layers	Weight %	Features	Ranks
Geomorphology	25%	River and Streams	5
		Alluvial plain	4
		Basement terrain	3
		Mountains	2
		Colluvium	2
		Rocky Outcrop	1
		Aswa Shear Zone	1
Lineament	5%	Pediplain	5
Drainage Density	15%	0.88 – 1	5
		0.8 - 0.87	5
		0.72 - 0.79	4
		0.64--0.71	4
		0.53--0.63	3
		0.4--0.52	2
		0.12--0.39	1
DEM	20%	Very high	5
		High	4
		Moderate	3
		Low	2
		Very low	1
Slope	20%	Very high	5
		High	4
		Moderate	3
		Low	2
		Very low	1
LULC	25%	Open Water	5
		Tree cover area	5
		Shrub cover area	4
		Grass Land	3
		Crop Land	3
		Vegetation Aquatic	3
		Lichen Mosses	2
		Bear Area	1
		Built up Area	1
Lithology	5%	Sedimentary rock	5
		Umruwaba formation	4
		Precambrian rock	1

Determinant factors

The geomorphology of an area is a vital element in the process of exploring the prospects of groundwater. This controls the movement of groundwater, affects the weathering process by creating superficial layers that vary in terms of permeability and degrees of porosity. Studies have demonstrated that unconsolidated overburden is able to develop reliable aquifers with notable thickness (Bala and Ike 2001; Mogaji *at el.*, 2011). Furthermore, they have demonstrated that concealed basement rocks might consist of folded and highly faulted areas, fracture systems that emanate from multiple tectonic events and incipient joints. The structures may in turn contain huge amounts of groundwater. As a result, the process of detecting and delineating such structures may facilitate the process of identifying zones with groundwater.

Lineaments, which are part of linear features, provide an overview of fractures and faults found in the study area. Because of this they might indicate areas with groundwater (Todd and Mays, 2005) and they may also act as conduits through which water might flow. These features are important because they help in identifying secondary structural disturbances that are useful in infer the movement of groundwater. The structures are normally inferred through digital remote sensing. Areas that fall around intersections of lineaments and lineaments themselves are regarded as favorable sites for groundwater because groundwater infiltrates and accumulates around those areas. As a result, it is presumed that the intensity of fracturing decrease as one moves away from lineaments implying that areas with groundwater are close to lineaments (Solomon and Quiel, 2006).

The stream patterns reflect the rates of precipitation in comparison to surface runoff (Edet, 1998; Gupta and Srivastava, 2010). Because it relates with permeability in an inverse manner then it is a vital element in the exploration of groundwater. This term was introduced by Gupta and Srivastava, (2010) and Horton, (1932) and it calculated as the ratio of cumulative stream length in relation to size of the area under study (Edet, 1998). Accordingly, areas with high drainage density are able to drain rain water faster than those with low density (Gupta & Srivastava, 2010; Melton, 1957). This implies that areas with high drainage density are unfavorable for groundwater whereas their counterparts with low density are favorable for it (Todd and Mays, 2005; Gupta and Srivastava, 2010). This literally means that drainage density

is linked directly with the amount of time runoff remains in a watershed. As a result, an area with low density allows water to collect on earth's surface for a longer time. This allows it to infiltrate into the ground. In contrast, an area with high density does not allow surface water to collect on earth's surface for a longer time. Because of this water does not infiltrate into the ground since it flows to other areas faster. As a result of this, areas with low density have higher potential for groundwater than their counterparts.

The LULC indicate the extent of utilization and requirement of groundwater in an area. As such, areas with dense vegetation are excellent for exploration of groundwater (Todd and Mays, 2005; Gupta and Srivastava, 2010). To date, the synoptic viewing conducted via remote sensing has been utilized to provide multispectral data used to classify LULC.

The topography of an area relates to relief setting of an area. It gives an idea of the direction under which groundwater flows and the influence it might have on discharge and recharge of groundwater. An area with low slope suggests the presence of groundwater whereas that with high slopes suggests poor potential for groundwater. The simple reason is that water tends to flow faster in hilly areas than in flat and less hilly ones.

3.3 Basic theory of resistivity method

3.3.1 Introductions

The conductivity and geophysical resistivity methods concern themselves with study of the effects of sub-surface on water flow when electric current flows on that surface. The electrical resistivity one are utilized extensively in evaluating shallow sub-surfaces especially those concerned with resolving hydrogeological and environmental problems. An alternating current (AC) or direct one of about 20Hz can be used for the investigation. The electrical survey is used to investigate variation in the subsurface electrical properties like the resistivity distribution. The subsurface resistivity variation can be correlated to geological parameters, for instance, the minerals and amount of water, fracturing, porosity, conductivity of saturate and lithology. The technique is also valuable in recognizing the various layers, variations and discontinuities within the layers of the subsurface because of its exceptional sensitivity to

subsurface resistivity. These peculiarities and variations are generally vital I the occurrence of groundwater (Owen *et al.*, 2005; Issah, 2015).

The occurrence of water controls is vital in the variation of ground resistivity. The degree of water saturation and network of opening space gives an estimation of the subsurface resistivity. This is because water is highly conductive and hence less resistive and current will move though regions of low resistance. Increase in salinity of ground water, increase saturation, increase porosity and degree of fracturing of rock, each of which tends to reduce resistivity. Increase in the degree of compaction within the lithology reduces the amount water and finally increases the resistivity. The occurrence of water reduces resistivity while the vicinity of pore air raises resistivity because air unsurprisingly has pronounced resistivity In the light of the fact that, the passage of current in the near surface results from movement of ions with the pore space, porosity controls the variation of resistivity. It is very tedious in estimating resistive anomalies than conductive anomalies, since the majority of minerals are non-conductive and rock structure has a tendency to affect resistivity (Cardimona, 2008; Issah, 2015).

3.3.2 Principle of Resistivity Methods

The majority of minerals forming rock are extremely non-conductive, and the passage electric current through is mainly ionic pore water. The vicinity and the degree of the dissolved ions in pore water determines their conductivity since pure water is less ionized (Milsom, 2003; Issah, 2015). The electrical properties of different materials are best explained by Ohm's law.

$$V = I \times R, \quad R = \frac{V}{I} \quad (3.1)$$

R is the constant of proportionality that represents the resistance. The conductance, which is the reciprocal of the law, is measured in Siemens.

The link provided in the above analysis holds only for earth materials. Nevertheless, the resistance, R , does not represent the constant of material. This is because it does not rest on material of medium, but also on its geometry. The resistance, R , which is presented in ohms, equals proportionally to the length of a material especially for wire. Also, it relates to cross-sectional area, A , of the material in an inverse manner.

$$R = \rho \frac{l}{A} \quad (3.2)$$

The resistivity ρ of a material has significant influence on the flow of electric current because it affects the resistance of that material. Because of this it can be regarded as resistance between opposing faces of unit cube in the light of current passing through it (Milsom, 2003).

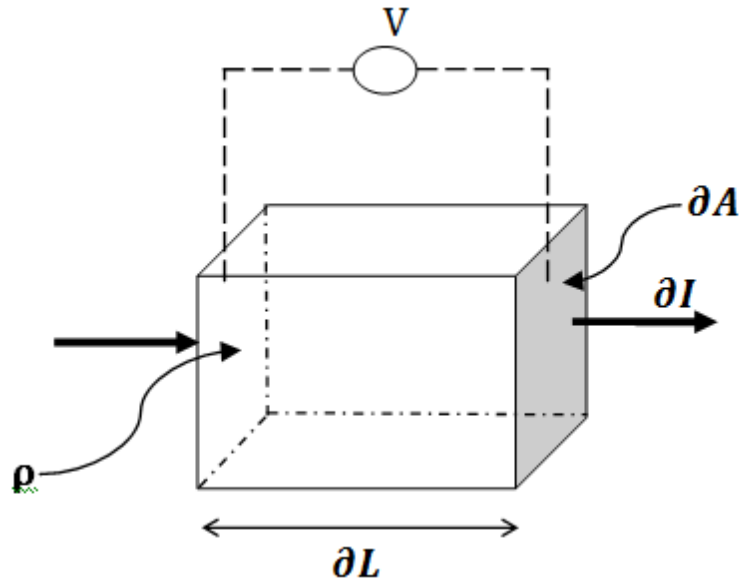


Figure 3.2: The basic definition of resistivity in a homogeneous block

A conducting block can be said to have resistivity given by Equation (3.2), which can be rearranged to give the following.

$$\rho = lR \cdot \frac{A}{l} \quad (3.3a)$$

$$\rho = \frac{V \cdot A}{I \cdot l} \quad (3.3b)$$

The density of the medium at any point would be regarded as the current that passes through it in a unit area. This density, J , relates to electric field strength E via an ohm's law given as;

$$J = \sigma E = \sigma \nabla V \quad (3.4)$$

Where $\sigma = \frac{1}{\rho}$

$$J = \frac{1}{\rho} E \quad (3.5)$$

$$J = \frac{1}{A} \frac{\nabla V}{\rho L} \quad (3.6)$$

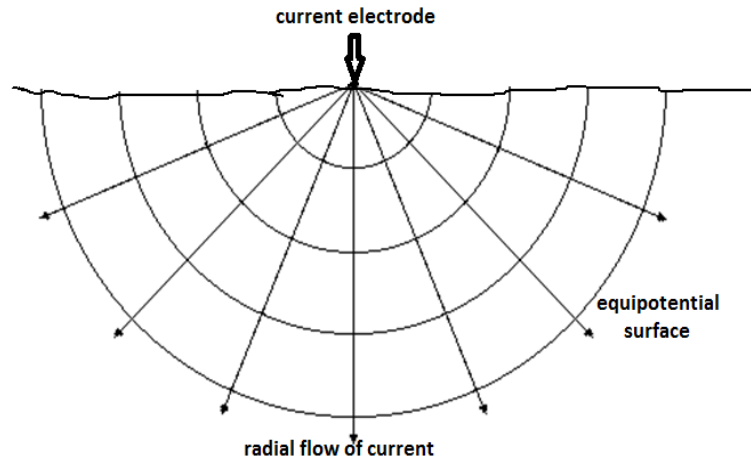


Figure 3.3: The current flowing from electrode to distribute current uniformly over the shell

The current's density reduces when distance from the source increases because it flows radially from electrode. As a consequence, it is distributed uniformly over the shells. From this, the voltage at a distance (r) is as shown above in figure 3.3

$$J = 1/\frac{1}{2}(4\pi r^2) = -\frac{1}{\rho} \frac{dv}{dr} \quad (3.7)$$

The equation (3.8) is a theoretical basis of the way current flows in a homogeneous isotropic subsurface with one current electrode. Current flows radially in an inverse manner. Hence, the resistivity ρ is given by

$$V(r) = \frac{I\rho}{2\pi r} \quad (3.8)$$

Practically, most of studies on resistivity use a minimum of one pair of current and potential electrodes (M. H. Loke, 1997). The values for potential electrode from such studies have symmetrical patterns provided by equation (3.4).

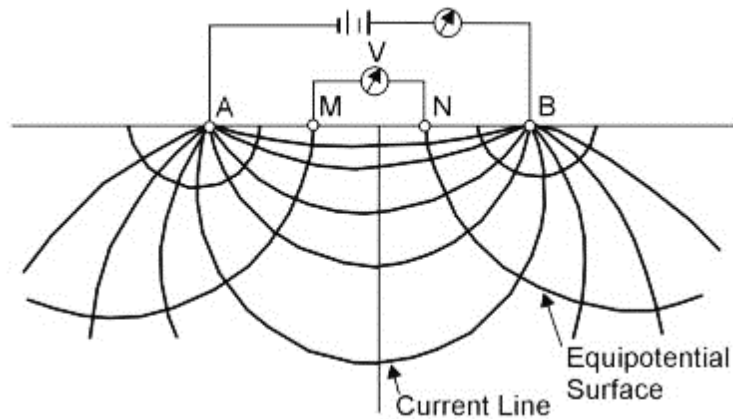


**Figure 3.4: The potential distribution from a pair of current electrodes
(U. S. Environmental Protection Agency, 2011)**

Consider an arrangement with potential electrodes M and N and current electrodes, A and B. Making use of equation (3.5), A and B would act as source and sink, respectively. This would give two points that would act as potential electrodes positions. In such a case, the electric potential would be impacted by sink and source to give potential difference between them.

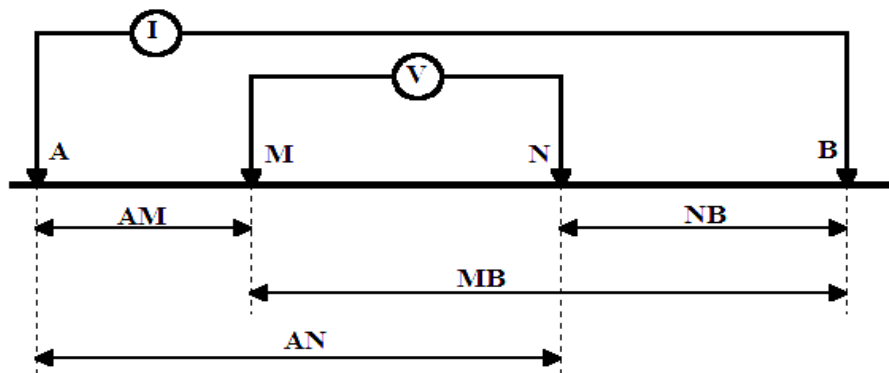


Figure 3.5: The generalized form of the electrode configuration used in resistivity measurements

The distance for electrode M is AM whereas that for B is MB. Conversely, for N the distances would be AN and NB. As a result, the potential V_M would be;

$$V_m = \frac{I\rho}{2\pi} \left(\frac{1}{AM} - \frac{1}{NB} \right) \quad (3.9a)$$

For V_N , it would be;

$$V_m = \frac{I\rho}{2\pi} \left(\frac{1}{AN} - \frac{1}{NB} \right) \quad (3.10)$$

Hence, the total difference between M and N would be;

$$\nabla V = V_M - V_N \quad (3.11)$$

$$\nabla V = \frac{I\rho}{2\pi} \left[\left(\frac{1}{AM} - \frac{1}{NB} \right) - \left(\frac{1}{AN} - \frac{1}{NB} \right) \right] \quad (3.12)$$

For arrays, potential at any given electrode would be the sum that each of them contributes.

Hence, the resistivity in a 4-electrode survey would be;

$$\rho = \frac{\Delta V}{I} K \quad (3.13)$$

Where

$$K = 2\pi I \left[\left(\frac{1}{AM} - \frac{1}{NB} \right) - \left(\frac{1}{AN} - \frac{1}{NB} \right) \right]^{-1} \quad (3.14)$$

K is a geometric factor that depends on positions of potential electrodes and current. Because sub-surfaces tend to be heterogeneous, resistivity attained are apparent (ρ_a). Worth noting that resistivity values measured on fields are never true, but apparent (Reynolds, 1997; Issah, 2015).

3.4 Electrode configuration for resistivity survey

It is possible to place the 4 electrodes A, B, M and N in (Figure 3.5) at arbitrary positions on the ground. Doing this would help in identifying the advantages that each of them provides in the arrangement. In spite of the fact that different arrangements offer varying resistivity, the Schlumberger, Wenner, and dipole-dipole configurations are the most common ones. For all the arrays, the four electrodes are collinearly arranged but with distinctive electrode separation and geometries are different (Lowrie, 2007). The geometry of the electrode of a configuration determines the apparent resistivity. The apparent resistivity is influenced by 4 distance-variables AM, AN, BM, and BN (Zohdy *et al.*, 1974).

3.4.1 Wenner Configuration

This is the simplest configuration because potential and current electrodes are placed at equal spacing a (Figure 3.6) (Kearey, 2002). The array has four electrodes that are placed collinearly at equal spaces. The two outermost electrodes act as current electrodes whereas the inner ones are potential electrodes. The electrode spacing extends from the midpoint as they maintain equal spaces between them. The apparent resistivity for this configuration is given by;

$$\rho_a = 2\pi a \frac{\Delta v}{I} \quad (3.15)$$

With this configuration, apparent resistivity can be determined from the field even though sensitivity would not necessarily be compared to other geometries of array. Normally, only a little amount of current is needed to create potential differences that would be measurable. The disadvantage with such an arrangement is that the electrodes would be repositioned for every sounding.

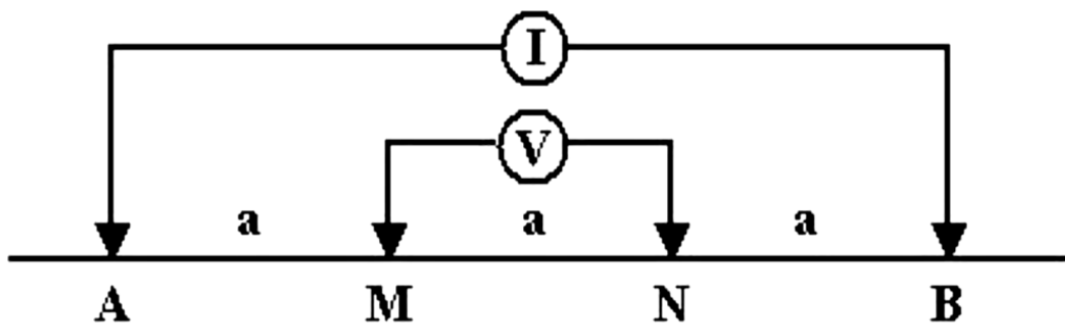


Figure 3.6: The Wenner array

3.4.2 Schlumberger configuration

This array is utilized widely in electrical prospecting, and it has four electrodes, which are arranged in a collinear manner with two of electrodes A and B acting as current electrodes and M and N as potential electrodes (Zohdy *et al.*, 1974) (Figure 3.7). The potential electrodes are normally placed at the center at a separation normally less than a fifth between current electrodes and they are kept constant whereas the current ones are varied.

The spacing of potential electrodes is presumed to be infinitesimal; hence, observed values should be adjusted (Dobrin and Savit, 1988). The following equation gives the apparent resistivity, (ρ_a) for this configuration;

$$\rho_a = \frac{\pi}{2} [S^2 - \left(\frac{a}{2}\right)^2] \frac{\Delta V}{I} \quad (3.16)$$

With the Schlumberger configuration, less electrodes are relocated for each sounding. To a large extent, the sounding of this configuration has good resolution and better depth of penetration, and easy field deployment. Its disadvantage is that it requires long current electrode cables.

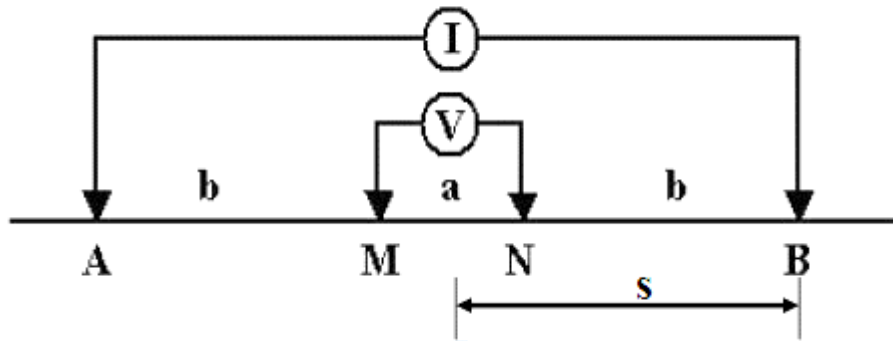


Figure 3.7: Schlumberger array

3.5. Field procedures for data collection

In this research work, both VES and Horizontal profile surveys using both Schlumberger and Wenner arrays configuration respectively were adopted throughout the analysis and field work. The vital field equipment used for the study was ABEM SAS Terrameter 1000 which displayed apparent resistivity value in digital form as obtained from Ohm's law. The Terrameter 1000 was powered by 12V D.C power source. The other materials included 4 hammers, a measuring tape, 12 metal electrodes (4 meters each) for VES and Profiling, cables, GPS to get the coordinates. The Schlumberger configuration was adopted with VES. This involved placing 4 electrodes systematically along a straight line; those on outside served as current electrodes whereas those on the inside served as potential electrodes. The current electrodes were displaced from the outside whereas the potential ones were not changed in any way in the process of changing the depths of measurements. Nevertheless, when the ratio of the distances are large, potential electrodes should be displaced outwards to ensure that potential difference

is not small (koefoed,1979; Alile,2008; Pervaiz *et al.*, 2010). The measurements of the position of both types of electrodes were marked such that $AB/2 \geq MN/2$.

Where $AB/2$ was the spacing for current electrode and $MN/2$ was for potential electrode.

Under normal circumstance, arrangements consist of one pair of potential electrode and another pair for current electrode. The pairs are then directed to the ground in straight lines to have direct contact with the earth. Once this is done, the spacing for current electrode should be extended. Here $AB/2 =$ Current electrode spacing. Its values increase as the study goes on whereas that for potential electrode is guided accordingly. Normally, the potential electrodes maintain small distances between them relative to the current ones (Milson, 1939;Alile, 2008). The main advantage of this method is that it only moves current electrodes whereas the potential ones are maintained at one point for three to four readings (Reinhard, 1976; Alile,2008). The ABEM SAS Terrameter 1000 resistivity meter records the readings automatically during the sounding process. It also computes resistance automatically and displays it digitally (Dobrin and king 1976; Alile 2008).

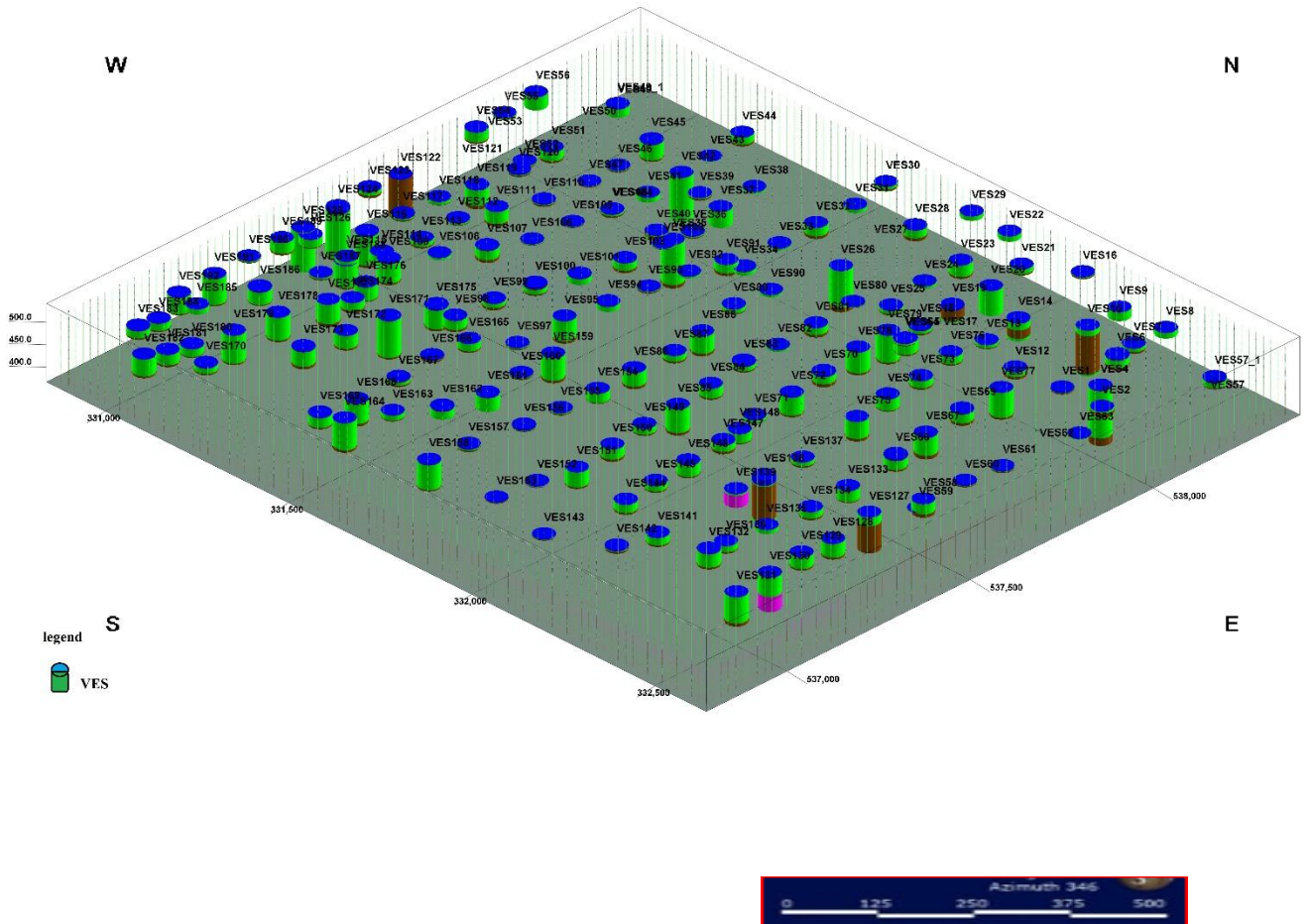


Figure 3.8: VES locations in Kapuri Area



Figure 3.9: Equipment's used for data collection

3.5.1 Horizontal electrical profiling

Horizontal electrical profiling used to determine subsurface layer, thickness of aquifer and the lateral variations extent. The electrode separation in this arrangement is fixed whereas the center is varied from time to time. In profiling technique, only variation and discontinuity in resistivity with lateral extensions of subsurface are recognized as anomalies underneath the profiles

In this study total of three (3) horizontal profiles (Fig 3.10) having a length of 1500m with spacing of 500m between each other running from east to west direction of study area, wenner configuration was utilized to conduct the study with the objectives of detecting subsurface geological layers and the extent. Total of 25 point where measured along each resistivity profile with the interval of 60m from each other, the measurement were taken at interval of $\left(\frac{AB}{2}\right)$ 10m,20m and 30m respectively at each point along the resistivity profile. ABEM SAS Terrametre resistivity meter was utilized to find the apparent resistivity of every horizontal

profile station; each point was recorded in universal traverse Mercator (UTM) coordinate with the aid of a Germin72 channel personal navigator (GPS) unit.

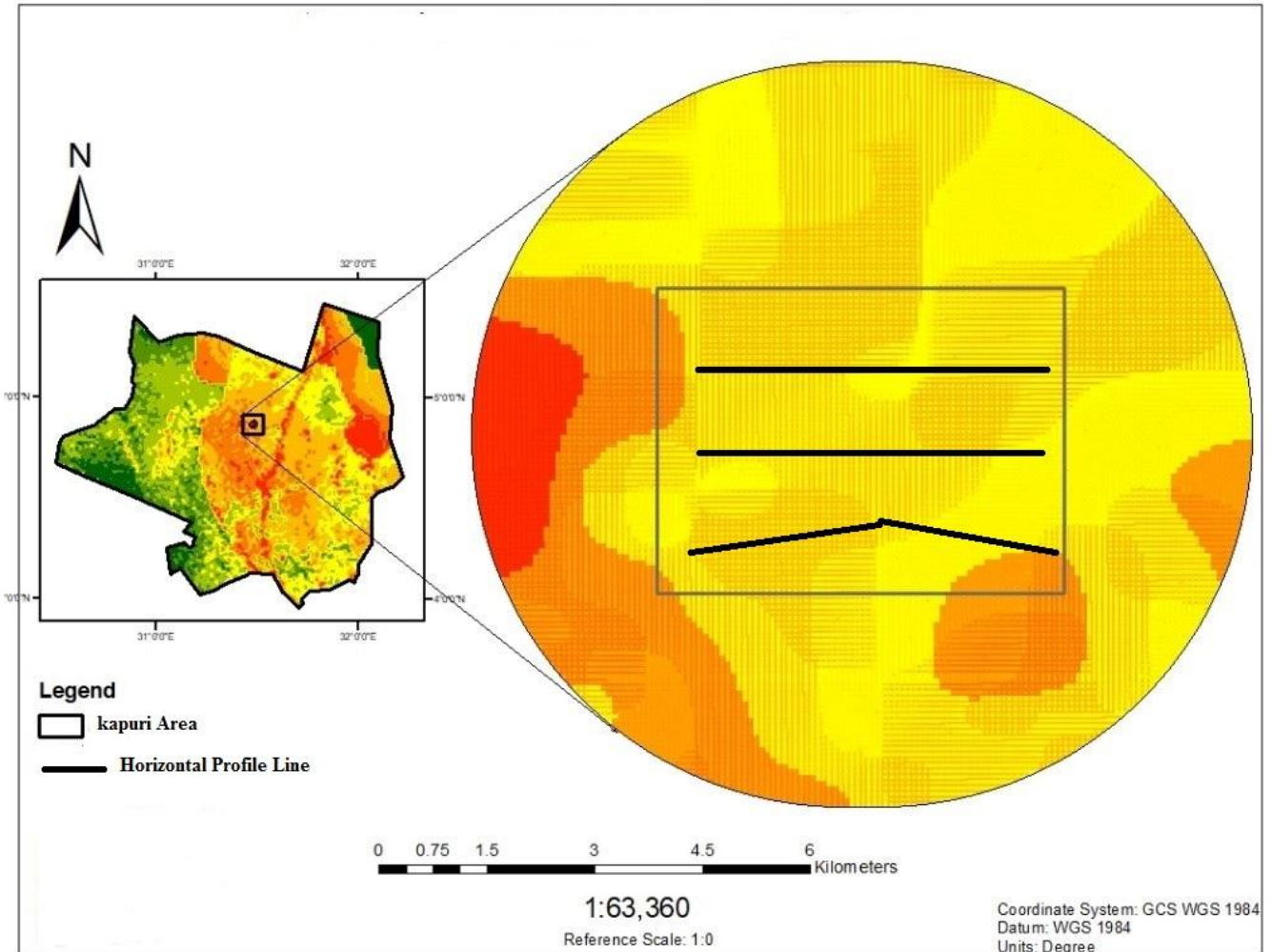


Figure 3.10: Horizontal profile location in Kapuri area

3.5.2 Vertical Electrical Sounding (VES)

This method, which is geophysical in nature, is used to evaluate geological medium. It attempts to evaluate the conductivity or electrical resistivity of those media. The estimation done in it is based on voltage of electrical field that current electrodes, which are grounded, induce on it. It is a form of galvanic technique. The rocks' electrical resistivity relies upon their liquid and lithology substances. As a result, by evaluating their nature, it is possible to tell whether a rock is able to produce groundwater or not. Schlumberger was the first person to develop VES method in 1934. Right from that time various VES systems have been developed and applied in different analysis (Keller and Frischknecht, 1966; Pervaiz *et al.*, 2010). However, the original one has remained to be the best of all. In this study, the VES system was utilized in different soundings with a view to correlating rock units with aquifer potential. The process entailed using electrodes (A and B) and measuring their potential difference in form of (DV). Throughout the study, the center point remained fixed, but the spacing between electrodes was increased a bit to provide data from deeper sections of sub-surfaces (Bhimasankaram and Gau, 1977). The depth of current electrodes was proportional to spacing between electrodes in all homogeneous grounds; thus, the variation that was conducted from time to time provided information relating to the way ground was stratified (koefoed,1979). The Schlumberger electrode configuration method was the best for the study area because it provided better results than other methods. Its advantages included high level of applicability, advantages in interpretation of results over Wenner method and high level of operationalization (Zohdy *et al.*,1974; Ward, 1990; Pervaiz *et al.*, 2010).

The VES survey that made use of the Schlumberger electrode configuration and a current electrode separation ($AB/2$) was utilized in the analysis. The readings started from 1.0 meter to a maximum of 160 meter. Throughout the study, the separation ($AB/2$) for the current electrodes was 1.0, 1.5, 1.8, 2.5, 3.5, 5, 8, 10, 13, 16, 20, 20, 25, 40, 45, 50, 63, 80, 100, 130 and 160m. Similar spacing of 20m and 40m indicated the rate at which spacing increased for potential electrode. Both readings were obtained for $AB/2$, but for $MN/2$ spacing different readings were made. The Schlumberger data was obtained from overlapping segments because the resistivity signals coming from the meter for every AB spacing kept on weakening. To address this challenge, the MN spacing was enlarged every time two values of AB were taken.

One reading was made for short spacing whereas the other one was made for the longer spacing. The separations (MN/2) for potential electrode were installed and enlarged at a rate of 0.5, 5.0, and 10m. This allowed for the readings of current electrode to be taken with high level of precision. About 192 VES surveys were conducted in the entire study area. To determine the accuracy of VES interpretation, 7 soundings were conducted near existing wells and their results correlated with each other. The instrument that measured apparent resistivity throughout the study was ABEM Terrameter SAS 1000 (Sweden). The instrument was not boosted in any way.

The 1-D inversion technique software (IX1D, Interpex, USA) was utilized to interpret VES data. The software produced the resistivity model by fitting the data that was obtained from field with least root mean square (RMS) error between the actual data and the synthetic one obtained from the model. An iteration method was then conducted until errors were fitted between synthetic and field data. The surface and position elevations for VES sites were recorded as well throughout the study using a GPS receiver. A computer software AutoCAD were used to generate thickness and the depth to the basement. .

3.6 Apparent resistivity

An electrical survey is conducted to evaluate the distribution of sub-surface resistivity by way of obtaining measurements from ground surface. Then true resistivity of sub-surface is determined from those measurements. The resistivity of ground relates to different geological parameters such as porosity, degree of water saturation within rocks, fluid content and minerals. For many years, the method has been utilized in geotechnical evaluations and hydrogeological mining. In the last few years, it has been extended to environmental surveys. To obtain the resistivity data, current electrodes (A and B in Fig (3.6)) are injected into the ground and voltage difference between potential electrodes (M and N) is determined. Out of this, the Voltage (V) and current (I) values are obtained and apparent resistivity (ρ_a) obtained as follows;

$$\rho_a = k \frac{V}{I} \quad (3.17)$$

k represents geometric factor that depend on the way the 4 electrodes are arranged. The above figure depicts a common array with its respective geometric factor. The resistivity meter yields a resistance value of, $R = \frac{V}{I}$, from which apparent resistivity value is computed as follows;

$$\rho_a = KR \quad (3.18)$$

An apparent resistivity is obtained from the analysis. The link between it and the true one need to be determined using a computer program. The process was followed in the current study to determine the true value.

3.6.1 Inversion and modeling

Modeling is the most popular method for interpretation of electrical resistivity geophysical data. Normally, a high speed digital computer is utilized in the determination of theoretical sounding curves. This process entails using an iterative method that starts with an initial model, which is then improved when calculated anomalies are compared with observed ones (M. Loke, 2001). To lessen the disparity between observed and calculated anomalies, the model parameters are adjusted (Elzein, 2007). When calculated anomalies do not fit the observed ones, the sub-surface is change till the Root Mean Square Error (RMSE) reduces below 10%. The model is appropriate when both values are fitted in the right way (Elzein, 2007).

3.6.2 Data Analysis and interpretation

The aim of interpretation of the resulting curves is to verify the thickness and resistivity of every layer from observed sensitivities and use results to develop a geological overview of area under investigation (Zohdy *et al.*,1990). To obtain quantitative results that are more accurate, the data should be processed to provide true resistivity distribution (Elzein, 2007). Interpretation of resistivity measurements therefore must be carried out with regards to the available geologic information of the area including geologic maps and borehole logs (if available). The graphical curve matching method (which is rather obsolete technique) or computer based techniques was used to interpret resistivity data (Zohdy *et al.*,1990). In graphical curve matching, the field curves are plotted on transparent logarithmic papers with similar modulus with master curves. Then they are shifted to master curves while keeping coordinate axes parallel till they match in a reasonable manner with either one of interpolated

curve or master curves. The resistivity values for various layers can then be determined by matching them to sets of master curves presuming layered Earth (Shewa, 2007).

CHAPTER FOUR

RESULTS AND DISCUSSIONS

This chapter provides the results obtained from the analysis in line with various objectives set at the beginning of the study.

4.1 Map lithology and geological structure, lineament, drainage, geomorphology change from remote sensing data

The data from Landsat ETM+8 was used to develop thematic maps using ArcGIS (10.3) software. The different thematic maps were described as shown below as Weighted overlay analysis of groundwater predictor factors in Kapuri area of Jubek state; mainly lithology, geomorphology change, Lineament , DEM, slope, drainage density, LULC are presented in Figures 4.1, 4.2, 4.3, 4.4,4.5 4.6, 4.7, 4.8 and 4.9 were all used to generate groundwater potential map with various zones (Figure 4.9).

4.1.1 Lithology of Kapuri Area

Lithology plays an important role in the distribution and occurrence of ground water in any region. The underlying geology of the study area comprises mainly of Precambrian rock of medium to high metamorphic grade. The Precambrian rock is composed principally of gneiss with amphibolite facies with subordinate meta-sediment. The Amphibolite dominance within a basement complex of the study area and been intruded by dyke swamp of doleritic composition (Figure 4.2).

Kapuri Area depicts covers thick burden of weathered materials and fractured bedrock from hydrogeological point of view and constitute a significant aquiferous unit by which forms potential ground water zone (Figure 4.1).

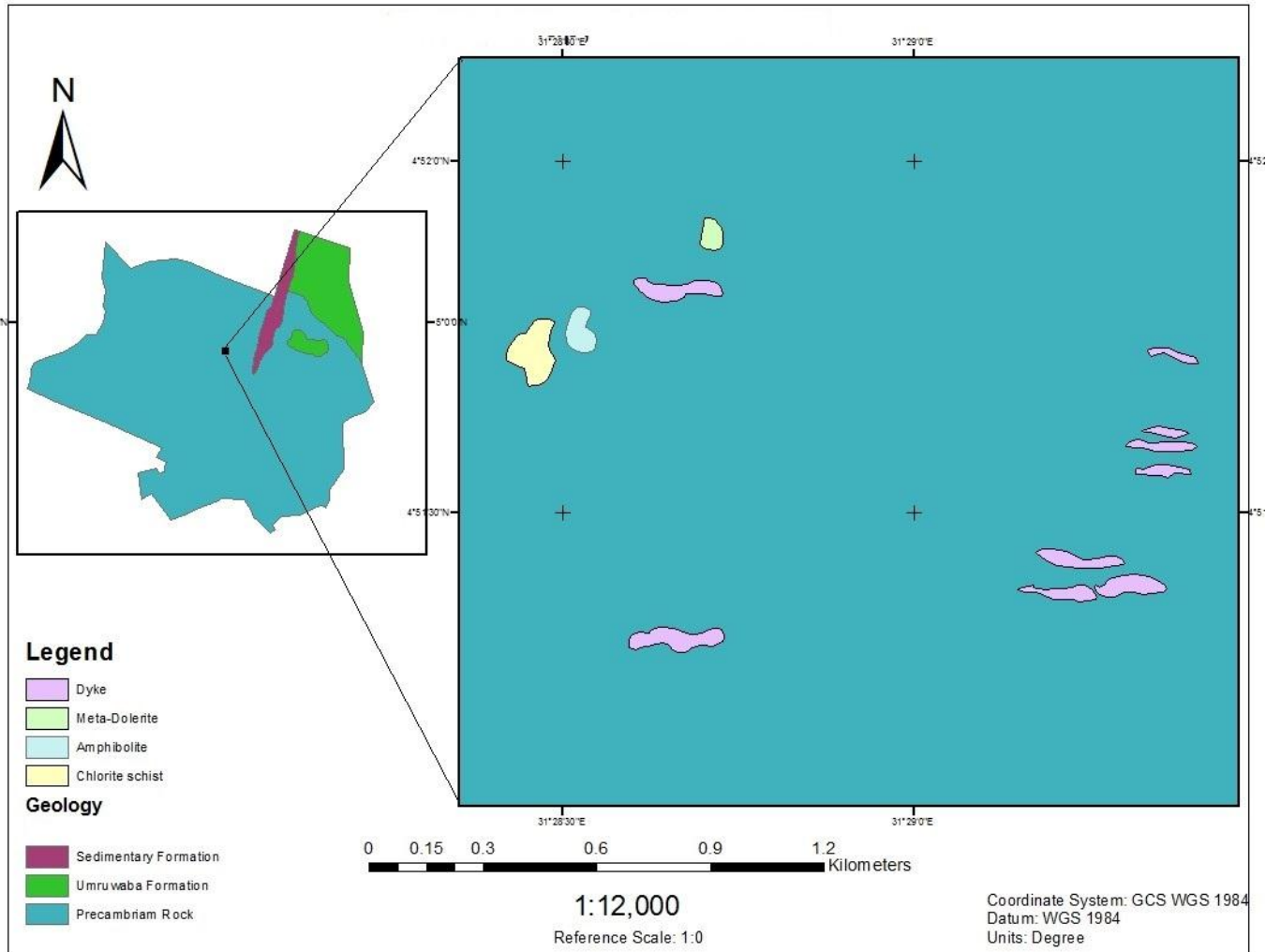


Figure 4.1: Lithology of Kapuri area



Figure 4.2: Different types of rock units in Kapuri Area. A) Gneiss, B) Chlorite schist, C) Amphibolite, D) Dolerite Dyke

4.1.2 Geomorphology of Kapuri Area

Geomorphology is concerned with the history and nature of landforms that form on earth's surface and other planets. Also, it is concerned with the way these landforms have evolved. The different geomorphology units generated from the analysis, which were obtained from satellite, are presented (Figure 4.3). The map portray vital geomorphic units, underlying geology, landforms, structures and geological controls that relate to groundwater occurrence and lithology. This helps in identifying areas that can produce groundwater. Their main focus of geomorphic mapping been on landform classification, linked between landform and processes, and process characterization. The remote sensing provide information relating to

distribution and location of landforms, surface elevation and surface-subsurface composition (Smith and Pain 2009; Prafull *et al.*, 2013). The landforms cover an important part within the exploration of groundwater (Horton 1945, Thornbury 1985) and consequently the highest weight can be found in (Table 3.1). The different classes that were identified in the analysis are provided in (Fig 4.2) such as. i) Rivers and Streams ii) Alluvial plain iii) Basement terrain iv) Rocky outcrop, V) Mountains, iv) Colluvium, iiv) Aswa Shear Zone.

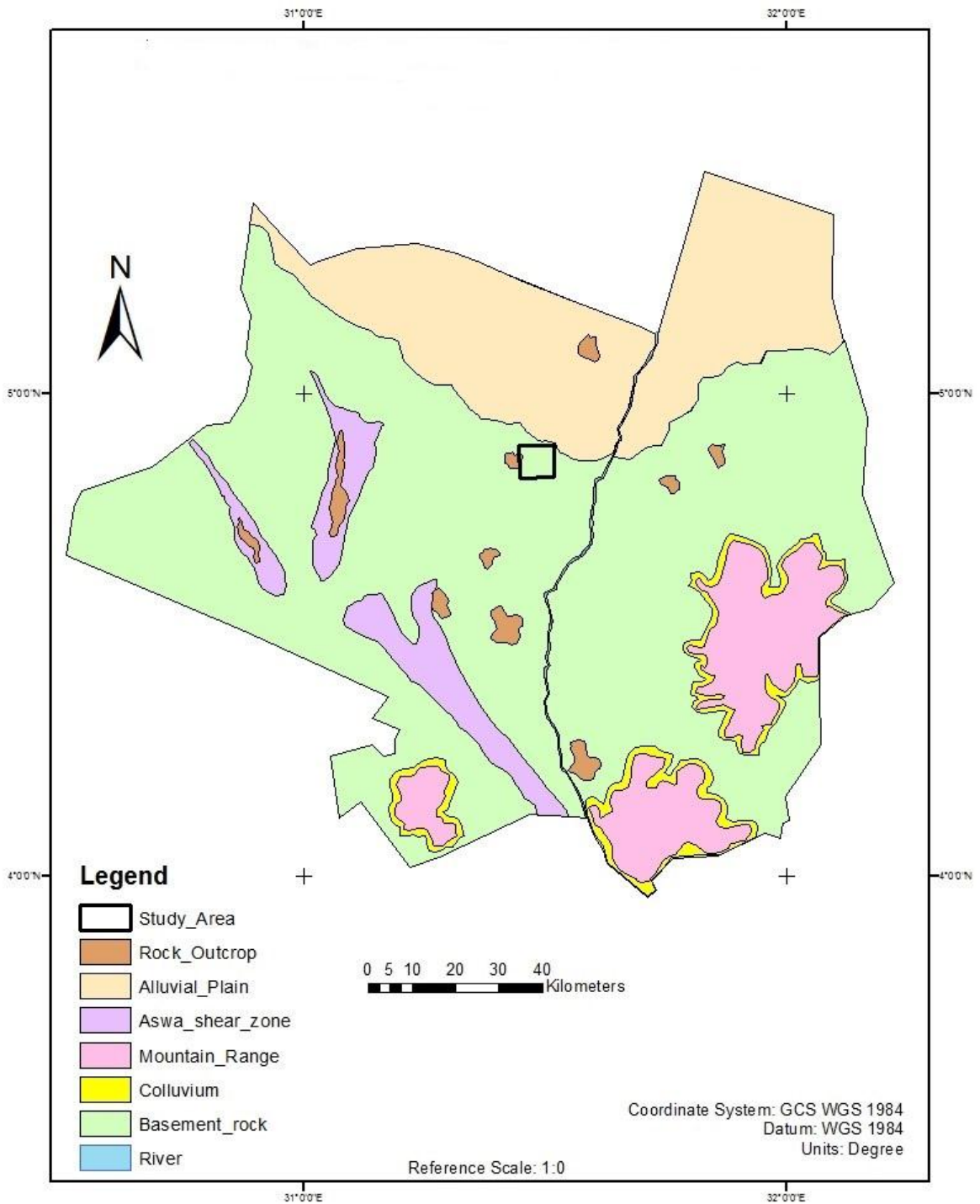


Figure 4.3: Geomorphology of Kapuri Area

4.1.3 Lineament Map

It is possible to express fracture and fault zones on satellite images as linear features. The mapping of lineaments is therefore an important aspect within hard-rock terrains. It indicates where groundwater occurs and possible movement of that water because it is impacted by linear features. Because of this analysis of lineaments during the process of exploring groundwater is vital because it acts as the first step in reconnaissance survey. Normally, the structural features such as fractures facilitate the flow of surface water thereby enhance secondary porosity of rocks (Fig.4.4). By analyzing lineaments, it is possible to have an overview of the way groundwater moves and is stored underground. Various studies have demonstrated that the potential of groundwater increases when lineament density increase (Shaban 2006, Awawdeh *et al.*, 2013; Teeuw 1995; Sener *et al.*, 2005). The analysis showed that the study area had many lineaments that resulted from tectonic activities that had occurred in the past. The lineaments followed three main directions namely N–S, NE–SW and E– W. A high drainage density indicates high lineament area. Areas with lineaments or those with intersections have the ability to accumulate groundwater because of weaker horizon.



Figure 4.4: Lineament Map, with rectangle inside the circle showing the study area

4.1.4 Drainage Density Map

Drainage density is a direct element for permeability then it is a vital aspect in exploration of groundwater. Normally, the characteristics of drainage system control the recharge of groundwater. Accordingly, an analysis of these characteristics is vital in the exploration of groundwater resources. In spite of this, it would be vital to note that recharge rate decrease with the density of drainage system implying that denser systems have lower recharge rate. Because of this low drainage densities allow groundwater to percolate and even accumulate in huge amounts. The process of identifying drainage density entails considering the number of drainage features within an area and then analyzing them. A high value suggests a high density of streams that induce fast response to rainfall. This results to runoff implying that water is not

given time to percolate into the ground. The calculation was achieved using by Spatial Analyst tool in ArcGIS software. In the study area drainage details were traced from satellite image. It was observed that drainage pattern was largely dendritic to sub-dendritic, but a rectangular pattern was observed as well (Fig.4.5). The drainage density map was classified into seven group: 0.12—0.39, 0.4—0.52, 0.53—0.63, 0.64—0.71, 0.72—0.79, 0.8—0.87, 0.88—1. Areas with low drainage density permit water to infiltrate thereby is likely to be good for drilling groundwater in comparison to those with high density. As a result of this, higher weights were given to areas with low drainage density whereas lower weights were given to those with high drainage density.

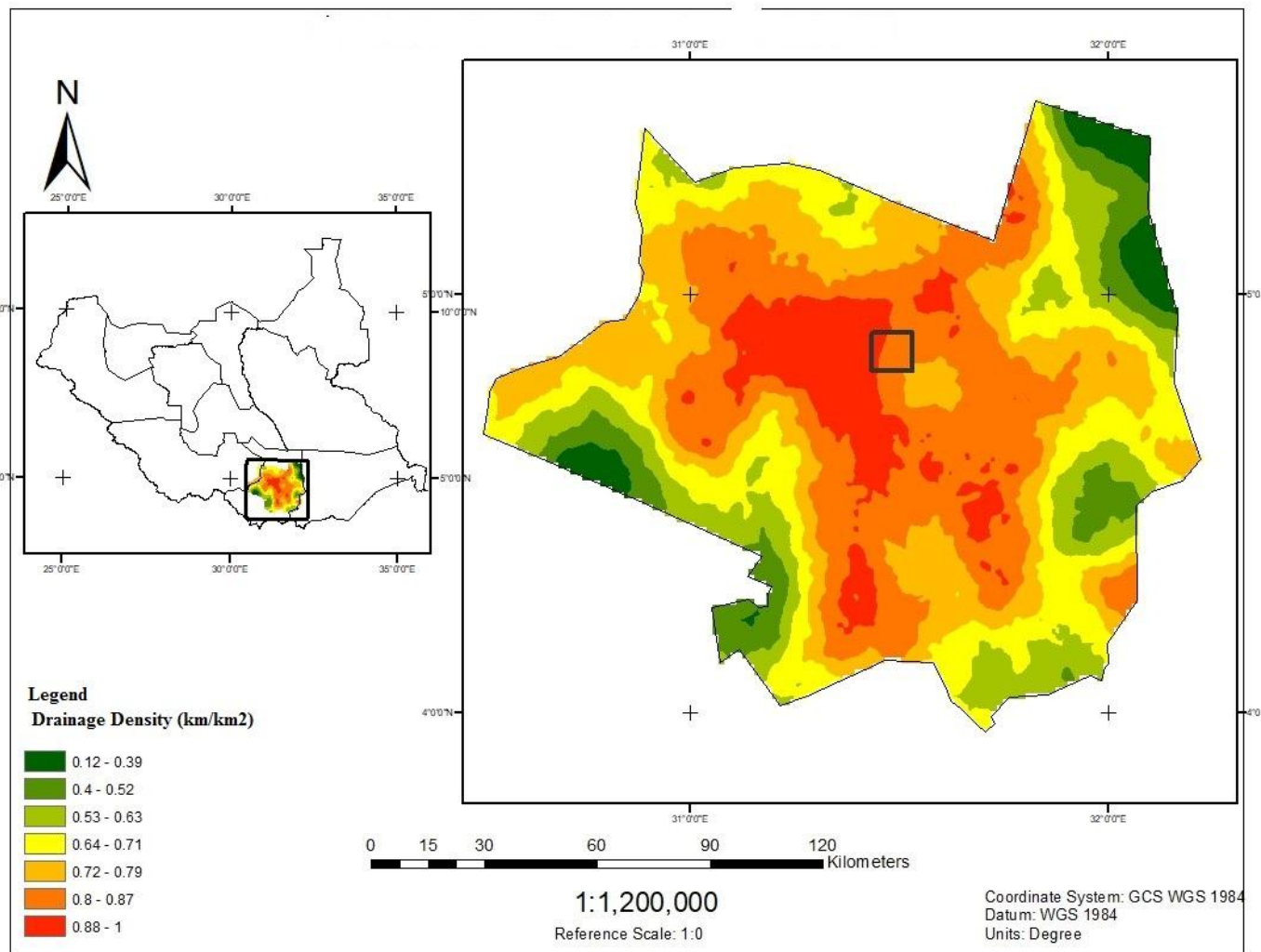


Figure 4.5: Drainage Density Map

4.1.5 Slope and DEM Map

Slope has great influence on runoff. It influences the infiltration of water from rainfall as well as surface water. The slope map was generated from DEM. The larger part of the study area was flat terrain except the western that was largely hilly with steep slope and was categorized into five groups (Fig 4.6 and Fig 4.7) i) very high slope, ii) high, iii) Moderate, iv) Low and v) very low. The larger part of the area lay between moderate, low and very low group. The area with minimum slope range was assigned highest rank because of the flat terrain whereas the one with maximum slope was given lowest rank because it had high rate of run-off that suggested the unavailability of groundwater.

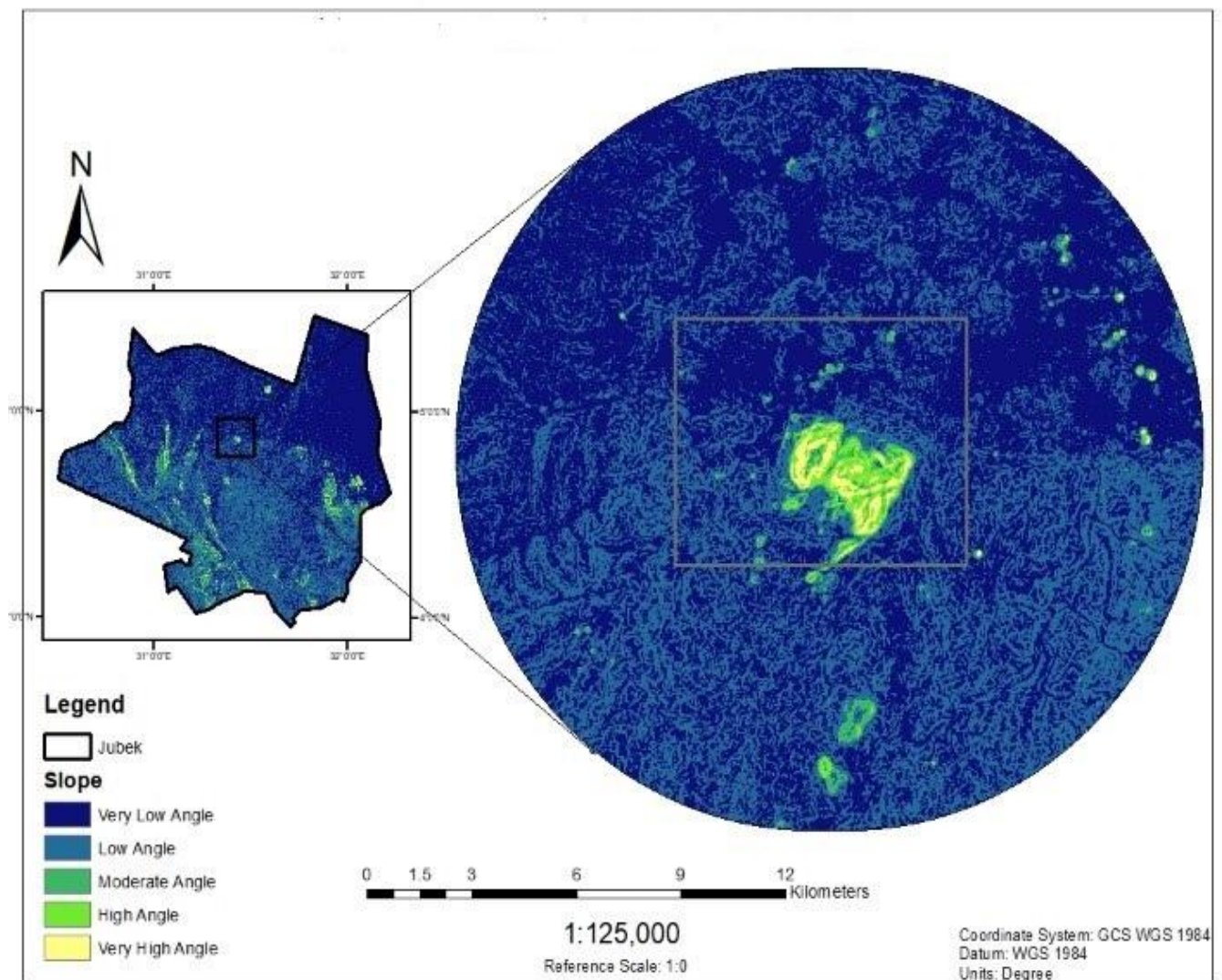


Figure 4.6: Slope map

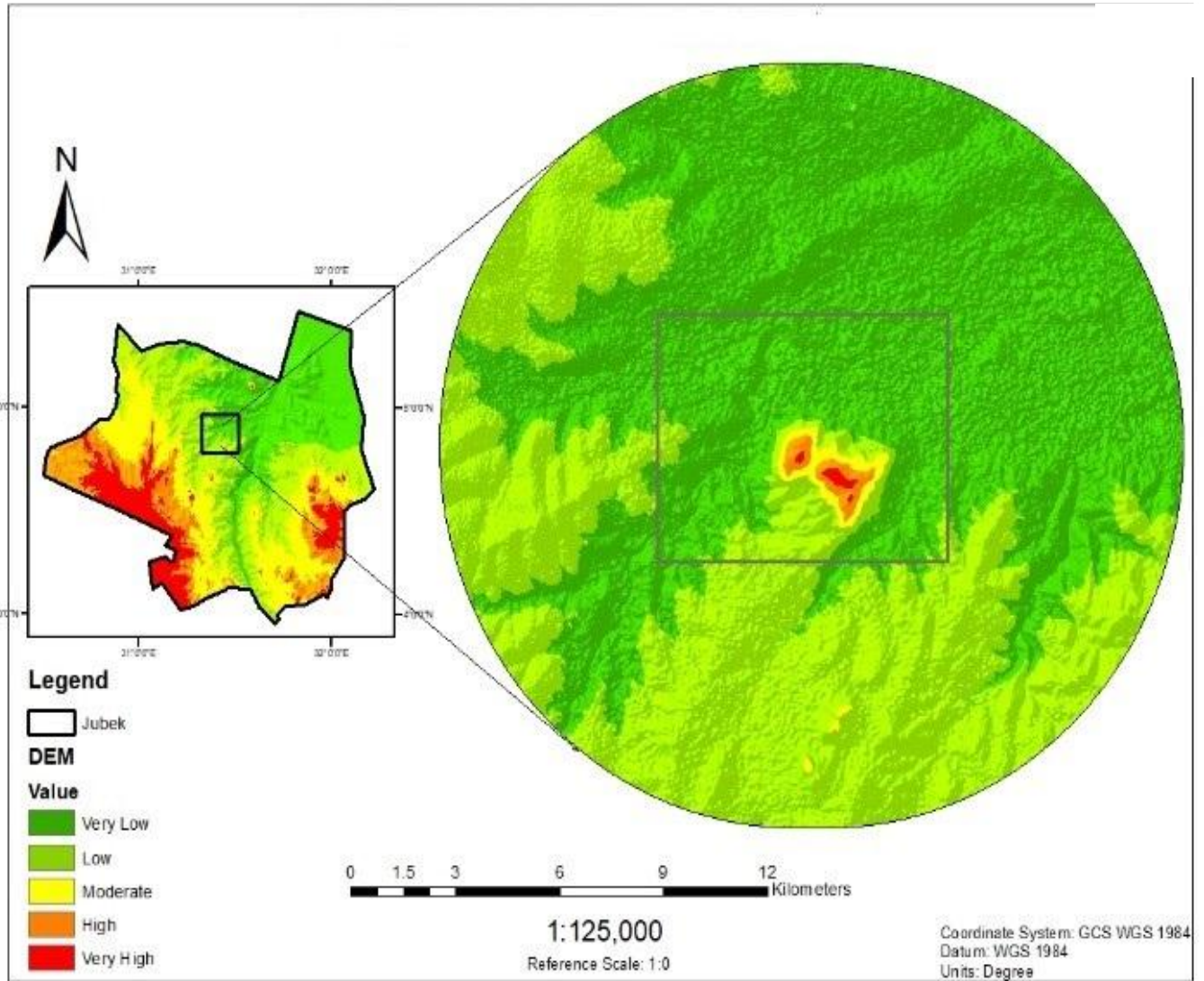


Figure 4.7: Drainage Density Map

4.1.6 Land Use Land Cover

Land use/land cover is a great significant in the exploration of groundwater. Because of this, the feature was evaluated in the analysis using thematic maps that were derived from remote sensing dataset. The map covering this element was prepared using a knowledge-based technique in conjunction with maximum likelihood classifier. The cover types identified in the analysis impacted the rate of recharge, evapotranspiration and run-off. The infiltration rate is proportional to vegetation cover; as a result, land use and cover were important in the analysis. An area with dense forest has high rate of infiltration and fewer run-offs. As such, it has high potential of groundwater. In contrast, an area without land cover has least rate of infiltration and more run-offs. Because of this it might not be rich in groundwater (Anbazhagan *at el.*, 2005; Rashid *at el.*, 2012). Water bodies play important roles in recharging the ground. Because of this water bodies and forests were assigned highest ranks in terms of groundwater potential throughout the analysis. Similarly, paddy and plantation fields tend to have excellent vegetation cover, which promote infiltration rate and reduce the rate of run-offs. Like in the above case, they were also assigned high ranks for groundwater potential. In contrast to the above, rocky areas and barren lands have low infiltration rates; as such, they were assigned least ranks. The land covered identified in the analysis included Tree cover area, shrub cover area, crop land, vegetation Aquatic, Lichen Mosses, Barren area, Built up area and open water bodies (Fig. 4.8).

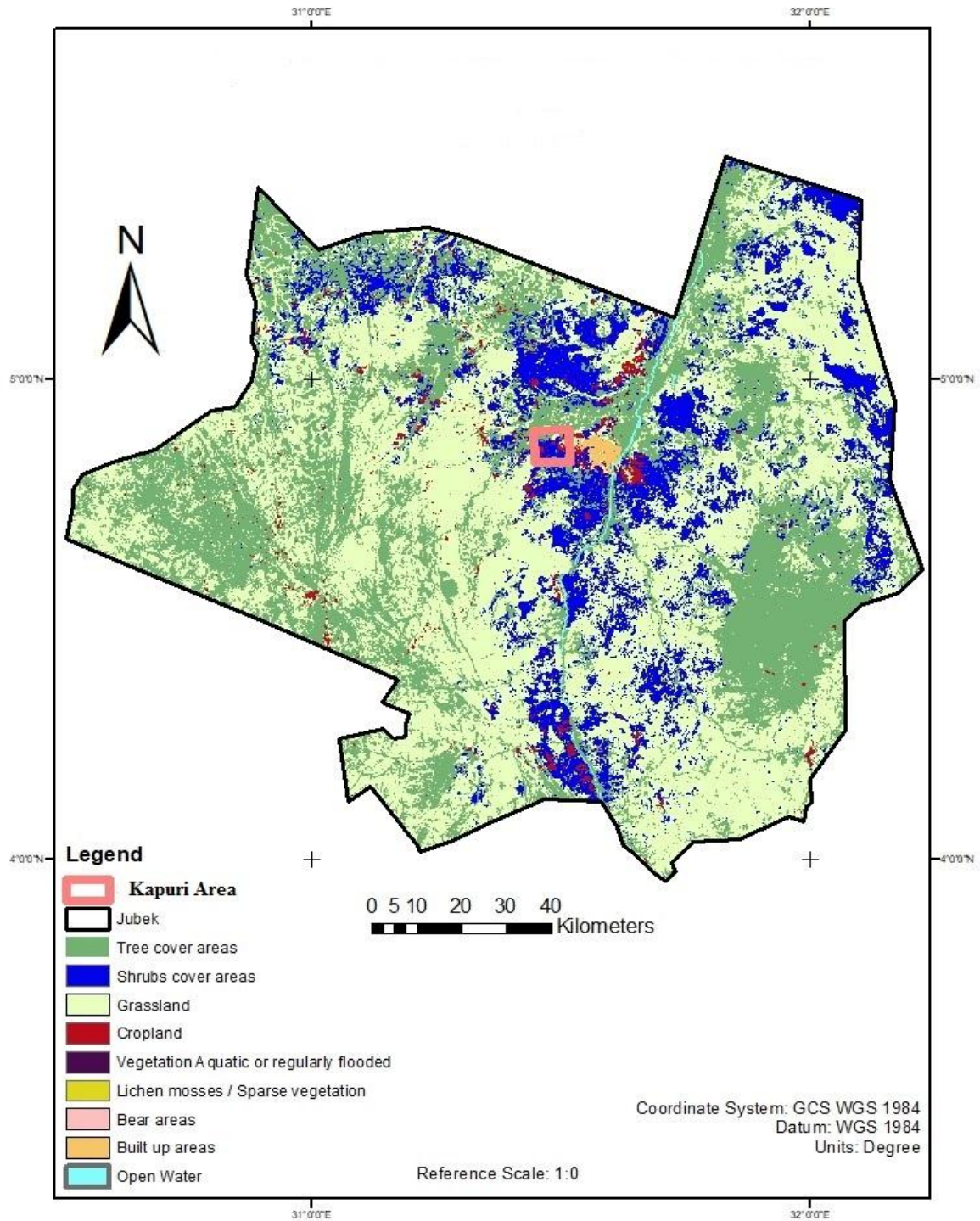


Figure 4.8: Land used Land cover Map

4.2 Verification of groundwater Potential Map using GIS and Remote Sensing.

4.2.1 Integration of Thematic Layers for modeling groundwater potential zone using GIS: (Weighted Index Overlay Model)

To help in identifying the areas with high rates of groundwater, thematic maps relating to lineament, geomorphology, drainage density, DEM, land use/ land cover and slope were developed via Spatial Analyst in ArcGIS. A map that was developed out of this analysis is provided in (Fig.4.9). The map was based on ranks and weights that were assigned to different features identified in the analysis and they were classified as i) Very good, ii) Good, iii) Good to Moderate, vi). Moderate, v) Moderate to poor, vi) poor and vii) Nil. The area with groundwater potential was identified as moderate out of the total area. Besides the above, the map provided the courses of streams, rivers, pediplains, alluvial plains, and sediments linked to lineaments that were identified of prospective areas for groundwater. The steep sloping areas that were underlain by gneiss were identified as poor because they did not provide traces of groundwater.

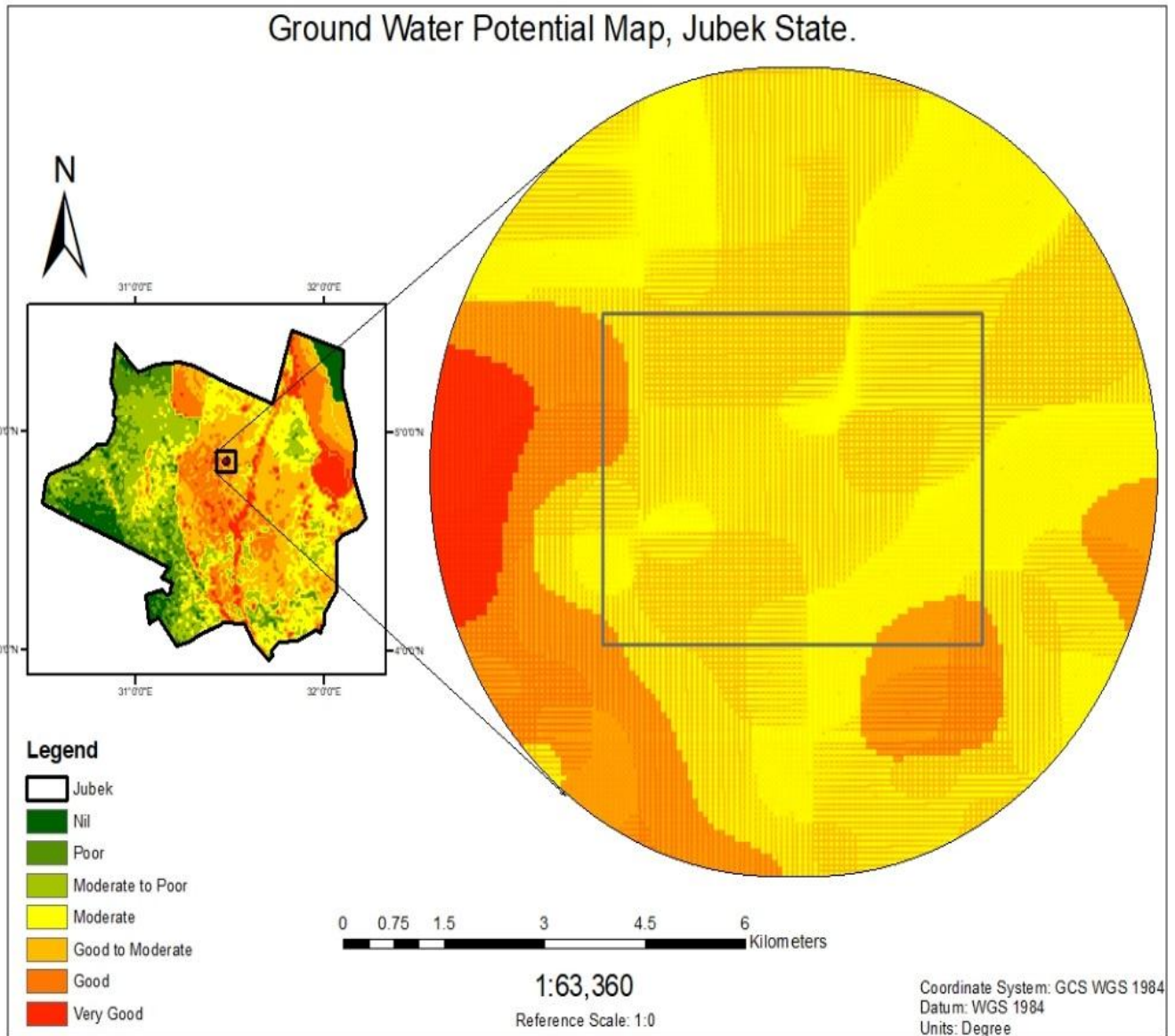
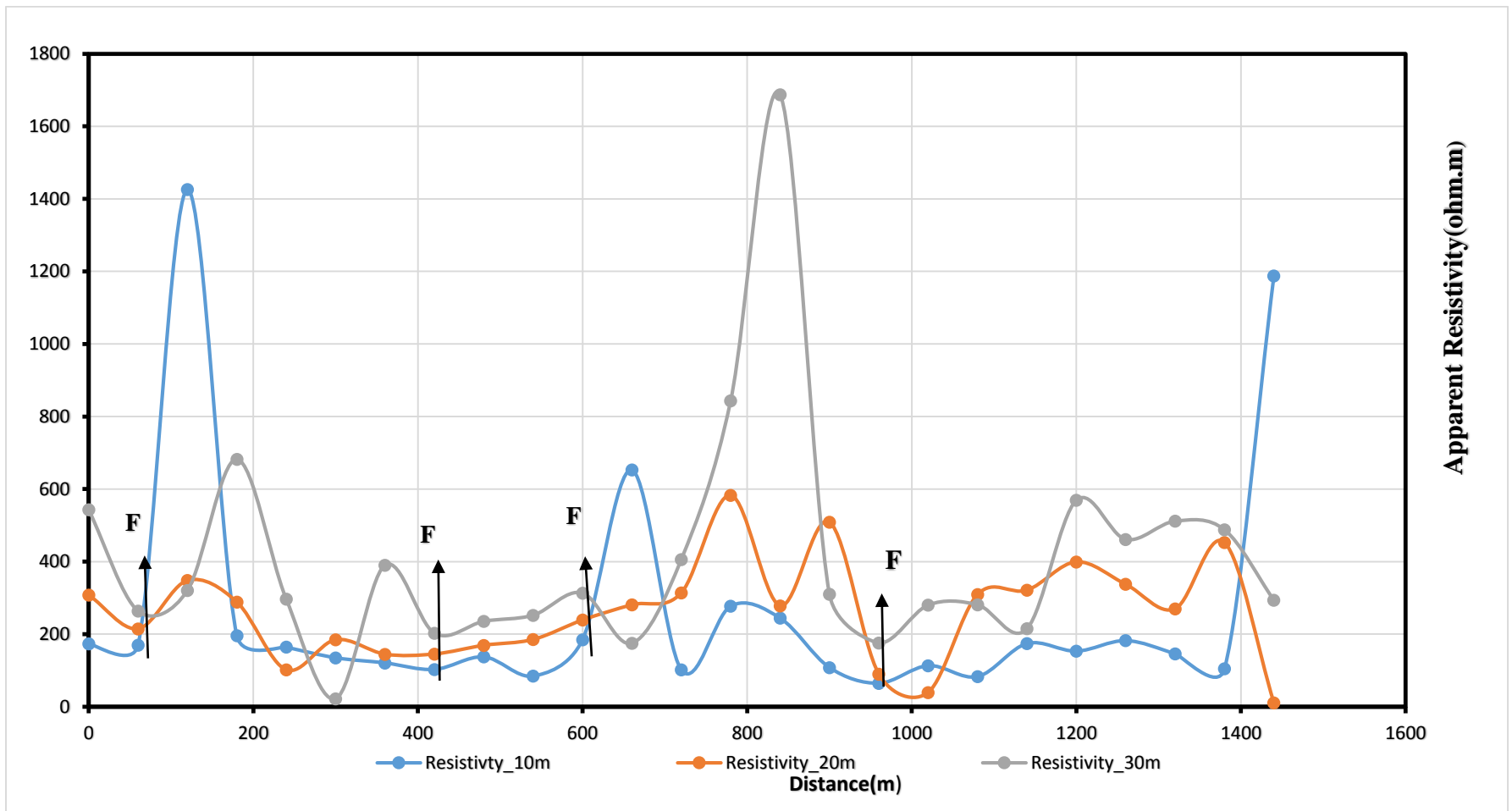


Figure 4.9: Groundwater potential map

4.3 Delineation thickness of aquifer as well as lateral extent from geophysical data

4.3.1 Profile I

Figure 4.10 present measured resistivity data along the profile the field. The pattern shows the point that was measured during the field work. Figure 4.10 depicts the measured apparent resistivity at the depth of 15m, 35m and 45m respectively which were carried out at the interval of 10m, 20m and 30m respectively. The figure (4.10) was generated through the use of Microsoft excel showing variation in resistivity throughout the area under investigation. Due to the geological nature of study area being a crystalline area, there are resistivity's values shows the subsurface structure of the study area. The profiling-I curve depicted a variation in resistivity throughout the Study area with low and high resistivity zones. The rate decreased suddenly between stations 4 to 13 (200m to 750m) with the resistivity ranges between 184 Ω .m to 313.19 Ω .m. At the interval of 10m which represent first layer of the subsurface structures, the resistivity is decreasing between stations 4 and 11(200m to 600m) and also between stations 13 and 24 (750m to 1420m) there resistivity ranges between 64.72 Ω .m to 195.54 Ω .m the resistivity value for the first layer indicate the topsoil moderate moisture. The second layer with resistivity value of 100 Ω .m to 500 Ω .m represents moderately fracture zone. The resistivity value between 200 Ω .m and 800 Ω .m indicates that the third layer is basement rock. Along the profile-I continues fracture have been identify and the point 2,8,11 and 17 with their resistivity ranges between 60 Ω .m to 300 Ω .m indicate the presence of fresh groundwater. Though the aquifer resistivity varies, it depends on the location where the study is being carried out.

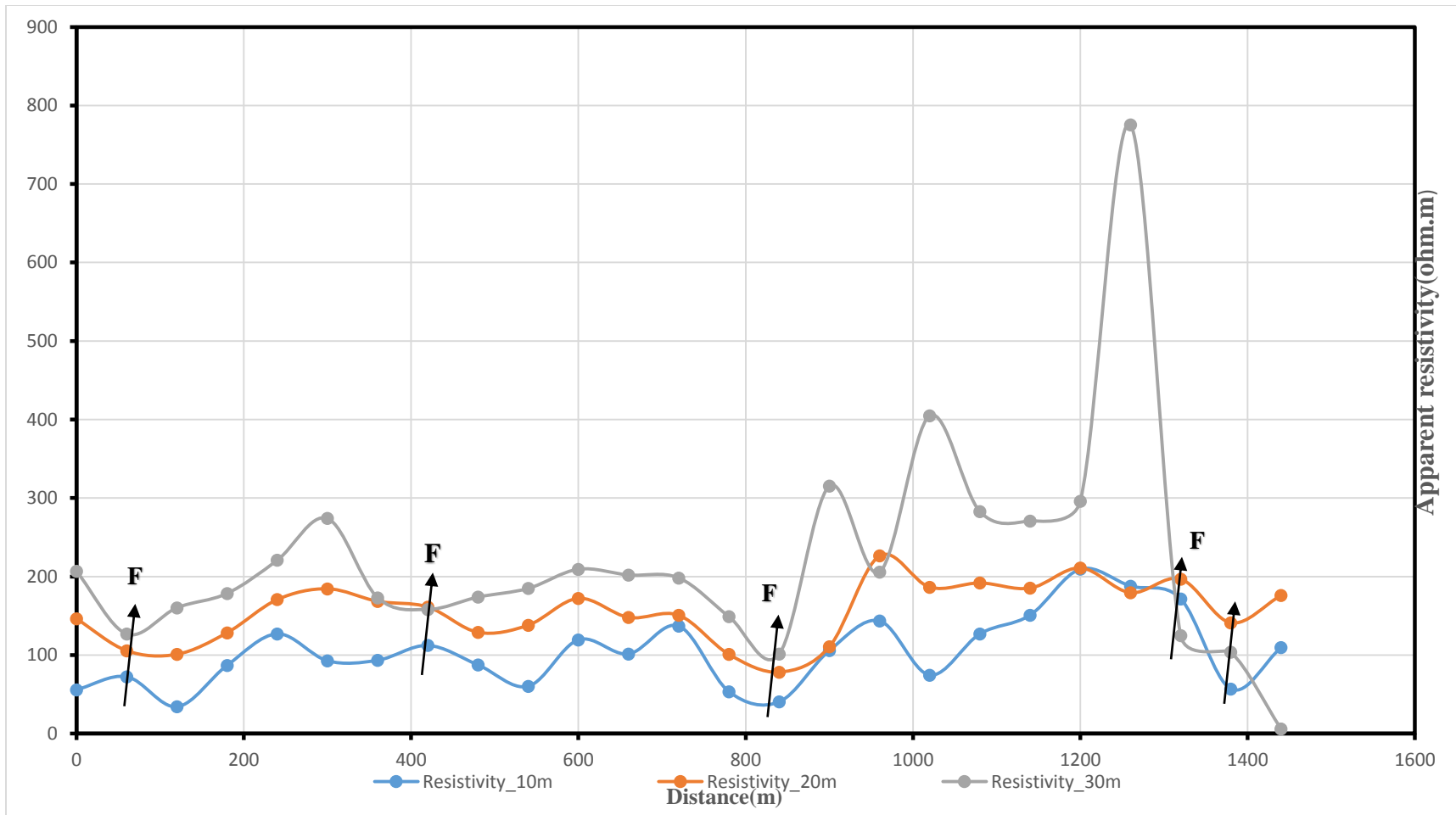


F= Fractures

Figure 4.10: profile N0.I

4.3.2 Profile II

The profile-II of the survey was positioned 500m horizontally to profile-I the pattern shows the point that was measured during the field work. Figure 4.11 shows the measured apparent resistivity at the depth of 15m, 35m and 45m respectively which were carried out at the interval of 10m, 20m and 30m respectively. From the result it indicates that top soil which is first layer is having approximate resistivity value that ranges between 55.81 Ω .m to 180 Ω .m. The second layer of this second profile has resistivity value ranges between 100.98 Ω .m to 190 Ω .m which indicates fractures zone. The resistivity value that ranges between 200 Ω .m to 400 Ω .m approximately represents basement which is third layer. Along the profile-II continues fracture have been identify at the point 2, 8, 12, 15 and 24 (100m, 410m, 820m, 1360m and 1380m) with their resistivity ranges between 40 Ω .m to 160 Ω .m indicate the presence of fresh groundwater .Looking at the two profiles carefully it will be observed that the resistivity values of profile's layers are similar and the fractures are continuous

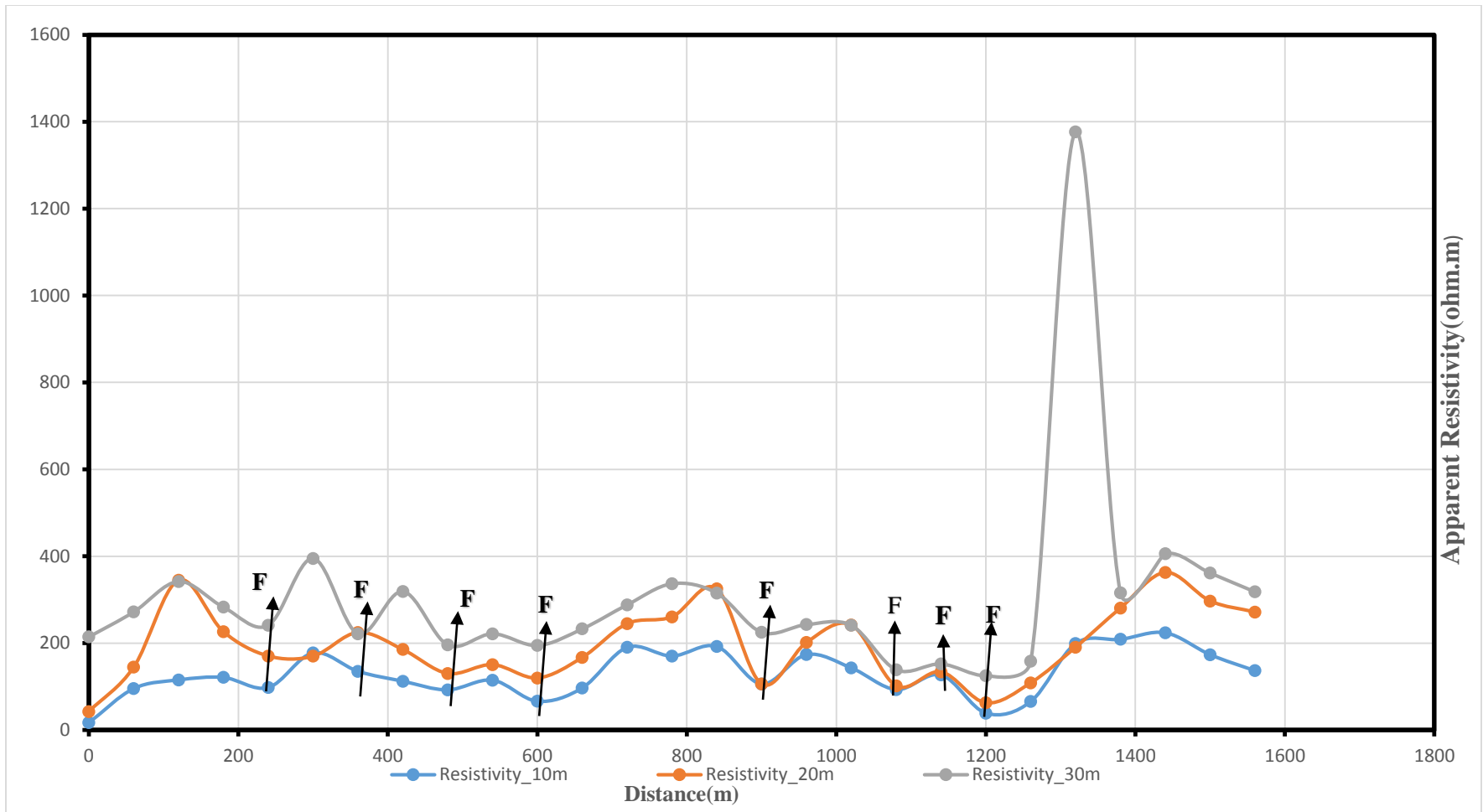


F= Fractures

Figure 4.11: Profile N0.II

4.3.3 Profile III

The profile-III of the survey was positioned 500m horizontally to profile-II the pattern shows the point that was measured during the field work. Figure 4.12 shows the measured apparent resistivity at the depth of 15m, 35m and 45m respectively which were carried out at the interval of 10m, 20m and 30m respectively. Preliminary review of the profile-III curve shows a variation in resistivity throughout the Study area with low and high resistivity zones. At the interval of 10m which represent first layer of the subsurface structures, the resistivity ranges between 10 Ω .m to 190 Ω .m the resistivity value for the first layer indicate the topsoil moderate moisture. The second layer with resistivity value of 40 Ω .m to 300 Ω .m represents moderately fracture zone. The resistivity value between 150 Ω .m and 300 Ω .m indicates that the third layer is basement rock. Along the profile-III continuous fracture zones have been identified at the point 5, 7,9,11,16,19,20 and 21 (240m,380m,500m,600m,900m,1100m1180m and 1200m), with their resistivity ranges between 30 Ω .m to 200 Ω .m indicate the terrain is partially or totally saturated with water.



F= Fractures

Figure 4.12: Profile N0.III

Figure 4.13: Cross section profile for all VES

4.4 3D Model showing groundwater potential zone

One hundred and ninety two (192) deep sounding using Schlumberger array were performed within the study area. The acquired field data and interpreted results are presented in tables, VES profile curves, geo-electric sections and 3D maps. Four geo-electric layers were interpreted applying both partial curve matching and computer software iterative technique. These layers correspond to the top soil, moderately weathered/fractured, fractured basement zone and fresh basement typical of the geological layering characteristics of the basement terrain. The geo electrical parameters interpreted from the 192 VES stations are present in Table 1. Four different curve types were interpreted; KH ($\rho_1 < \rho_2 > \rho_3 < \rho_4$), HA ($\rho_1 < \rho_2 > \rho_3 < \rho_4$), QH ($\rho_1 > \rho_2 > \rho_3 < \rho_4$), QA ($\rho_1 > \rho_2 > \rho_3 < \rho_4$), Q ($\rho_1 > \rho_2 > \rho_3$), A ($\rho_1 < \rho_2 < \rho_3$) and H ($\rho_1 > \rho_2 < \rho_3 < \rho_4$). The interpreted VES results were used to model the subsurface rock in 2-D geo-electric sections (Figure 4.13). The model gave insights into the geometry and thickness variation of the various lithologic units along the cross section. Four major layers that correspond comparatively to the top soil, clay, weathered/ fractured basement and fresh basement, typical of the four basic lithological units defined in basement hydrogeology were interpreted (Salami and Ogbamikhumi, 2017; Bayode *et al.*, 2005). It is observed that for more than 50% of the sounding points, the resistivity of the bedrock is not less than 5000 Ω m. As demonstrated by Salami and Ogbamikhumi, (2017) and Hazell, et al.,(1992)the bedrock can be described as incompetent and mostly fractured.

The first layer on the geo- electric section is the top soil characterized by clayey sand with resistivity value between 10.9-650.9 Ω m (Abiola *et al.*, 2013)) and thickness ranging between 0.19-2.35m. The second layer described as moderately weathered/fractures has resistivity values between 30- 500 Ω m and thickness between 2.5- 4.5m. The third layer is defined as the fractured basement, and constitutes the main potential aquifer in the study area, with resistivity values between 50 -450 Ω m, and thickness between 2.5 and 7m. The fourth layer is the fresh basement which extends to infinity into the subsurface. It has resistivity value between 600 - 10000 Ω m. This can extend to infinity with depth because of its crystalline nature (Figure 4.14)

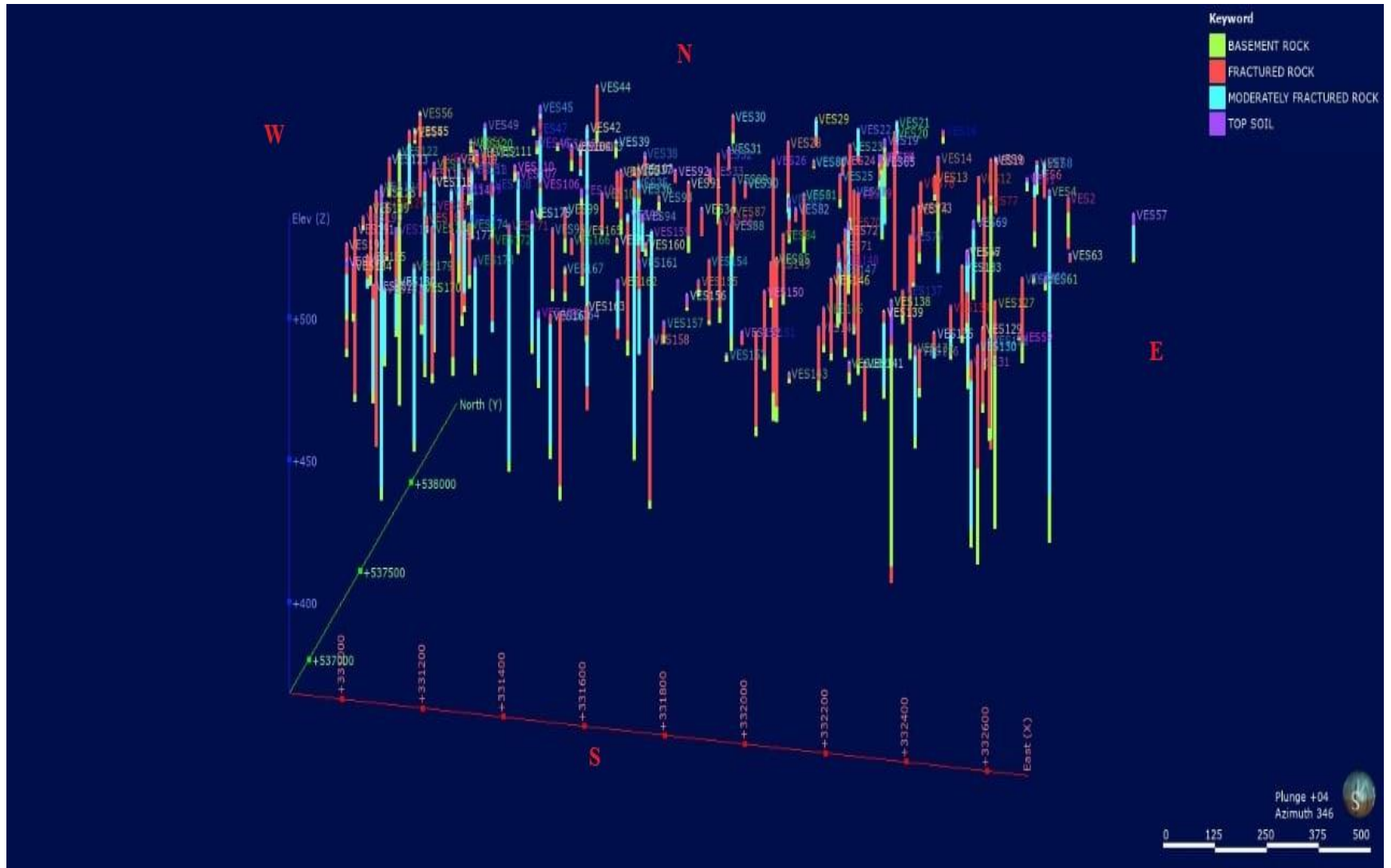


Figure 4.14: VES logs of Kapuri Area

4.4.1 3D resistivity Model for subsurface geological structures

The 3D image was generated using leapfrog software as shown in the figure (4.14, 4.15 and 4.16) below. In the 3D model the top layer as shown in the figure below having resistivity value ranges from 500Ωm to 1000Ωm with the average thickness of 0.45M and most part they are clearly seen because of the thin thickness. It's mainly composed of Sandy clay underlain by less resistive gneiss.

Normally, to establish an electrical resistivity scale, necessary to interpret the results. The result for geological formations that flourish in the site are as follows:

- Top soil resistivity ranges from 500Ωm to 1000Ωm.
- Moderately weathered rock resistivity ranges from 200Ωm to 500Ωm.
- Fractured rock resistivity ranges from 20Ωm to 100Ωm.
- Fresh basement rock resistivity ranges from 1000Ωm above.

Special care was given to the process of analyzing and interpreting the results especially to the horizons that were below 100Ω m. This reflected the presence of fractured rock formation that might accumulate underground water (Figure 4.15).

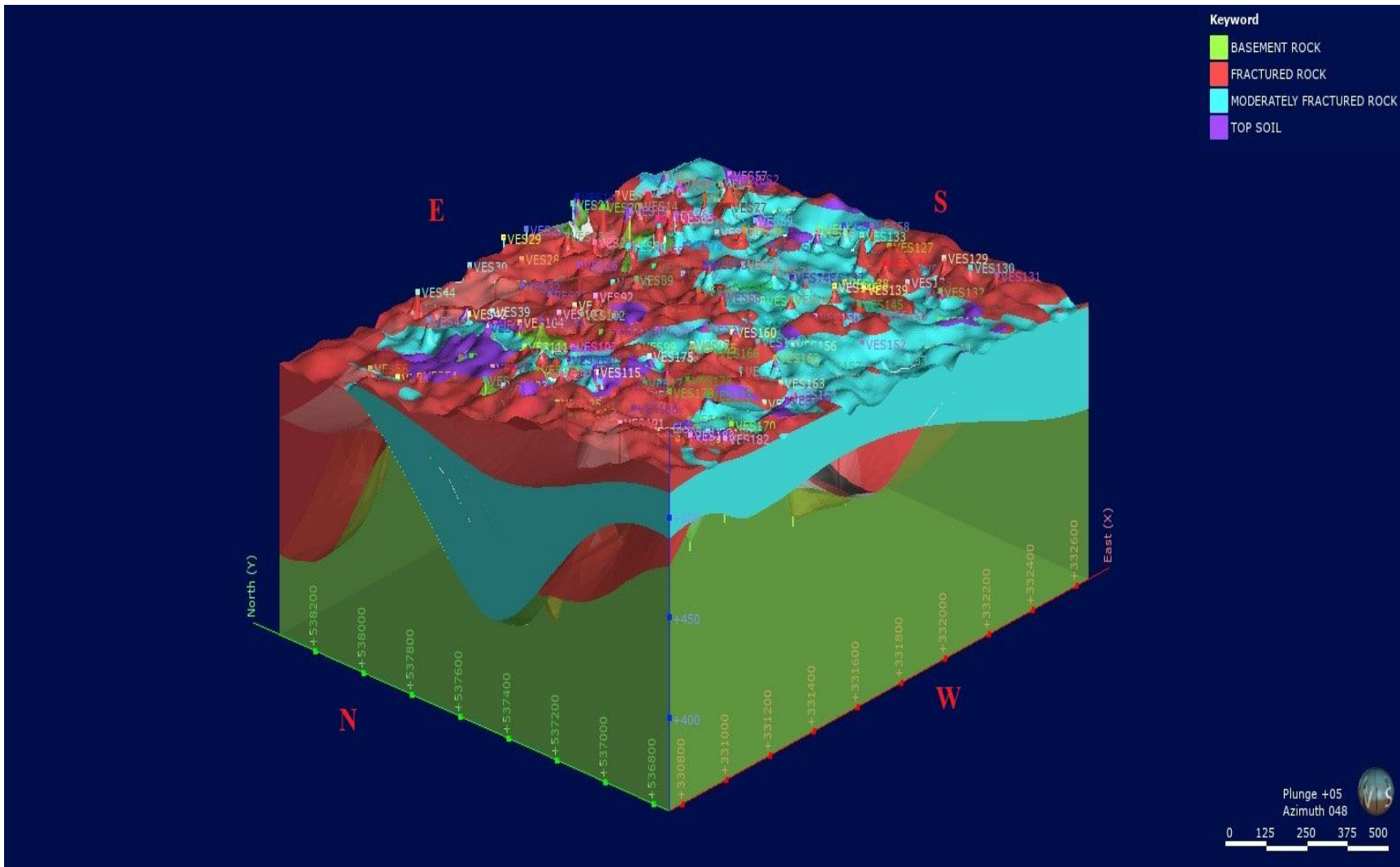


Figure 4.15: 3D Resistivity models showing North face of Kapuri Area

3D model Interpretation enable visualization of the resistant terrain evolution, from the sector's top part to the deepest zones, which are assumed to represent moderately fractured, fractured and basement rock. Moderately fractured and fractured rock is extend to eastern part of the study area overlaying the basement rock. The top soil is not clearly seen in the model because in most of the VES points it shows thin layer having a thickness of less than 1m. This model has proven the presence of moderately fractured and fractured rock only in the eastern and western part of the Kapuri area and the extension depth seems limited.

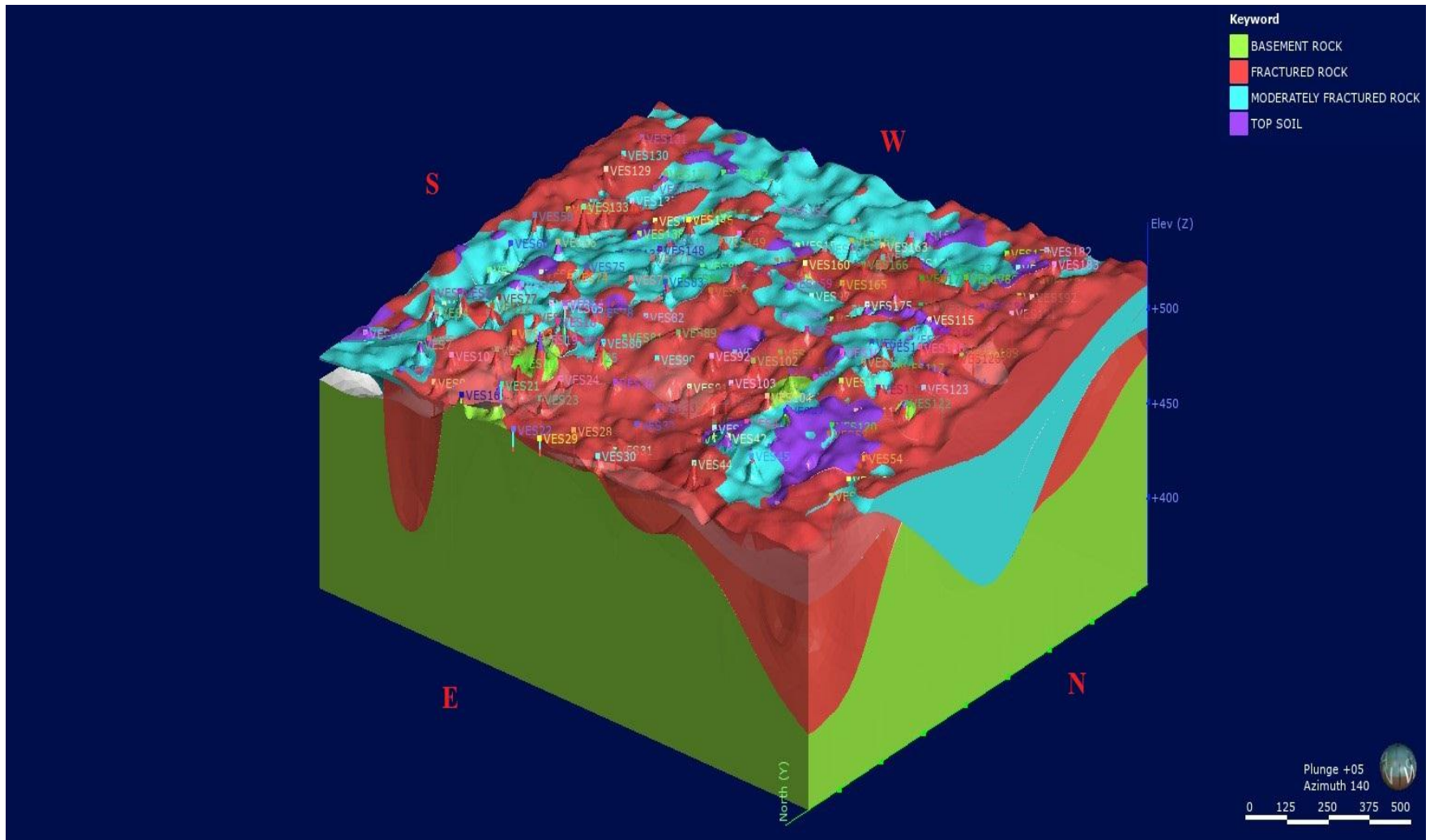


Figure 4.16: 3D Resistivity models showing south face Kapuri Area

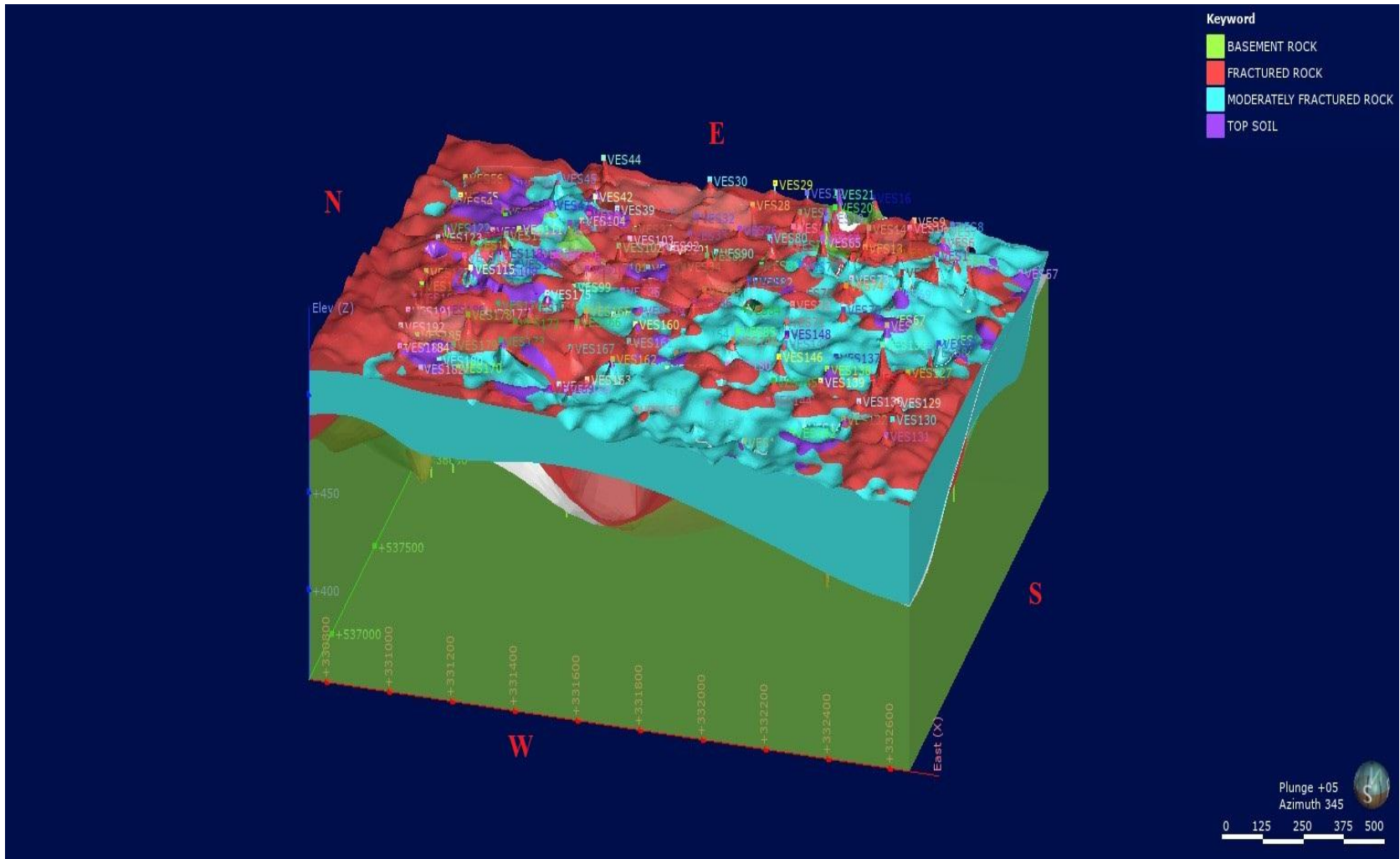


Figure 4.17: 3D Resistivity models showing East face Kapuri Area

CHAPTER FIVE

CONCLUSION AND RECOMMENDATION

5.1 Conclusion

This chapter concludes the study by summarizing the findings in line with the various objectives identified at the start of the study.

In this study, from the first objective it can be concluded that Kapuri area is located in zone with good potential for groundwater exploitation partly in the western and south eastern parts, while central and northern parts of the study area characterized by moderate to good groundwater prospects. It is further concluded that steep sloping mountains underlain by compact lithology and high drainage density are classified as poor prospective areas, while low drainage density, gently sloping area, stream courses, alluvial plains, pediplains, rivers, and with associated lineaments are identified as good prospective zones.

The horizontal profiling results identified numerous fractured zones along the profile, while the three level probe depth (15m, 15m, 35m and 45m) determined the continuity of these fractures with depth. It is concluded for the fractured zones spanning all the probed depths mark local aquifers.

The 3D geo-electrical model indicates that the area is underlain by four geologic section which include top soil (sandy clay), moderately weathered, fractured and fresh basement. Moderately weathered material ranging from less than one meter to several meters in thickness separate the overburden from the underlying weathered and fractured bedrock, while the basal layer is comprised of compact and massive fresh basement. The fractured and the moderately weathered rock make up the aquiferous zone within the study area.

5.2 Recommendation

Results obtained from the present study is a baseline for further geophysical investigation. Drilling should be carried out in fractured zone. It is recommended that 2D and 3D electrical resistivity imaging be carried out for mapping fractured at higher resolution.

REFERENCES.

- Abdullahi, N. K., Udensi, E. E., Iheakanwa, A., and Eletta, B. E. (2018). Geo-electrical Method Applied to Evaluation of Groundwater Potential and Geo-electrical Method Applied to Evaluation of Groundwater Potential and Aquifer Protective Capacity of Overburden Units. *British Journal of Applied Science & Technology*, 4(14):pp 2024–2037.
- Abiola, O., Ogunribido T. H. T., Omoniyi B. A., and Ikuepamitan, O. (2013). Geoelectric Assessment of Groundwater Prospects in. *Geosciences*, 3(1), 23–3. <https://doi.org/10.5923/j.geo.20130301.03> ,17.Nov.2019.
- Agarwal, R., and Garg, P. K. (2016). Remote sensing and GIS based groundwater potential and recharge zones mapping using multi-criteria decision making technique. *Water Resour. Manage.* 30, 243–260.
- Amin, S. (2006). Use of remote sensing and GIS to determine recharge potential zones: the case of Occidental Lebanon. *Hydrogeol J*, 14:, 433–443.
- Abiola O., Ogunribido T. H. T., Omoniyi B. A., I. O. (2013). Geoelectric Assessment of Groundwater Prospects in. *Geosciences*, 3(1), 23–33. <https://doi.org/10.5923/j.geo.20130301.03>
- Agarwal, R., and Garg, P. K. (2016). Remote sensing and GIS based groundwater potential and recharge zones mapping using multi-criteria decision making technique. *Water Resour. Manage.* 30, 243–260.
- Aghakouchak, A. (2014). A multivariate approach for persistence-based drought prediction : Application to the 2010 – 2011 East Africa drought. *JOURNAL OF HYDROLOGY*. <https://doi.org/10.1016/j.jhydrol.2014.09.063>
- Alabi, A.A; Bello, A. S. O., and Oyerinde, H. O. (2010). Determination of groundwater potential in Legos state university,Ojo,Using geoelectric methods(vertical electrical sounding and Horizontal profile Report opinoin,24: 68-75.
- Alile, O. M, and Amadasun, C. (2008). Direct Current probing of the Subsurface Earth for Water Bearing Layer in Oredo Local Government Area, Edo State, Nigeria. *Nig. J. Appl. Sci.*, 25: 107–116.
- Amajor, L.C., and Ofoegbu, C. (2007). Determination of polluted aquifers by stratigraphically controlled biochemical mapping; Examples of the eastern Niger Delta, Nigeria,

- Groundwater and mineral resources of Nigeria,. *Vieweg, Braunschweig/Wiesbaden*, pp62–73.
- Anbazzhagan, S., Ramasamy, S. M., & Gupta, D. S. (. (2005). Remote sensing and GIS for artificial recharge study,runoff estimation and planning in Ayyar basin, Tamil Nadu, India. *Environmental Geology*, 48, 158–170.
- Anomohanran, O. (2011). Underground water exploration of Oleh , Nigeria using the electrical resistivity method. *Scientific Research and Essays*, 6(20), 4295–4300.
- Anornul, G. K., Kabo-bah, A. T. and Anim-Gyampo, M. (2012). Evaluation of Groundwater Vulnerability in the Densu River Basin of Ghana. *American Journal of Human Ecology, Volume 1, .*
- Awawdeh, M., Obeidat, M., and Al-mohammad, M. (2013). Integrated GIS and remote sensing for mapping groundwater potentiality in the Tulul al Ashaqif , Northeast Jordan. <https://doi.org/10.1007/s12517-013-0964-8>
- Awomeso, A., Orebiyi, O., and Oyedokun, O. (2008). Geophysical investigations for groundwater exploration in a crystalline basement, southwest Nigeria. *New York Science Journal*, 1(4), 19–35.
- Bala, A. N., Ike, E. C (2001). The aquifer of the crystalline basement rocks in Gusau area, North-western Nigeria. *J. Min. Geol.*, 37(2), 177–184.
- Barten, P. K. (2006). Overveiw of forest hydrology and forest management effects. Sustainable Forest Management Network – Hydro-Ecological Landscapes. In *Project Workshop, Amherst, Massachusetts: University of Western Ontario*,.
- Battaglin W., Ltay, L., and Parker R, L. G. (1993). Applications of a gis for modeling the sensitivity of water resources to alternations in climate in the gunnisan river basin, Colorado. *Water Resour Bull, Am Water Res Assoc*, 25(6):1021–1028.
- Bayode, S., Ojo, J. S., and Olorunfemi, M. O. (2005). Geoelectric characterisation of aquifer types in the Basement Complex of part of Osun State, Nigeria. *Global Journal of Pure and Applied Sciences.*, 12, 377–385.
- Berhe, S. M. (1991). Tectonic Evolution of the Pan-African Mozambique Belt in NE and E Africa: In *Extended Abstract International Field Geotraverse /Workshop through The Mozambique Belt. Tanzania July 23-August 6, 1991*.
- Bhimasankaram, V.L. S, and Gaur, V. k (1977). Lectures on exploration Geophysicists,

- geophysics for geologists and engineers. *Assoc Explor Centre Explor Geophys, Hyderabad, India.*
- Bruijnzeel, L. A. (2004). Hydrological functions of tropical forests: Not Seeing the Soil for Trees. *Agriculture, Ecosystems and Environment*, 104(1), 185–228.
- Cardimona, S. (2008). 2008. Electrical Resistivity Techniques for Subsurface Investigation. *Department of Geology and Geophysics, University of Missouri-Rolla, Rolla, MO.*
- Chowdhury, A., Jha, M.K., Chowdary, V.M. and Mal, B. C. (2009). “Integrated Remote Sensing and GIS-Based Approach for Assessing Groundwater Potential in West Mednipur District, West Bengal, India. *International Journal of Remote Sensing*, 30, pp. 231–250.
- Clark, L. (1985). Groundwater abstraction from Basement Complex areas of Africa Lewis Clark, 18, 25–34.
- Coker, J.O (2012). Vertical electrical sounding (VES) methods to delineate potential groundwater aquifers in Akobo area, Ibadan, South-western, Nigeria. *Journal of Geology and Mining Research*, Vol. 4(2), pp. 35–42.
- Dahab, A. H. (2012). Geoelectric investigation of groundwater potential in Khor Abu Habil drainage basin. *Journal of Science and Technology*, 13(2).
- Dar IA, Sankar K, D. M. (2010). Deciphering groundwater potential zones in hard rock terrain using geospatial technology. *Environ Monit Assess*, 173, 597–610.
- Das, S., Behera, S.C., kAr, A., Narendra, P. and Guha, S. (1997). Hydrogeomorphological mapping in groundwater exploration using remotely sensed data – A case study in Keonjhar district in Orissa. *Journal of Indian Society of Remote Sensing*, 25, pp. 247–259.
- Deane and Mohamed. (1960). The mineral deposit of Sudan. *Hunting Technical service, Rept (Unpublished).*
- Dobrin, M. B., and King, F. R. (1976). Introduction to Geophysical prospecting. *McGraw-Hill Book, New York*, p. 630.
- Edet, A.E. (1998). Application of remote sensing data to groundwater exploration: a case study of the Cross River State, south-eastern Nigeria. *Hydrogeology Journal*, 6 (3), 394–404.
- Egai, A.O., and Imasuen, O. I. (2013). Geo-electric Characterization of Subsurface crude oil

- Leachate plume in Aguobiri, Southern Nigeria. *Research Journal of Engineering and Applied Sciences (RJEAS) Seattle USA, Vol 2 (6)*, pp. 427–433.
- Egai, A. O. (2013). Environmental impacts of crude oil activities in Aguobiri, Southern Ijaw LGA, and Bayelsa State. *Unpublished M.Sc. Thesis University of Benin, Nigeria*.
- Elmahdy, S.I., and Mohamed, M. M. (2015). Probabilistic frequency ratio model for groundwater potential mapping in Al Jaww plain, UAE. *Arabian. J. Geosci.*, 8, 2405–2416.
- Elzein, M. (2007). Geoelectrical and hydrogeological characteristics of the groundwater aquifers in the Gezira area, Central Sudan. *Unpublished Doctoral Dissertation, University of Khartoum*.
- Fashae, O. a., Tijani, M. N., Talabi, A. O., and Adedeji, O. I. (2013). Delineation of groundwater potential zones in the crystalline basement terrain of SW-Nigeria: an integrated GIS and remote sensing approach. *Applied Water Science*, 4(1), 19–38. <https://doi.org/10.1007/s13201-013-0127-9>
- Fashae, O. A., Tijani, M. N., Talabi, A. O., and Adedeji, O. I. (2014). Delineation of groundwater potential zones in the crystalline basement terrain of SW-Nigeria : an integrated GIS and remote sensing approach, 19–38. <https://doi.org/10.1007/s13201-013-0127-9>
- Fronlch, R.K., Urish, D.W., Fuller, J., and Reilly, M. (1994). Use of geoelectrical method in groundwater pollution surveys in coastal environment. *Journal of Applied Geophysics*, 32, 139–154.
- Garhi, M. (2013). Integrating Remote Sensing and GIS for Identification of Groundwater Prospective Zones in the Narava Basin , Visakhapatnam Region , Andhra Pradesh, 81, 248–260.
- Gressando, Y. (1999). Application of geophysical techniques for groundwater investigation in Lake Naivasha area, Kenya. *Unpublished Doctoral Dissertation University of Khartoum*.
- Gumma, M. K., and Pavelic, P. (2013). Mapping of groundwater potential zones across Ghana using remote sensing , geographic information systems , and spatial modeling, 3561–3579. <https://doi.org/10.1007/s10661-012-2810-y>
- Gupta, M., and Srivastava, P. K. (2010). Integrating GIS and remote sensing for

identification of groundwater potential zones in the hilly terrain of Pavagarh, Gujarat, India. *Water International*, 35(2), 233–245.

<https://doi.org/10.1080/02508061003664419>

Gustavsson, M., Kolstrup, E., and Seijmonsbergen, A. C. (2006). A new symbol and GIS based detailed geomorphological mapping system: renewal of a scientific discipline for understanding landscape development. *Geomorphology*, 77, 90–111.

Hamil, L and Bell, F. (1986). Groundwater Resources Development. *John Wiley & Sons.*, PP.133 – 210.

Harinarayana, P., Gopalakrishna, G.S. and Balasubramanian, A. (2000). Remote sensing data for ground water development and management in Keralapura watersheds of Cauvery basin, Karnataka, India. *The Indian Mineralogists*, 34, pp. 11–17.

Hazell, J. R. T; Cratchley, C. R and Jones, C. R. C. (1992). The hydrogeology of crystalline aquifers in northern Nigeria and geophysical techniques used in their exploration. *Geological Society, London, Special Publications*, 66(1):, 155–182.

Heath, R. C. (1987). Basic Ground-Water Hydrology, North Carolina: United States Geological Survey.

Holmes, A. (1951). The sequence of Precambrian Orogenic belts in South and Central Africa. *18th Int. Geol. Congr., London, 1948*, 4, pp. 254–269.

Horton, R. E. (1932). Drainage basin characteristics. *Transactions of the American Geophysical Union*, 13, 350–361.

Hunting Geology and Geophysics Limited, Elstree Way, Boreadamwood, Hertfordshire, E. (n.d.). Exploration-Juba Area.pdf.

Islam, S., and Susskind, L. (2015). Understanding the water crisis in Africa and the Middle East: How can science inform policy and practice?

<https://doi.org/10.1177/0096340215571906>

Issah, M. M. (2015). Geophysical investigation for groundwater in the tain district of the brong ahafo region of ghana using the 2d Cves Method By Mohammed Mansuru Issah B . Sc . Physics (Hons) A Thesis Submitted to the Department of Physics , Kwame Nkrumah University of Sc.

Jaiswal, R.K., Mukherjee, S., Krishnamurthy, J. and Saxena, R. (2003). Role of remote sensing and GIS techniques for generation of groundwater prospect zones toward rural

development – an approach. *International Journal of Remote Sensing*, 24, pp. 993–1008.

- Jatau, B. S., and Agelaga, A. G. (2013). Groundwater Investigation in Parts of Kaduna South and Environs using Wenner Offset Method of Electrical Resistivity Sounding. *Journal of Earth Sciences and Geotechnical Engineering*, 3(1), 41–54.
- Jha, M.K., Chowdary, V., and Chowdhury, A. (2010). Groundwater assessment in Salboni Block, West Bengal (India) using remote sensing, geographical information system and multi-criteria decision analysis techniques. *Hydrogeology Journal*, 18 (7), 1–16.
- Kanta, L., Jha, M. K., and Chowdary, V. M. (2018). Assessing the accuracy of GIS-based Multi-Criteria Decision Analysis approaches for mapping groundwater potential. *Ecological Indicators*, 91(August 2017), 24–37.
<https://doi.org/10.1016/j.ecolind.2018.03.070>
- Kearey, P., Michael, B., and Ian, H. (2002). *An Introduction to Geophysical Exploration. third ed.:Blackwell Science Ltd.*
- Keller, G.V and Frischknecht, F. C. (1966). *Electrical Methods in Geophysical Prospecting.* Pergamon, Oxford, UK.
- Korford, G. D., (1979). *Geosounding principles, resistivity sounding measurements.* Elsevier, New York.
- Krishnamurthy J, S. G. (1995). Role of geological and geomorphological factors in ground water exploration: a study using IRS LISS data. *Int J Remote Sens* 16:2595–2618.
- Kumar, P. K., Gopinath, G., and Seralathan, P. (2007). Application of remote sensing and GIS for the demarcation of groundwater potential zones of a river basin in Kerala, southwest coast of India. *International Journal of Remote Sensing*, 28(24), 5583–5601.
- Kumar, P. K. D., Gopinath, G., and Seralathan, P. (2007). International Journal of Remote Application of remote sensing and GIS for the demarcation of groundwater potential zones of a river basin in Kerala , southwest coast of India, (August 2014), 37–41.
<https://doi.org/10.1080/01431160601086050>
- Kuria D, Gachari M, and Macharia M, M. E. (2012). Mapping groundwater potential in Kitui District, Kenya using geospatial technologies. *Int J Water Res Environ Eng* 4(1):15–22.
- Kumar, R. V. (2012). Remote Sensing and GIS in Identification of Groundwater Potential Zones : A Study at Thirumullaivasal Village , Nagapattinam District , 173, 2776–2779.

- <https://doi.org/10.4028/www.scientific.net/AMM.170-173.2776>. 12.Nov.2018.
- Lillesand T. M., and Kiefer, R. (2000). Remote sensing and image interpretation. *Wiley, New York*.
- Loke, M. (2001). Tutorial: 2-d and 3-d electrical imaging surveys. Copyright (1996-2012).
- Loke, M. H. (1997). Electrical imaging surveys for environmental and engineering studies, A practical guide to 2D and 3D survey, Short Training Course Lecture Note..
- Lowrie, W. (2007). Fundamentals of Geophysics. *Second Edition Ed. Zürich : Cambridge University Press*.
- Lucy, M., Willis, A., John, G., and Hezekiah, C. (2016). Geophysical Investigation and Characterization Of Groundwater Aquifers In Kangonde Area , Machakos County In Kenya Using Electrical Resistivity Method . *Journal of Applied Geology and Geophysics*, 4(2), 23–35. <https://doi.org/10.9790/0990-0402012335>
- Macdonald, A. M., Davies, J., and Peart, R. J. (2001). Geophysical methods for locating groundwater in low permeability sedimentary rocks : examples from southeast Nigeria. *Journal of African Earth Sciences.*, 32(1), 115–131.
- Machiwal, D., Rangi, N., and Sharma, A. (2014). Integrated knowledge- and data-driven approaches for groundwater potential zoning using GIS and multi-criteria decision making techniques on hard-rock terrain of Ahar, (Cgwb 2011). <https://doi.org/10.1007/s12665-014-3544-7>
- Mandal, U., Sahoo, S., Munusamy, S.B., Dhar, A., Panda, S.N., Kar, A., Mishra, P. K. (2016). Delineation of groundwater potential zones of coastal groundwater basin using multicriteria decision making technique. *Water Resour. Manage.*, 30, 4293–4310.
- Mbonu, P.D.C., Ebeniro, J. Ofoegbu, C., and Ekine, A. (1991). Geo-electric sounding for the determination of aquifer characteristics in parts of the Umuahia area of Nigeria. *Geophysics*, 56;, 284–291.
- Melton, M. A. (1957). An analysis of the relations among the elements of climate, surface properties, and geomorphology. *Technical Report 11. New York: Department of Geology, Columbia University*.
- Milsom, J. (2003). *Field Geophysics. THIRD EDITION ed. The Atrium, Southern Gate, Chichester: John Wiley & Sons Ltd*.
- Mogaji, K. A., Aboyeji, O. S., and Omosuyi, G. O. (2011). Mapping of lineaments for

groundwater targeting in the basement complex region of Ondo State , Nigeria , using remote sensing and geographic information system (GIS) techniques, 3(August), 150–160.

- Mohammed, O. (1960). Geology, hydrology and Minerals occurrence in Southern Region. *Unpublished Rept. Geo.Min Resources department., Ministry of Industry and Mining, Khartoum.*
- Muchingami, I., Hlatywayo, D. J., Nel, J. M., and Chuma, C. (2012). Electrical resistivity survey for groundwater investigations and shallow subsurface evaluation of the basaltic-greenstone formation of the urban Bulawayo aquifer. *Physics and Chemistry of the Earth*, 50-52(January 2017), 44–51. <https://doi.org/10.1016/j.pce.2012.08.014>
- Mukund, B., Patil, V., Bhaskarrao, J., and Aarti, B. (2017). Comparative study of Wenner and Schlumberger electrical resistivity method for groundwater investigation : a case study from Dhule district (M . S .), India. *Applied Water Science*. <https://doi.org/10.1007/s13201-017-0576-7>
- Murasingh, S. (2014). Analysis of Groundwater Potential Zones Using Electrical Resistivity , Rs & Gis Techniques in a Typical Mine Area of Odisha.
- Murthy K.S.R. (2000). “Groundwater Potential in a Semi-Arid Region of Andhra Pradesh: A Geographical Information System Approach. *International Journal of Remote Sensing*, vol. 21, n, pp. 1867–1884.
- Mwega, B. W. (2016). Geo-Electric Investigation of the Aquifer Characteristics and Ground Water Potential Of The Lake Chala Watershed, Taita Taveta County.
- Nag, S. K. (2005). Application of lineament density and hydrogeomorphology to delineate groundwater potential zones of Bagmundi block in Purulia district, West Bengal. *Journal of Indian Society of Remote Sensing*, 33 (4), 522–529.
- Nicola, M. and Van-de Giesien, N, (2005). Spatial Distribution of Groundwater Production and Development Potential in the Volta River basin of Ghana and Burkina Faso. *International Water Resources Association, June, Volume 30* , p. 239–249.
- Okiongbo, K. S., and Akpofure, E. (2012). Determination of Aquifer Properties and Groundwater Vulnerability Mapping Using Geoelectric Method in Yenagoa City and Its Environs in Bayelsa State , South South Nigeria, 2012(June), 354–362.
- Osej, J. O., Asokhai, M. B. and Okolie, E. C (2006). Determination of groundwater potential

in Obiaruku and Environs Using surface geoelectric sounding.

- Owen, R. J., Gwavava, O. and Gwaze, P. (2005). Multi-electrode resistivity survey for groundwater exploration in the Harare greenstone belt, Zimbabwe. *Hydrogeology Journal*.
- Owor, M., Batte, A. G., and Muwanga, A., and Sigrist, P. W (2008). Vertical electrical sounding as an exploration technique to improve on the certainty of groundwater yield in the fractured crystalline basement aquifers of eastern Uganda. *Hydrogeology Journal*, 16, 1683–1693.
- Persits, F, Ahlbrandt, T, Tuttle, M Charpentier, R, Brownfield, M, andTakahashi, K. (2002). Map showing geological, oil and gas fields and geologic provinces of Africa. *USGS Open File Report*, 97 - 470 A.
- Pervaiz, S., Allah, B. Muhammed, A., and Rana, T. (2010). The use of vertical electrical sounding resistivity method for the location of low salinity groundwater for irrigation in Chaj and Rachna Doabs. *Environ Earth Sci*, 60:, 1113–1129. <https://doi.org/10.1007/s12665-009-0255-6>. 12.Oct.2019.
- Pradeep, K. J., (1998). Remote sensing techniques to locate ground water potential zones in upper Urmil river basin District Chatarpur, Central India. *J Ind Soc Remote Sens*, 26(3), 135–147.
- Rashid, M., Lone, M. A., and Romshoo, S. A. (2011). Geospatial tools for assessing land degradation in Budgam district, Kashmir Himalaya, India. *Journal Earth System Science*, 120(3), 423–433.
- Rashid, M., Lone, M. A., and Ahmed, S. (2012). Integrating geospatial and ground geophysical information as guidelines for groundwater potential zones in hard rock terrains of south India, 4829–4839. <https://doi.org/10.1007/s10661-011-2305-2>
- Ravindran, A. A., Ramanujam, N. and Somasundaram, P. (2012). Wenner array resistivity and sp logging for ground water exploration in sawerpuram teri deposits, thoothukudi district, tamil nadu, india. *Asian Research Publishing Network (ARPN). All Rights Reserved., October.Vo.*
- Ravindran, K.V. and Jayaram, A. (1997). Groundwater prospects of Shahbad Tehsil, Baran district, eastern Rajasthan and remote sensing approach. *Journal of Indian Society of Remote Sensing*, 25, pp. 239–246.

- Reynolds, J. M. (1997). An introduction to applied and environmental geophysics. Chichester. *John Wiley and Sons Limited*.
- Saidi, S., Mannai, S. H. H., Bouri, F. J. S., and Anselme, B. (2017). GIS-based multi-criteria analysis and vulnerability method for the potential groundwater recharge delineation , case study of Manouba phreatic aquifer , NE Tunisia. *Environmental Earth Sciences*. <https://doi.org/10.1007/s12665-017-6840-1>
- Salami, S.A and Ogbamikhumi, A. (2017). Geo-Electrical Investigation for Groundwater Potential of Ihievbe Ogben , Edo North , South Western Nigeria. *J. Appl. Sci. Environ. Manage.*, Vol. 21 (7, 1291–1296.
- Sarkar, B.C., Deota, B.S., Raju, P.L.N. and Jugran, D. (2001). A geographical information system approach to evaluation of groundwater potential of shamri microwatershed in the shimla taluk,Himachal pradesh. *Indian Society of Remote Sensing* , 2993), 151– 164.
- Sener, E., and Davraz, A, O. M. (2005). An integration of GIS and remote sensing in groundwater investigation: a case study in Burdur, Turkey. *Hydrogeol J*, 13, :826–834.
- Shahid, S., Nath, S.K. and Patra, H. P. (2000). Groundwater assessment and management within typical laterites around Salbni District Midnapur (W.B). *Jour. of Indian Water Worrks*, XXXII(2), 101– 106.
- Shanshal, Z. M. (2018). Electrical resestivity investigation for groundwater of three villages in sumel district-, 23(1).
- Shewa, T. (2007). Assessment of Groundwater and its vulnerability to pollution by Vertical Electrical Sounding in Ada’A plain. *Unpublished Masters Dissertation, Addis Ababa University*.
- Sikdar, P.K., Chakraborty, S., Adhya, E., and Paul, P. K. (2004). Land use/land cover changes and groundwater potential zoning in and around Raniganj coal mining area, Bardhaman District, West Bengal: a GIS and remote sensing approach. *J. Spat. Hydro.*, 4(2), 1–24.
- Singh, A. K., Parkash, B., and Choudhury, P. R. (2007). Integrated use of SRM, Landsat ETM + data and 3D perspective views to identify the tectonic geomorphology of Dehradun valley, India. *International Journal of Remote Sensing*, 28(11), 2430–2414.
- Smith, M. and Pain, C. (2009). Applications of remote sensing in geomorphology. *Progress in Physical Geography*, 33 (4), 568–582.

- Solomon, S. and Quiel, F. (2006). Groundwater study using remote sensing and geographic information systems (GIS) in the central highlands of Eritrea. *Hydrogeology Journal*, 14 (6), 729–741.
- Sreedevi, P. D., Subrahmanya, K., and Ahmed, S. (2005). Integrated approach for delineating potential zones to explore for groundwater in the Pageru River basin, Cuddapah District, Andhra Pradesh, India. *Hydrogeology Journal*, 13, 534–543.
- Srinivasan, K., Poongothai, S., and Chidambaram, S. (2013). Identification of groundwater potential zone by using gis and electrical resistivity techniques in and around the wellington reservoir, cuddalore district, Tamilnadu, India. *European Scientific Journal*, vol.9, No., pp. 1857 – 7881.
- Srivastava, P. K., and Bhattacharya, A. K. (2006). Groundwater assessment through an integrated approach using remote sensing, using remote sensing, GIS and resistivity techniques: a case study from a hard rock terrain. *International Journal of Remote Sensing*, 27(20), 4599–4620.
- Srivastava, P. K., and Bhattacharya, A. K. (2006). Groundwater assessment through an integrated approach using remote sensing, using remote sensing, GIS and resistivity techniques: a case study from a hard rock terrain. *International Journal of Remote Sensing*, 27(20), 4599–4620.
- Subramanya, K. (2008). *Engineering Hydrology*,.
- Srinivas, Y. Muthuraj, D., and Chandrasekar, N. (2008). Resistivity studies to delineate structural features near Abhishekapatti, Tirunelveli, Tamil Nadu ... Resistivity studies to delineate structural features near. *J. Ind. Geophys. Union*, Vol.12, No(January), pp.157–163.
- Taylor, P., Singh, P., Thakur, J. K., and Kumar, S. (2013). Delineating groundwater potential zones in a hard- rock terrain using geospatial tool., (December 2014), 37–41. <https://doi.org/10.1080/02626667.2012.745644>
- Todd, D.K. and Mays, L. W. (2005). Groundwater hydrology. *John Wiley & Sons.*, 3rd ed. Ho.
- Todd, D. K. (1980). Groundwater Hydrology. 2nd Edn (New York: John Wiley & Sons), pp. 23–63.
- Tomas, A., Sharma, A.K., Manoj, K.S. and Anil, S, (1999). Hydrogeomorphological

- mapping in assessing groundwater by using remote sensing data- A case study in Lehra Ganga block, Sangrur district, Punjab. *Journal of Indian Society of Remote Sensing*, 27, pp. 31–42.
- Tiwari, B., and Rai, A. (1996). Hydromorphological Mapping for groundwater prospecting using Landsat–MSS images – A case study of part of Dhanbad district, Bihar; *J. Indian Soc. Remote Sensing*, 24(4), 281–285.
- Teeuw, R. M. (1995). Groundwater exploration using remote sensing and a low-cost geographical information system. *Hydrogeol J*, 3(3), :21–30.
- U. S. Environmental Protection Agency. (2011). United States Environmental Protection Agency. [Http://www.epa.gov](http://www.epa.gov) [Online] Available At:
- UNESCO. (2004). Groundwater resources of the world and their use.
- Upton K, Ó. Dochartaigh, B.E., and Bellwood.-H. (2018). Africa Groundwater Atlas: Hydrogeology of South Sudan. British Geological Survey. http://earthwise.bgs.ac.uk/index.php/Hydrogeology_of_South_Sudan (p. 1).
- Van Dongen, P. and Woodhouse, M. (1994). Finding groundwater. A project manager guide to techniques and how to use them. In *UNDP -- World Bank Water and Sanitation programme*.
- Vail, J. R. (1987). Late Proterozoic terrains in the Arabian-Nubian Shield and their characteristic mineralization. *Geol. Jour.*, 22, pp. 161–175.
- Vandas, S. J., Winte., T. C. and Battaglin, W. A. (2002). Water and the environment (AGI Environmental Awareness Series). *l.:American Geological Institute Publications*.
- Van-Dycke, A., S. and Menyeh, A. (2013). Geo-Electrical Investigation Of Groundwater Resources And Aquifer Characteristics In Some Small Communities In The Gushiegu And Karaga Districts Of Northern Ghana. *International Journal of Scientific & Technology Research*, March.2(3).
- Ward, S. H. (1990). Resistivity and induced polarization methods. Geotechnical and Environmental Geophysics. *Society of Geophysics, Exploration, vol 1*.
- Water, U. (2007). Coping with Water Scarcity: Challenge of the twenty-first century. prepared for World water day 2007. Retrieved from [http://www.unwater.org/wwd07/downloads/ Documents/escarcity.pdf](http://www.unwater.org/wwd07/downloads/Documents/escarcity.pdf).
- Whiteman, A. . (1971). The Geology of Sudan Republic. *Clarendon, Press Oxford*.

WHO. (2010). Water for Health, (Geneva 27).

Zohdy, A. A. R., Eaton, G. P., and Mabey, D. R. (1974). Application of surface geophysics to ground-water investigations., p. 11 6.

Zohdy, A.A.R., Eaton, G.P., and Mabey, D. R. (1990). Application of surface geophysics to Groundwater Investigations. *Series in Techniques of Water Resources Investigations of the United States Geophysical Survey*, 2, 8–55.

APPENDIX I.

1 .Horizontal profile survey sheet.

Wenner Electrical Resistivity Data Sheet

(E.P)

Location..... Date.....

Coordinate.....EN

Altitude..... Profile Number.....

$$\rho a = 2\pi a \Delta V / I$$

Where, a=10, 20, 30

Interval	Ohms-m	Remark
10		
20		
30		

2. Sample of Horizontal profile.

Wenner Electrical Resistivity Data Sheet

(H.P)

Location.....*Kapur*..... Date.....*05/03/2018*.....
 Coordinate.....*0332400*.....E.....*0537990*.....N
 Altitude.....*497 m*..... Profile Number.....*I-P:1*.....

$$\rho_a = 2\pi a \Delta V / I$$

Where, a=10, 20, 30

Interval	Ohms-m	Remark
10	<i>3688.7 Ohm.m</i>	
20	<i>3268.4 Ohm.m</i>	
30	<i>3841.7 Ohm</i>	

Wenner Electrical Resistivity Data Sheet

(H.P)

Location.....Kapuri..... Date.....07/03/2018.....
 Coordinate.....0331041.....E.....0637356.....N
 Altitude.....517 M..... Profile Number.....II, P.25.....

$$\rho_a = 2\pi a \Delta V / I$$

Where, a=10, 20, 30

Interval	Ohms-m	Remark
10	253255 Ohm-m	
20	108678 Ohm-m	
30	427332 Ohm-m	

Wenner Electrical Resistivity Data Sheet

(H.P)

Location.....Kapuri..... Date.....07/03/2018.....
 Coordinate.....0332517.....E.....0536983.....N
 Altitude.....500 M..... Profile Number.....III - P.1.....

$$\rho_a = 2\pi a \Delta V / I$$

Where, a=10, 20, 30

Interval	Ohms-m	Remark
10	557.071 Ohm	
20	453.11 Ohm	
30	1651.75 Ohm	

Appendix II.

2.1. VES survey sheet.

Schlumberger Electrical Resistivity Data Sheet

(V.E.S)

Location..... Date.....

Coordinate.....EN

Altitude..... VES Number.....

$$\rho_a = \pi \Delta V / I * [(AB/2)^2 - (MN/2)^2] / MN$$

AB/2	MN/2	Ohms-m	Remark
1.0	0.5		
1.5	0.5		
1.8	0.5		
2.5	0.5		
3.5	0.5		
5.0	0.5		
8.0	0.5		
10	0.5		
13	0.5		
16	0.5		
20	0.5		
20	5.0		
25	5.0		
32	5.0		
40	5.0		
40	10		
45	10		
50	10		
80	10		
100	10		
130	10		
160	10		

2.2. Sample of VES.

Slumberger Electrical Resistivity Data Sheet

(V.E.S)

Location..... Kepun Date..... 10th/03/018
 Coordinate..... 055.2266 E 053.8095 N
 Altitude..... 491 M VES Number..... -11

$$\rho_a = \pi \Delta V / I * [(AB/2)^2 - (MN/2)^2] / MN$$

AB/2	MN/2	Ohms-m		Remark
1.0	0.5	2881.5	Ohm-m	
1.5	0.5	2404.8	"	
1.8	0.5	1882.01	"	
2.5	0.5	7184.4	"	
3.5	0.5	5084.4	"	
5.0	0.5	1183.6	"	
8.0	0.5	471.44	Ohm-m	
10	0.5	273.33	"	
13	0.5	230.70	"	
16	0.5	255.47	"	
20	0.5	145.24	"	
20	5.0	2813.7	Ohm-m	
25	5.0	2155.3	"	
32	5.0	1557.6	"	
40	5.0	7185.8	"	
40	10	2542.1	"	
45	10	1920.9	"	
50	10	1594.9	"	
63	10	940.37	Ohm-m	
80	10	531.62	"	
100	10	383.67	"	
130	10	230.70	"	
160	10	122.87	"	

Slumberger Electrical Resistivity Data Sheet

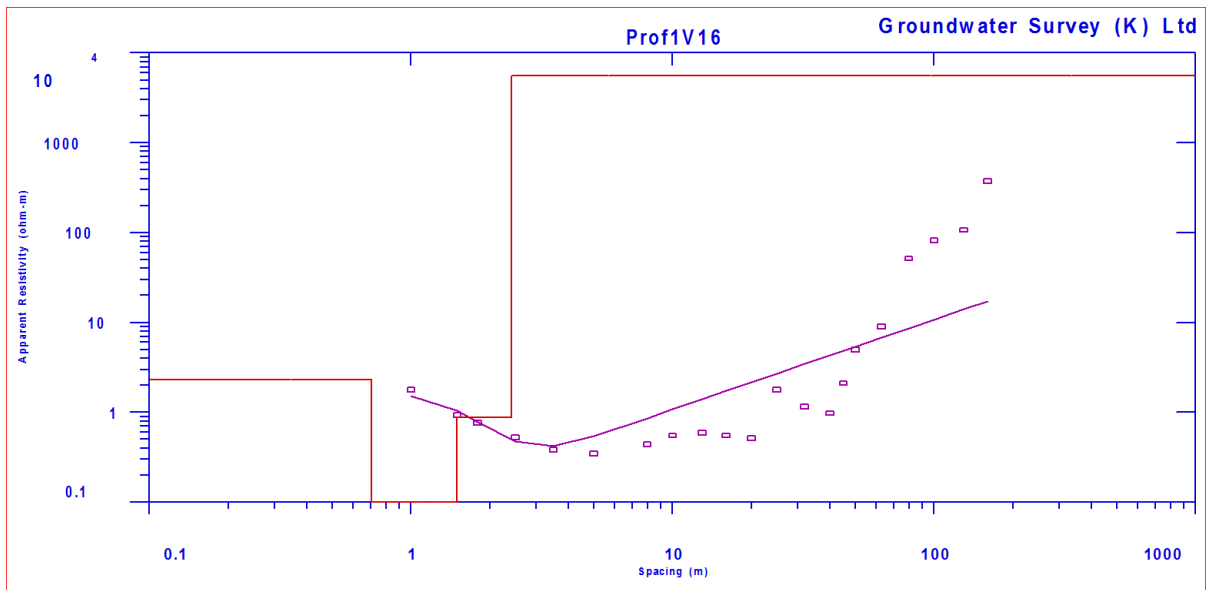
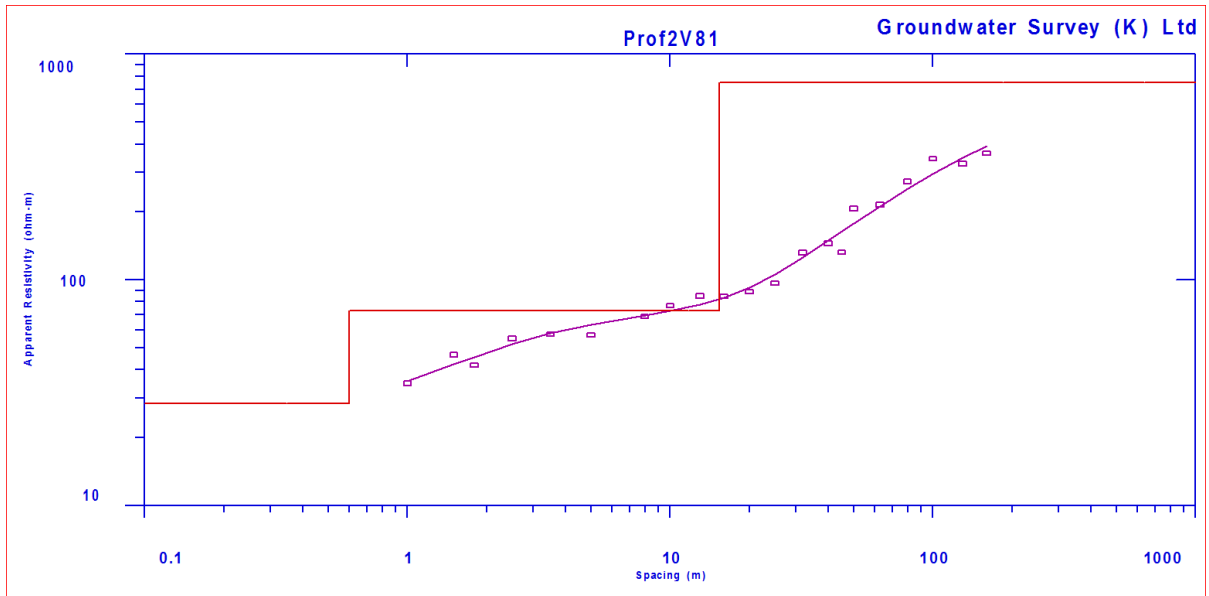
(V.E.S)

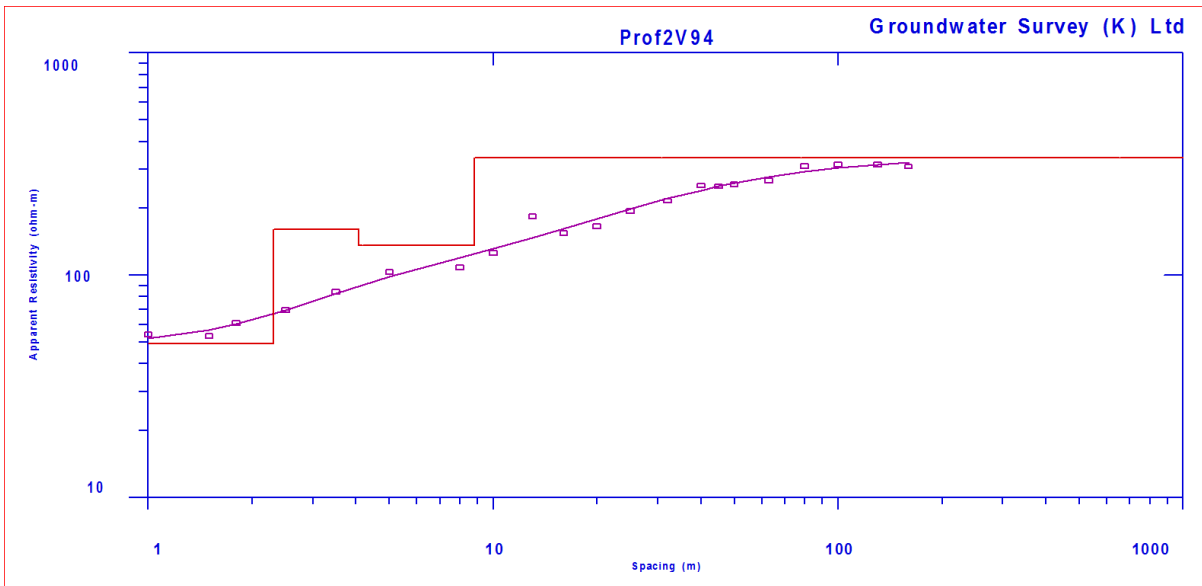
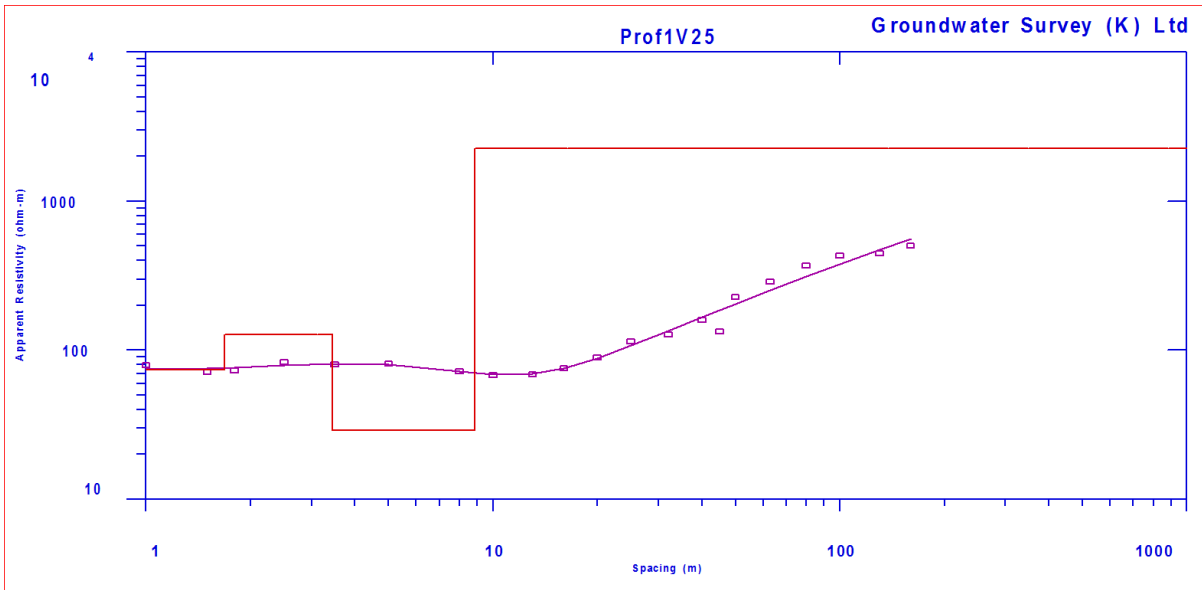
Location..... Ko Qui Date..... 10th/03/2018
 Coordinate... 0538307 E 0538307 N
 Altitude..... 484 M VES Number..... -9

$$\rho_a = \pi \Delta V / I * [(AB/2)^2 - (MN/2)^2] / MN$$

AB/2	MN/2	Ohms-m	Remark
1.0	0.5	8872.1	Ohm.m
1.5	0.5	7309.8	"
1.8	0.5	2878.8	"
2.5	0.5	1050.7	"
3.5	0.5	346.06	"
5.0	0.5	127.89	"
8.0	0.5	52.599	Ohm.m
10	0.5	10.031	"
13	0.5	15.046	"
16	0.5	17.554	"
20	0.5	7.5229	"
20	5.0	154.10	"
25	5.0	92.783	"
32	5.0	55.168	"
40	5.0	12.538	"
40	10	117.86	Ohm.m
45	10	42.630	"
50	10	47.645	"
63	10	30.092	"
80	10	25.076	"
100	10	15.046	Ohm.m
130	10	5.0153	"
160	10	25.076	"

2.3. Electrical resistivity models and curves.





2.4: Summary of VES interpretations with their positions in kapuri area.

N0 of VES	Longitude (M)	Latitude (M)	N0 of Layers	Resistivity(Ωm) ρ_i					Thickness(m) T_i					RMS error
				ρ_1	ρ_2	ρ_3	ρ_4	ρ_5	T1	T2	T3	T4	T5	
VES1	332400.63	537990.5	3	7.73	452	24592	—	—	1.5427	0.58749	—	—	—	84.39%
VES2	332500.04	537999.6	4	43.9	69.18	9995	21.81	—	0.621	4.6051	7.7126	—	—	8.61%
VES3	332533.01	538136	4	15.8	33.12	178	17717	—	0.7552	0.60303	53.622	—	—	8.29%
VES4	332437.72	538057.5	4	201	406.8	549.6	13953	—	1.9751	17.651	87.648	—	—	21.44%
VES5	332386.13	538090	4	48.4	1158	8506	57.5	—	3.7677	0.35863	10.862	—	—	8.51%
VES6	332372.31	538168.9	4	99.5	546	46.92	32958	—	4.344	4.2681	11.929	—	—	67.12%
VES7	332367.65	538218.5	4	3.29	0.505	753.9	11696	—	0.5391	0.93557	6.2353	—	—	88.27%
VES8	332361.21	538312.9	4	103	17.89	72.77	4.811	—	0.6896	4.7546	6.4929	—	—	29.14%
VES9	332241.84	538305.3	4	25071	247	56.48	14.22	—	0.26	1.253	14.073	—	—	9.75%
VES10	332255.7	538204.9	5	23.2	7.856	0.675	1882	19 .1	0.5328	10.689	1.7187	85.476	—	10.53%
VES11	332266.05	538095	4	277	45.68	3588	393.7	—	2.1054	2.4857	11.453	—	—	9.61%
VES12	332280.94	537982.3	3	381	67.18	4722	—	—	0.3838	9.8935	—	—	—	14.24%
VES13	332162.68	538022.4	3	229	93.46	805.6	—	—	0.3196	6.6427	—	—	—	5.33%
VES14	332145.5	538126	4	101	132.8	1291	77.77	—	1.9381	14.568	18.986	—	—	8.08%
VES15	332132.12	538231	4	6.18	0.505	2.046	9901	—	0.8146	4.3154	3.5887	—	—	96.90%
VES16	332101	538245	4	2.3	0.1	0.881	5577	—	0.7077	0.78681	0.9305	—	—	234.14%
VES17	332104.16	537963	4	3.63	1.801	4.262	5018	—	0.5312	1.7062	16.577	—	—	231.11%
VES18	332042.98	537962	4	147	765.8	31.18	918.3	—	2.7248	1.5887	4.2397	—	—	10.69%
VES19	332028.01	538063	4	97	171.4	4216	253.2	—	2.9921	7.3153	14.784	—	—	9.89%
VES20	332026.19	538171	4	190	97.07	35.92	111.9	—	0.3477	0.20425	51.18	—	—	49.62%
VES21	332004	538276	4	137	50.01	0.55	1647	—	0.8031	7.108	2.9102	—	—	14.83%
VES22	331885.93	538361.3	4	9866	608.3	161.8	3.949	—	0.2308	0.96381	8.5008	—	—	15.50%
VES23	331903.67	538210.7	5	2.93	1.996	0.495	214.1	72 4	0.3503	1.1646	1.7493	5.0746	—	272.14%
VES24	331913.19	538102.4	4	19	31.07	18.11	72.88	—	0.7457	1.5814	0.9949	—	—	337.59%
VES25	331935.67	537988.3	4	73.9	124.8	29.42	2260	—	1.684	1.7555	5.4255	—	—	10.78%
VES26	331760.4	538027	4	108	20.48	58.3	3194	—	0.3565	3.8454	75.392	—	—	14.51%
VES27	331743.23	538134.4	4	126	26.29	13.23	27.91	—	1.2958	1.553	1.2057	—	—	66.72%
VES28	331740.05	538249.9	4	7.4	1.923	10.83	11387	—	1.4602	4.1682	12.681	—	—	16.12%
VES29	331014.58	538066.7	3	99	74.24	13.06	—	—	0.1017	11.85	—	—	—	340.77%
VES30	331584.49	538325.5	3	42.7	0.923	6635	—	—	0.4212	5.6327	—	—	—	68.40%
VES31	331598.36	538227.8	3	32.5	9.36	18.37	—	—	0.6867	4.2008	—	—	—	50.46%
VES32	331601.22	538118.6	4	224	62.52	5.541	574.5	—	0.5878	8.7259	9.6867	—	—	119.93%
VES33	331607.41	538012.4	4	8.04	29.96	23.32	58.7	—	0.5391	0.30661	0.4242	—	—	1579.87%
VES34	331613.73	537909.3	4	128	36.23	62.16	1865	—	2.2385	0.14542	2.1844	—	—	9.48%

VES35	331454.82	537873.7	4	71.4	5.897	13245	43851	—	0.6517	2.4878	13.635	—	—	61.56%
VES36	331451.29	537931.5	4	43.3	49.49	9.624	1550	—	1.6195	0.48282	1.7245	—	—	31.14%
VES37	331423.68	538035.4	4	77	22.34	512.3	2.018	—	0.2298	3.7335	23.232	—	—	31.54%
VES38	331413.15	538138.1	4	5.79	27.98	21.34	32.37	—	0.7143	0.91568	0.7208	—	—	299.94%
VES39	331369	538034.2	4	8.85	157.5	6.615	2223	—	0.1928	1.2602	1.0086	—	—	15.67%
VES40	331411.89	537872.6	4	51.2	93.66	30.08	59114	—	0.2307	6.441	5.5106	—	—	10.17%
VES41	331299.07	537961.7	5	329	37.53	1107	35.2	⁶³ 5	0.868	0.99877	2.314	4.6459	—	34.75%
VES42	331290.31	538062.1	4	151	6.508	594.1	9.637	—	0.6698	0.26062	90.8	—	—	11.98%
VES43	331269.02	538162.1	3	250	633.7	45.77	—	—	0.1051	0.19357	—	—	—	113.76%
VES44	331266.11	538252	4	63.3	155	11.88	31313	—	0.2042	0.12606	15.361	—	—	32.69%
VES45	331269.02	538162.1	5	127	456	42.72	213	⁸⁸ 61	4.2994	2.29	6.9783	3.0698	—	57.06%
VES46	331180.25	537999.3	4	571	107.3	25.91	1422	—	0.5061	2.0592	0.6399	—	—	10.10%
VES47	331197.67	537903.1	3	500	47.53	76149	—	—	0.308	0.69409	—	—	—	248.19%
VES48	331303.72	537862.6	4	87.4	164	24.56	16356	—	0.846	3.406	0.8512	—	—	47.49%
VES49	331009	538169	5	8.03	7.176	15.9	6.506	⁸⁵ .1	1.636	0.54581	3.7577	0.3223	—	49.63%
VES50	331913.19	538102.4	4	92.3	24.19	64.07	12463	—	0.937	0.44859	20.555	—	—	19.63%
VES51	331935.67	537988.3	4	111	53.51	188.2	1695	—	1.316	0.37414	19.84	—	—	12.41%
VES52	331760.4	538027	4	120	384.6	65.82	2836	—	0.328	0.99788	6.4772	—	—	9.55%
VES53	331743.23	538134.4	4	2136	117	79.75	3539	—	0.2619	0.96986	8.5419	—	—	9.11%
VES54	331740.05	538249.9	4	51.6	69.54	292.7	1237	—	0.2619	3.9614	17.609	—	—	10.68%
VES55	331584.49	538325.5	4	865	82.16	16.75	2802	—	0.5056	1.0461	2.0925	—	—	8.14%
VES56	331598.36	538227.8	4	131	27.93	91.73	741.6	—	0.5965	0.79416	14.896	—	—	7.03%
VES57	331515.46	538332.7	4	17	3.212	272.5	20173	—	0.6336	0.75492	0.974	—	—	16.04%
VES58	332000	537916	5	76.1	13.18	30.25	108.8	## ##	0.2896	1.3504	0.2294	20.88	—	8.77%
VES59	332506	537494.3	3	4.07	0.542	63453	—	—	0.1908	0.32226	—	—	—	154.22%
VES60	332511.6	537614.2	3	27.8	0.744	68799	—	—	0.3746	0.29334	—	—	—	97.08%
VES61	332514.37	537714.1	4	7.82	20.27	1.185	66021	—	0.3757	0.89422	0.4578	—	—	50.73%
VES62	332516.14	537813.2	4	243	40.9	93903	—	—	0.4795	8.06	—	—	—	19.98%
VES63	332041.65	537962	4	8.04	29.96	23.32	58.7	—	1.4369	0.30661	0.4242	—	—	6048.37%
VES64	3332062	537900	5	102	110	31.13	23.37	⁷² 2	1.7279	1.5262	0.2633	1.7189	—	15.72%
VES65	332025.81	538171	4	81.7	22.22	364	7649	—	0.681	0.47621	24.175	—	—	11.87%
VES66	332004.42	538275.7	4	108	350.1	51.91	37492	—	5.5101	9.2342	10.666	—	—	9.77%
VES67	332500.04	537999.6	4	154	48.02	203.8	9234	—	1.4716	0.405	39.298	—	—	16.68%
VES68	332327	537691	4	95.5	32.55	25.15	774	—	1.7366	0.11585	0.3636	—	—	5.94%
VES69	332437.72	538057.5	3	52.7	389.3	6091	—	—	2.901	19.382	—	—	—	20.46%
VES70	332367.65	538218.5	3	61.8	204.6	52344	—	—	3.9954	15.849	—	—	—	991.60%
VES71	331894.03	537721.4	3	212	121.2	597.5	—	—	1.0057	6.463	—	—	—	6.60%
VES72	330888.88	537903.9	4	49.5	15.61	111.5	22900	—	1.0057	0.55194	39.445	—	—	9.97%
VES73	331290.31	538062.1	4	97.6	28.44	147.6	997.8	—	1.1381	0.71057	14.37	—	—	5.90%

VES74	332184	537731	4	252	37.13	132.6	1186	—	0.6249	0.2788	25.169	—	—	13.43%
VES75	332200	537631	4	141	11.35	148.5	54498	—	0.5354	0.3974	37.297	—	—	33.24%
VES76	332150	537937	4	10.4	158	27.71	856.1	—	0.3656	11.848	3.8098	—	—	9.93%
VES77	332314	537911	4	13.7	38.95	184.7	1563	—	0.2765	4.1389	51.615	—	—	9.88%
VES78	332013	537821	4	5.7	4.879	154.1	3284	—	0.5302	4.0533	42.245	—	—	164.32%
VES79	332000	537916	4	48.2	9.289	143	13852	—	0.384	0.21866	59.672	—	—	9.62%
VES80	331149	537103	4	101	21.97	113.2	268.3	—	0.882	0.93827	0.1108	—	—	9.28%
VES81	331577	537796	3	28.4	72.76	748.5	—	—	0.6008	14.824	—	—	—	9.26%
VES82	331782	538362	4	8.04	29.96	23.32	58.7	—	0.6008	0.30661	0.4242	—	—	****%
VES83	332184	537731	4	126	317.3	16.04	12218	—	3.6102	3.8771	5.4257	—	—	19.85%
VES84	332200	537631	4	40.9	110.6	29.89	5649	—	0.3438	14.015	7.1856	—	—	11.13%
VES85	332150	537937	4	117	67.18	142.3	2390	—	0.2887	5.1736	46.882	—	—	5.28%
VES86	332314	537911	4	65.4	36.25	167.1	25317	—	0.4049	4.0247	26.186	—	—	9.63%
VES87	332013	537821	4	50.2	17.54	73.2	787.8	—	0.5175	0.45275	12.068	—	—	6.53%
VES88	332553	538254	4	42.8	83.09	281	85509	—	1.2601	9.5248	28.62	—	—	11.77%
VES89	3332062	537900	4	57.1	151	44.94	2714	—	1.3405	3.5401	4.8016	—	—	8.16%
VES90	331540.74	537364.1	4	8.04	29.96	23.32	58.7	—	1.4369	0.30661	0.4242	—	—	3571.23%
VES91	331462.17	537841.8	4	14.8	139.5	51326	—	—	0.1459	18.916	—	—	—	21.90%
VES92	331145.64	537408.5	4	8.04	29.96	23.32	58.7	—	1.4369	0.30661	0.4242	—	—	3137.85%
VES93	332400.63	537990.5	4	19.2	49.14	4.063	11554	—	0.6736	0.10325	1.3594	—	—	98.00%
VES94	331882.87	537937.5	4	49.4	160.7	135.8	337.1	—	2.3051	1.7617	4.7433	—	—	6.74%
VES95	331089.39	537349.9	4	1501	276.5	105.6	12612	—	0.4448	2.3862	41.577	—	—	9.72%
VES96	331537	537408	3	64.8	4.879	398.7	—	—	1.0015	0.84543	—	—	—	20.20%
VES97	330966.54	537374.2	4	518	48.06	97.2	12407	—	0.2417	2.5691	18.995	—	—	10.88%
VES98	332000	537916	4	116	111.5	187.5	1940	—	1.5736	18.471	1.699	—	—	8.67%
VES99	332000	537916	4	46.6	183.1	65.42	1235	—	1.9417	1.4089	7.5454	—	—	9.82%
VES100	331405.72	537548	4	213	1079	42.91	13521	—	3.6584	2.4443	9.6947	—	—	67.93%
VES101	331432.44	537642	4	32.9	48.41	4361	—	—	1.4068	11.156	—	—	—	9.71%
VES102	330993.15	536877	4	50.4	3.088	52.54	17320	—	1.5782	0.32749	15.662	—	—	158.54%
VES103	330995.27	536930.7	4	15	3.441	29.8	1146	—	1.0533	0.98978	0.6095	—	—	59.69%
VES104	331045.8	537156.2	4	100	180.9	24.09	89463	—	1.9439	2.6924	0.8172	—	—	47.91%
VES105	331007.02	537024	4	16.8	2.609	9.307	79334	—	0.4596	0.68562	0.4481	—	—	115.76%
VES106	331088.78	537279.7	4	26.9	2.074	64.25	60293	—	0.4626	0.92519	1.0381	—	—	37.85%
VES107	331091.37	537345.6	4	18.5	265.5	65433	—	—	2.7418	20.138	—	—	—	46.75%
VES108	330938.15	537324.4	4	1022	24.85	0.411	—	—	0.462	2.8881	—	—	—	60.72%
VES109	330946.47	537225.6	4	262	15.75	152.8	24717	—	2.0901	0.80673	42.446	—	—	29.64%
VES110	330950.13	537127.9	4	243	35.51	9.29	1249	—	1.2412	0.11426	1.4221	—	—	226.17%
VES111	330954.23	537027.4	4	266	102.8	385.7	2401	—	0.5099	5.7514	21.247	—	—	8.23%
VES112	331468.84	537203.2	4	89.7	444.3	32.91	2508	—	1.3955	0.74832	2.5738	—	—	12.42%

VES113	331477.37	537103.1	3	####	62.46	49785	—	—	0.1374	9.2712		—	—	18.55%
VES114	331467.71	536998.3	4	276	224.6	81.48	26629	—	0.9589	3.8374	14.048	—	—	22.27%
VES115	331463.72	536902.7	4	2270	189.5	19.19	37905	—	1.5428	13.059	5.7864	—	—	65.73%
VES116	331301.13	537253.8	4	257	140.4	355.5	1263	—	2.9517	3.7789	61.206	—	—	3.99%
VES117	331285.37	537151.5	4	180	71.57	287.8	3424	—	2.2768	2.5462	0.4698	—	—	61.82%
VES118	331267.41	537053.6	4	144	72.92	53.12	1521	—	0.3559	2.2417	4.3581	—	—	4.33%
VES119	331180.05	536875	3	69.4	548.5	48784	—	—	2.2768	34.26	—	—	—	24.05%
VES120	331173.5	537317.6	3	29.3	19.71	34382	—	—	2.5523	1.6514	—	—	—	26.40%
VES121	331171.05	537217	3	331	159	5204	—	—	0.4054	6.0666	6.2166	—	—	7.40%
VES122	331943.82	537219.7	4	382	817.9	1356	2416	—	1.1366	10.661	71.805	—	—	9.77%
VES123	331948.69	537118.3	4	260	113.9	1337	5443	—	0.5156	8.1719	2.4498	—	—	6.57%
VES124	331938.05	537020.2	3	273	721.4	6184	—	—	8.2575	98.595	—	—	—	13.03%
VES125	331925.63	536922.2	4	133	21.01	157.3	1194	—	1.6298	0.54139	82.891	—	—	10.78%
VES126	331772.08	537352	4	187	36.68	121.8	92644	—	0.6029	1.0045	18.048	—	—	9.66%
VES127	331772.52	537250.4	4	179	81.49	4954	9310	—	1.1016	18.123	58.151	—	—	9.43%
VES128	331768.53	537153.9	4	727	28	157	20618	—	1.6033	1.5252	28.506	—	—	7.67%
VES129	331743.19	537028.4	4	205	95.82	167.8	1258	—	0.7451	1.7773	24.1	—	—	5.19%
VES130	331621.86	537380.5	4	115	185.2	867.1	1054	—	0.7911	43.479	23.03	—	—	5.77%
VES131	331633.95	537281.4	4	92.7	48.98	241	5179	—	0.5584	6.5111	52.081	—	—	8.73%
VES132	331641.38	537182	4	115	32.72	266.9	1215	—	2.3499	1.0582	28.447	—	—	9.45%
VES133	331613.98	537086	3	161	91.1	80549	—	—	0.6906	24.221	—	—	—	10.78%
VES134	331554.81	537009.6	4	66.6	57.18	168.2	47461	—	1.2705	8.9437	4.798	—	—	14.55%
VES135	331512.13	536921.1	3	82.9	27.99	595.8	—	—	0.4626	4.8145	—	—	—	5.93%
VES136	331471.27	537301.4	4	79.7	18.15	149.1	1509	—	0.3341	1.847	11.374	—	—	9.33%
VES137	332382.62	537424.2	4	344	72.81	37.02	6218	—	0.2587	4.1264	4.4408	—	—	9.94%
VES138	332379.29	537326.1	4	187	25.32	4357	8	—	13.787	2.2845	77.86	—	—	9.70%
VES139	332353.43	537120.3	4	88	62.83	327.4	4288	—	0.5823	3.7878	23.287	—	—	9.46%
VES140	332234	537148	4	300	81.77	116.4	983.8	—	0.2227	2.4503	8.1277	—	—	8.13%
VES141	332227.08	537456.3	4	91.3	10.21	144.5	1946	—	1.3064	0.58067	15.722	—	—	14.89%
VES142	332220.63	536955.1	3	55.8	2.788	13151	—	—	2.5523	1.5138	—	—	—	59.74%
VES143	332088.6	536888.8	3	12.4	2.82	1666	—	—	1.0579	0.84015	—	—	—	64.18%
VES144	332110.35	537089.8	4	112	49.4	104.8	5821	—	0.3967	1.9934	15.911	—	—	6.24%
VES145	332100.79	537180.9	4	25.4	4.764	76.58	4828	—	1.3877	0.45715	10.826	—	—	10.09%
VES146	332094.35	537276.4	4	226	35.04	89.9	19429	—	10.826	0.22087	30.575	—	—	31.39%
VES147	332082.94	537383.6	4	42.6	8.19	83.03	12085	—	1.6877	1.0749	12.78	—	—	6.74%
VES148	332075.52	537435.4	4	19.5	4.724	209.6	4632	—	0.9167	0.55435	18.703	—	—	9.99%
VES149	331936.38	537314.8	4	110	14.73	38.18	38395	—	0.707	0.73135	11.758	—	—	9.46%
VES150	331943.82	537219.7	5	235	11.68	40.9	121.1	66 57	0.4546	0.57681	2.7233	19.138	—	8.82%
VES151	331948.69	537118.3	4	1808	20.81	45.82	1821	—	0.3266	0.18999	32.925	—	—	9.85%

VES152	331938.05	537020.2	3	34	47.49	20948	—	—	1.8133	6.931	—	—	—	9.67%
VES153	331925.63	536922.2	3	7.02	0.819	60252	—	—	0.7032	0.18487	—	—	—	62.17%
VES154	331772.08	537352	4	325	52.51	75.13	2620	—	0.3695	0.95338	20.265	—	—	7.00%
VES155	331772.52	537250.4	4	32	54.36	5.279	21015	—	1.2637	1.3151	0.743	—	—	9.23%
VES156	331768.53	537153.9	3	69.8	16.46	898.2	—	—	3.5462	0.95725	—	—	—	9.35%
VES157	331743.19	537028.4	4	36.3	8.547	175	34340	—	2.4936	0.93804	1.726	—	—	9.29%
VES158	331733.09	536930.7	4	95.6	25.76	177.5	8088	—	1.768	1.6705	53.708	—	—	8.64%
VES159	331621.86	537380.5	4	123	184.8	404.2	21630	—	0.5392	2.4142	47.375	—	—	8.57%
VES160	331633.95	537281.4	4	27.6	34.26	6.46	1765	—	0.8082	0.37799	1.0765	—	—	9.61%
VES161	331641.38	537182	4	88.9	96.58	233.5	455.6	—	2.104	8.0622	21.48	—	—	6.47%
VES162	331613.98	537086	4	14.7	27	223.3	142.9	—	3.6146	0.30629	13.307	—	—	7.22%
VES163	331554.81	537009.6	4	14.3	19.37	136.2	343.9	—	0.1377	2.3034	8.5085	—	—	8.34%
VES164	331512.13	536921.1	4	105	5.4	90.62	15506	—	0.5148	0.15941	60.391	—	—	6.82%
VES165	331471.27	537301.4	4	220	41.65	82.14	1234	—	0.6208	4.0909	12.098	—	—	7.17%
VES166	331468.84	537203.2	4	8.04	29.96	23.32	58.7	—	1.4369	0.30661	0.4242	—	—	3591.87%
VES167	331477.37	537103.1	4	520	9956	27.42	17401	—	0.7192	1.4938	5.6905	—	—	36.78%
VES168	331467.71	536998.3	4	95.3	119.6	338.2	10449	—	0.7202	2.9332	39.171	—	—	9.18%
VES169	331463.72	536902.7	4	136	214.8	275.7	1271	—	2.4248	1.3075	20.308	—	—	2.69%
VES170	331180.05	536875	4	163	119.8	124.2	998	—	2.0921	0.77037	10.93	—	—	7.13%
VES171	331301.13	537253.8	4	194	194.4	395.4	28242	—	1.9425	1.782	79.391	—	—	13.54%
VES172	331285.37	537151.5	4	160	9.996	102.9	385.1	—	0.3417	0.31339	28.446	—	—	8.84%
VES173	331267.41	537053.6	4	83.9	226.6	1325	48406	—	2.8831	32.503	3.1964	—	—	10.79%
VES174	331202	537253	4	329	21.22	126.6	78475	—	0.3964	0.2781	17.975	—	—	8.03%
VES175	331332.63	537351.2	4	87.5	178.6	396.7	897.4	—	4.4435	6.6057	34.705	—	—	5.02%
VES176	331173.5	537317.6	4	626	311.2	12.85	6269	—	0.8606	25.509	4.3323	—	—	8.40%
VES177	331171.05	537217	4	334	90.02	121.5	44115	—	0.4925	3.3233	39.629	—	—	5.91%
VES178	331149	537103	4	81.9	37.94	93.05	8990	—	0.9676	6.8834	43.548	—	—	8.43%
VES179	331128.75	537002	4	95.8	6.962	387	28557	—	0.8646	0.64698	61.398	—	—	7.31%
VES180	331108.58	536908.3	4	165	35.01	302.6	979.9	—	0.9688	0.45503	16.426	—	—	5.67%
VES181	331091.05	536859.5	4	175	13.12	227.3	19305	—	0.7745	0.41619	22.828	—	—	9.28%
VES182	331076.63	536809.4	4	397	54.51	313.6	74363	—	0.6082	4.7165	32.745	—	—	7.90%
VES183	330993.15	536877	4	150	161.6	176.2	5853	—	2.2759	0.33482	15.268	—	—	15.52%
VES184	330995.27	536930.7	4	122	35.31	142.8	27491	—	0.7913	0.80449	14.732	—	—	15.81%
VES185	331007.02	537024	4	1095	118.6	33.45	624.9	—	0.2424	2.5531	2.2611	—	—	13.33%
VES186	331045.8	537156.2	4	676	136.9	246.4	1945	—	3.6073	26.131	1.2383	—	—	9.44%
VES187	331088.78	537279.7	4	279	38.11	1.621	4662	—	0.3684	2.4093	0.9453	—	—	10.47%
VES188	331091.37	537345.6	4	6636	415.9	214.3	1257	—	0.3643	4.7811	43.624	—	—	8.85%
VES189	330938.15	537324.4	4	211	31.06	54.74	8644	—	0.4408	0.44821	23.145	—	—	10.37%
VES190	330946.47	537225.6	4	42.4	12.55	27.85	270.2	—	0.7997	1.1387	1.378	—	—	22.44%

VES191	330950.13	537127.9	4	84.9	40.93	156	32442	—	0.4842	2.305	55.578	—	—	10.47%
VES192	330954.23	537027.4	4	38.1	10.1	137.2	36809	—	1.0479	0.31827	36.109	—	—	18.24%

Appendix III.

3.1.3D Model data used for leapfrog software.

LOCATION ID	DEPTH TOP	DEPTH BASE	GEOLOGY CODE
VES56	0	0.596	Top soil
"	0.596	1.39	Moderately fractured
"	1.39	16.28	Fractured rock
"	16.28		Fractured rock
VES49	0	1.63	Top soil
"	1.6	2.49	Moderately fractured
"	2.49	4.91	Moderately fractured
"	4.91	9.12	Moderately fractured
"	9.12		Fractured rock
VES44	0	0.2	Top soil
"	0.2	0.33	Moderately fractured
"	0.33	15.69	Fractured zone
"	15.69		Basement rock
VES43	0	0.1	Top soil
"	0.1	0.29	Moderately fractured
"	0.29		Fractured rock
VES38	0	1.43	Top soil
"	1.43	1.74	Moderately fractured
"	1.74	2.16	Moderately fractured
"	2.16		Fractured zone
VES34	0	2.23	Top soil
"	2.23	2.38	Fractured rock
"	2.38	4.56	Fractured rock
"	4.45		Fractured rock
VES30	0	0.42	Top soil
"	0.42	6.05	Fractured rock
"	6.05		Basement rock
VES22	0	0.23	Top soil
"			
"	0.23	1.19	Moderately fractured
"	1.19	9.69	Moderately fractured
"	9.69		Fractured rock
VES21	0	0.83	Top soil
"	0.83	7.91	Moderately fractured

LOCATION ID	DEPTH TOP	DEPTH BASE	GEOLOGY CODE
"	7.91	10.82	Top soil
"	10.82		Basement rock
VES16	0	0.7	Top soil
"	0.7	1.49	Fractured rock
"	1.49	2.42	Fractured rock
"	2.42		Basement rock
VES8	0	0.68	Top soil
"	0.68	5.44	Moderately fractured
"	5.44	11.93	Fractured rock
"	11.93		Fractured rock
VES55	0	0.5	Top soil
"	0.5	1.55	Moderately fractured
"	1.55	3.64	Fractured rock
"	3.64		Basement rock
VES60	0	0.64	Top soil
"	0.64	1.51	Fractured rock
"	1.51		Basement rock
VES45	0	2.83	Top soil
"	2.83	4.61	Moderately fractured
"	4.61	10.85	Fractured rock
"	10.85	36.69	Moderately fractured
"	36.69		Basement rock
VES42	0	0.66	Top soil
"	0.66	0.93	Fractured rock
"	0.93	91.73	Moderately fractured
"	91.73		Fractured rock
VES37	0	0.33	Top soil
"	0.33	4.07	Fractured rock
"	4.07	27.3	Moderately fractured
"	27.3		Fracture rock
VES33	0	1.43	Top soil
"	1.43	1.74	Fractured rock
"	1.74	2.16	Fractured rock
"	2.16		Fractured rock
VES29	0	0.49	Top soil
"	0.49	6.56	Moderately fractured
"	6.56		Fracture rock

LOCATION ID	DEPTH TOP	DEPTH BASE	GEOLOGY CODE
VES23	0	0.31	Top soil
"	0.31	0.71	Fractured rock
"	0.71	8.67	Fractured rock
"	8.67	25.56	Fractured rock
"	25.56		Basement rock
VES20	0	0.19	Top soil
"	0.19	0.39	Moderately fractured
"	0.39	51.57	Fractured rock
"	51.57		Fractured rock
VES15	0	0.84	Top soil
"	0.84	5.16	Fractured rock
"	5.16	8.75	Fractured rock
"	8.75		Basement rock
VES9	0	0.26	Top soil
"	0.26	1.51	Moderately fractured
"	1.51	15.58	Fractured rock
"	15.58		Fractured rock
VES7	0	0.53	Top soil
"	0.53	1.47	Fractured rock
"	1.47	7.71	Moderately fractured
"	7.71		Basement rock
VES54	0	1.019	Top soil
"	1.019	4.98	Fractured rock
"	4.98	22.59	Moderately fractured
"	22.59		Basement rock
VES51	0	1.31	Top soil
"	1.31	1.45	Fractured rock
"	1.45	20.57	Moderately fractured
"	20.57		Basement rock
VES46	0	0.92	Top soil
"	0.92	1.82	Fractured rock
"	1.82	2.13	Fractured rock
"	2.13		Basement rock
VES41	0	0.82	Top soil
"	0.82	1.82	Fractured rock
"	1.82	4.13	Moderately fractured
"	4.13	8.78	Fractured rock

LOCATION ID	DEPTH TOP	DEPTH BASE	GEOLOGY CODE
"	8.78		Moderately fractured
VES36	0	1.619	Top soil
"	1.619	2.1	Fractured rock
"	2.1	3.82	Fractured rock
"	3.82		Basement rock
VES32	0	0.58	Top soil
"	0.58	9.31	Fractured rock
"	9.31	19	Fractured rock
"	19		Basement rock
VES28	0	1.46	Top soil
"	1.46	5.628	Fractured rock
"	5.628	18.31	Fractured rock
"	18.31		Basement rock
VES24	0	0.96	Top soil
"	0.96	1.83	Fractured rock
"	1.83	3.8	Fractured rock
"	3.8		Fractured rock
VES19	0	2.95	Top soil
"	2.95	10.27	Basement rock
"	10.27	26.26	Basement rock
"	26.26		Moderately fractured
VES14	0	1.93	Top soil
"	1.93	16.5	Fractured rock
"			
"	16.5	35.49	Basement rock
"	35.49		Moderately fractured
VES10	0	0.532	Top soil
"	0.532	11.22	Fractured rock
"	11.22	12.94	Fractured rock
"	12.94	98.41	Basement rock
"	98.41		Fractured rock
VES6	0	4.34	Top soil
"	4.34	8.61	Moderately fractured
"	8.61	20.54	Fractured rock
"	20.54		Basement rock
VES57	0	3.76	Top soil
"	3.76	4.12	Fractured rock
"	4.12	14.98	Moderately fractured

LOCATION ID	DEPTH TOP	DEPTH BASE	GEOLOGY CODE
"	14.98		Basement rock
VES52	0	0.63	Top soil
"	0.63	1.44	Moderately fractured
"	1.44	2.51	Fractured rock
"	2.51		Basement rock
VES47	0	0.307	Top soil
"	0.307	1	Fractured rock
"	1		Basement rock
VES40	0	0.77	Top soil
"	0.77	6.33	Fractured rock
"	6.33	11.07	Fractured rock
"	11.07		Basement rock
VES35	0	0.64	Top soil
"	0.64	5.95	Fracture rock
"	5.95	90.58	Moderately fractured
"	90.58		Basement rock
VES31	0	0.87	Top soil
"	0.87	5.07	Fractured rock
"	5.07		Fractured rock
VES26	0	0.357	Top soil
"	0.357	4.2	Fractured rock
"	4.2	82.019	Fractured rock
"	82.019		Basement rock
VES25	0	1.65	Top soil
"	1.65	3.47	Fractured rock
"	3.47	8.94	Fractured rock
"	8.94		Basement rock
VES18	0	2.718	Top soil
"	2.718	4.35	Moderately fractured
"	4.35	8.88	Fractured rock
"	8.88		Basement rock
VES13	0	0.32	Top soil
"	0.32	6.96	Fractured rock
"	6.96		Basement rock
VES12	0	0.38	Top soil
"	0.38	10.27	Fractured rock
"	10.27		Basement rock

LOCATION ID	DEPTH TOP	DEPTH BASE	GEOLOGY CODE
VES4	0	1.975	Top soil
"	1.975	19.62	Moderately fractured
"	19.62	107.22	Moderately fractured
"	107.22		Basement rock
VES2	0	0.619	Top soil
"	0.619	5.22	Fractured rock
"	5.22	13.83	Basement rock
"	13.83		Fractured rock
VES21	0	0.8	Top soil
"	0.8	7.91	Fractured rock
"	7.91	10.82	Fractured rock
"	10.82		Basement rock
VES120	0	2.55	Top soil
"	2.55	4.2	Fracture rock
"	4.2		Basement rock
VES110	0	1.24	Top soil
"	1.24	1.35	Fractured rock
"	1.35	2.77	Fractured rock
"	2.77		Basement rock
VES104	0	1.94	Top soil
"	1.94	4.63	Fractured rock
"	4.63	5.45	Fractured rock
"	5.45		Basement rock
VES102	0	1.57	Top soil
"	1.57	1.9	Fractured rock
"	1.9	17.56	Fractured rock
"	17.56		Basement rock
VES91	0	0.45	Top soil
"	0.45	19.06	Fracture rock
"	19.06		Basement rock
VES90	0	1.43	Top soil
"	1.43	1.74	Fractured rock
"	1.74	2.16	Fractured rock
"	2.16		Fractured rock
VES81	0	0.6	Top soil
"	0.6	15.42	Fractured rock
"	15.42		Basement rock

LOCATION ID	DEPTH TOP	DEPTH BASE	GEOLOGY CODE
VES74	0	0.62	Top soil
"	0.62	0.9	Fractured rock
"	0.9	26.07	Fractured rock
"	26.07		Basement rock
VES73	0	1.13	Top soil
"	1.13	1.84	Fractured rock
"	1.84	16.21	Fractured rock
"	16.21		Basement rock
VES63	0	1.43	Top soil
"	1.43	1.74	Fractured rock
"	1.74	2.16	Fractured rock
"	2.16		Fractured rock
VES60	0	0.64	Top soil
"	0.64	1.51	Fractured rock
"	1.51		Basement rock
VES122	0	1.13	Top soil
"	1.13	11.79	Basement rock
"	11.79	83.6	Basement rock
"	83.6		Basement rock
VES119	0	2.27	Top soil
"	2.27	36.53	Moderately fractured
"	36.53		Basement rock
VES111	0	0.51	Top soil
"	0.51	6.26	Fractured rock
"	6.26	27.51	Moderately fractured
"	27.51		Basement rock
VES105	0	0.45	Top soil
"	0.45	1.14	Fractured rock
"	1.14	1.59	Fractured rock
"	1.59		Basement rock
VES101	0	2.13	Top soil
"	2.13	13.28	Fractured rock
"	13.28		Moderately fractured
VES92	0	1.43	Top soil
"	1.43	1.74	Fractured rock
"	1.74	2.16	Fractured rock
"	2.16		Fractured rock
VES89	0	1.34	Top soil

LOCATION ID	DEPTH TOP	DEPTH BASE	GEOLOGY CODE
"	1.34	4.88	Fractured rock
"	4.88	9.68	Fractured rock
"	9.68		Basement rock
VES82	0	1.43	Top soil
"	1.43	1.74	Fractured rock
"	1.74	2.16	Fractured rock
"	2.16		Fractured rock
VES75	0	0.53	Top soil
"	0.53	0.93	Fractured rock
"	0.93	38.23	Fractured rock
"	38.23		Basement rock
VES72	0	1.43	Top soil
"	1.43	1.98	Fractured rock
"	1.98	41.43	Fractured rock
"	41.43		Basement rock
VES64	0	1.72	Top soil
"	1.72	3.25	Fractured rock
"	3.25	3.51	Fractured rock
"			
"	3.51	5.23	Fracture rock
"	5.23		Basement rock
VES123	0	0.51	Top soil
"	0.51	8.68	Fractured rock
"	8.68	11.13	Basement rock
"	11.13		Basement rock
VES118	0	0.35	Top soil
"	0.35	2.59	Fractured rock
"	2.59	6.95	Fractured rock
"	6.95		Basement rock
VES112	0	1.39	Top soil
"	1.39	2.14	Moderately fractured
"	2.14	4.71	Fractured rock
"	4.71		Basement rock
VES106	0	0.46	Top soil
"	0.46	1.38	Fractured rock
"	1.38	1.9	Fractured rock
"	1.9		Basement rock
VES100	0	3.65	Top soil

LOCATION ID	DEPTH TOP	DEPTH BASE	GEOLOGY CODE
"	3.65	6.1	Basement rock
"	6.1	15.79	Fractured rock
"	15.79		Basement rock
VES93	0	0.63	Top soil
"	0.63	0.78	Fractured rock
"	0.78	2.13	Fractured rock
"	2.13		Basement rock
VES88	0	1.26	Top soil
"	1.26	10.78	Fractured rock
"	10.78	39.4	Moderately fractured
"	39.4		Basement rock
VES83	0	3.61	Top soil
"	3.61	7.48	Moderately fractured
"	7.48	12.91	Fractured rock
"	12.91		Basement rock
VES76	0	0.36	Top soil
"	0.36	12.21	Fractured rock
"	12.21	16.02	Fractured rock
"	16.02		Basement rock
VES71	0	1	Top soil
"	1	7.46	Fractured rock
"	7.46		Basement rock
VES65	0	0.68	Top soil
"	0.68	1.15	Fractured rock
"	1.15	25.33	Moderately fractured
"	25.33		Basement rock
VES61	0	1.47	Top soil
"	1.47	1.88	Fractured rock
"	1.88	2.53	Fractured rock
"	2.53		Basement rock
VES124	0	8.25	Top soil
"	8.25	106.85	Moderately fractured
"	106.85		Basement rock
VES117	0	2.27	Top soil
"	2.27	4.82	Fractured rock
"	4.82	5.29	Moderately fractured
"	5.29		Basement rock
VES113	0	0.13	Top soil

LOCATION ID	DEPTH TOP	DEPTH BASE	GEOLOGY CODE
"	0.13	9.48	Fractured rock
"	9.48		Basement rock
VES107	0	2.74	Top soil
"	2.74	22.8	Moderately fractured
"	22.8		Basement rock
VES99	0	1.94	Top soil
"	1.94	3.35	Fractured rock
"	3.35	10.89	Fractured rock
"	10.89		Basement rock
VES94	0	2.3	Top soil
"	2.3	3.05	Fractured rock
"	3.05	6.8	Moderately fractured
"	6.8		Moderately fractured
VES87	0	0.51	Top soil
"	0.51	0.97	Fracture rock
"	0.97	13.03	Fractured rock
"	13.03		Basement rock
VES84	0	0.35	Top soil
"	0.35	14.3	Fractured rock
"	14.3	21.49	Fractured rock
"	21.49		Basement rock
VES77	0	0.27	Top soil
"	0.27	4.41	Fractured rock
"	4.41	56.03	Fractured rock
"	56.03		Basement rock
VES70	0	3.3	Top soil
"	3.3	19.15	Moderately fractured
"	19.15		Basement rock
VES66	0	5.51	Top soil
"	5.51	14.74	Moderately fractured
"	14.74	25.41	Fractured rock
"	25.41		Basement rock
VES60	0	0.64	Top soil
"	0.64	1.51	Fracture rock
"	1.51		Basement rock
VES125	0	1.62	Top soil
"	1.62	2.17	Fractured rock
"	2.17	85.06	Fractured rock

LOCATION ID	DEPTH TOP	DEPTH BASE	GEOLOGY CODE
"	85.06		Fractured rock
VES116	0	2.95	Top soil
"	2.95	6.73	Fractured rock
"	6.73	67.13	Moderately fractured
"	67.13		Basement rock
VES114	0	0.95	Top soil
"	0.95	4.79	Moderately fractured
"	4.79	18.09	Fractured rock
"	18.09		Basement rock
VES108	0	0.46	Top soil
"	0.46	3.35	Fracture rock
"	3.35		Fracture rock
VES98	0	1.58	Top soil
"	1.58	20.04	Fractured rock
"	20.04	21.74	Fractured rock
"	21.74		Basement rock
VES95	0	0.44	Top soil
"	0.44	2.83	Moderately fractured
"	2.83	44.4	Fracture rock
"	44.4		Basement rock
VES86	0	0.4	Top soil
"	0.4	4.42	Fractured rock
"	4.42	30.61	Fractured rock
"	30.61		Basement rock
VES85	0	0.28	Top soil
"	0.28	5.46	Fractured rock
"	5.46	52.34	Fractured rock
"	52.34		Basement rock
VES78	0	0.64	Top soil
"	0.64	4.69	Fractured rock
"	4.69	46.93	Fractured rock
"	46.93		Basement rock
VES69	0	2.9	Top soil
"	2.9	22.28	Moderately fractured
"	22.28		Basement rock
VES67	0	1.47	Top soil
"	1.47	1.87	Fractured rock

LOCATION ID	DEPTH TOP	DEPTH BASE	GEOLOGY CODE
"	1.87	41.17	Moderately fractured
"	41.17		Basement rock
VES59	0	0.17	Top soil
"	0.17	0.97	Fractured rock
"	0.97		Basement rock
VES189	0	0.44	Top soil
"	0.44	0.88	Fractured rock
"	0.88	24.03	Fractured rock
"	24.03		Basement rock
VES188	0	0.36	Top soil
"	0.36	5.14	Moderately fractured
"	5.14	48.77	Moderately fractured
"	48.77		Basement rock
VES176	0	0.86	Top soil
"	0.86	26.37	Moderately fractured
"	26.37	30.7	Fracture rock
"	30.7		Basement rock
VES175	0	4.44	Top soil
"	4.44	11.04	Moderately fractured
"	11.04	45.75	Moderately fractured
"	45.75		Basement rock
VES165	0	0.61	Top soil
"	0.61	4.7	Fractured rock
"	4.7	16.8	Fractured rock
"	16.8		Basement rock
VES164	0	0.51	Top soil
"	0.51	0.67	Fractured rock
"	0.67	61.06	Fractured rock
"	61.06		Basement rock
VES154	0	0.38	Top soil
"	0.38	1.11	Fractured rock
"	1.11	21.38	Fractured rock
"	21.38		Basement rock
VES149	0	0.68	Top soil
"	0.68	1.42	Fractured rock
"	1.42	13.17	Fractured rock
"	13.17		Basement rock
VES148	0	0.91	Top soil

LOCATION ID	DEPTH TOP	DEPTH BASE	GEOLOGY CODE
"	0.91	1.46	Fractured rock
"	1.46	20.94	Moderately fractured
"	20.94		Basement rock
VES68	0	1.73	Top soil
"	1.73	1.85	Fractured rock
"	1.85	2.21	Fractured rock
"	2.21		Basement rock
VES133	0	0.69	Top soil
"	0.69	24.91	Fractured rock
"	24.91		Basement rock
VES127	0	0.1	Top soil
"	0.1	19.22	Fractured rock
"	19.22	77.37	Basement rock
"	77.37		Basement rock
VES190	0	0.79	Top soil
"	0.79	1.93	Fractured rock
"	1.93	3.31	Fractured rock
"	3.31		Basement rock
VES187	0	0.36	Top soil
"	0.36	2.67	Fractured rock
"	2.67	3.65	Fractured rock
"	3.65		Basement rock
VES177	0	0.49	Top soil
"	0.49	3.81	Fractured rock
"	3.81	43.44	Fractured rock
"	43.44		Basement rock
VES174	0	0.39	Top soil
"	0.39	0.67	Fractured rock
"	0.67	18.64	Fractured rock
"	18.64		Basement rock
VES166	0	1.43	Top soil
"	1.43	1.74	Fractured rock
"	1.74	2.16	Fractured rock
"	2.16		Fractured rock
VES163	0	0.13	Top soil
"	0.13	2.44	Fractured rock
"	2.44	10.95	Fractured rock

LOCATION ID	DEPTH TOP	DEPTH BASE	GEOLOGY CODE
"	10.95		Basement rock
VES155	0	1.26	Top soil
"	1.26	2.58	Fractured rock
"	2.58	3.32	Fractured rock
"	3.32		Basement rock
VES150	0	0.45	Top soil
"	0.45	1.03	Fractured rock
"	1.03	3.75	Fractured rock
"	3.75	22.89	Fracture rock
"	22.89		Basement rock
VES147	0	1.68	Top soil
"	1.68	2.76	Fracture rock
"	2.76	15.54	Fracture rock
"	15.54		Basement rock
VES137	0	0.33	Top soil
"	0.33	4.46	Fractured rock
"	4.46	8.9	Fractured rock
"	8.9		Basement rock
VES134	0	1.27	Top soil
"	1.27	10.27	Fracture rock
"	10.27	15.06	Moderately fractured
"	15.06		Basement rock
VES128	0	1.6	Top soil
"	1.6	3.12	Fractured rock
"	3.12	31.63	Fractured rock
"	31.63		Basement rock
VES191	0	0.48	Top soil
"	0.48	2.78	Fractured rock
"	2.78	58.36	Fractured rock
"	58.36		Basement rock
VES186	0	3.6	Top soil
"	3.6	29.73	Fractured rock
"	29.73	30.97	Moderately fractured
"	30.97		Basement rock
VES178	0	0.86	Top soil
"	0.86	7.85	Fractured rock
"	7.85	51.39	Fractured rock

LOCATION ID	DEPTH TOP	DEPTH BASE	GEOLOGY CODE
"	51.39		Basement rock
VES173	0	2.88	Top soil
"	2.88	35.38	Moderately fractured
"	35.38	38.58	Basement rock
"	38.58		Basement rock
VES167	0	0.71	Top soil
"	0.71	2.21	Basement rock
"	2.21	8.75	Fractured rock
"	8.75		Basement rock
VES162	0	3.61	Top soil
"	3.61	3.92	Fractured rock
"	3.92	17.22	Moderately fractured
"	17.22		Fracture rock
VES156	0	3.54	Top soil
"	3.54	4.49	Fractured rock
"	4.49		Basement rock
VES151	0	0.32	Top soil
"	0.32	0.62	Fractured rock
"	0.62	33.57	Fractured rock
"	33.57		Basement rock
VES146	0	1.26	Top soil
"	1.26	2.13	Fractured rock
"	2.13	26.24	Fractured rock
"	26.24		Basement rock
VES138	0	13.78	Top soil
"	13.78	16.07	Fractured rock
"	16.07	93.93	Basement rock
"	93.93		Fractured rock
VES135	0	0.46	Top soil
"	0.46	5.27	Fractured rock
"	5.27		Moderately fractured
VES129	0	0.74	Top soil
"	0.74	2.52	Fractured rock
"	2.52	26.62	Fractured rock
"	26.62		Basement rock
VES185	0	0.79	Top soil
"	0.79	1.32	Fractured rock

LOCATION ID	DEPTH TOP	DEPTH BASE	GEOLOGY CODE
"	1.32	8.51	Fracture rock
"	8.51		Moderately fractured
VES179	0	0.86	Top soil
"	0.86	1.51	Fractured rock
"	1.51	62.9	Moderately fractured
"	62.9		Basement rock
VES172	0	0.34	Top soil
"	0.34	0.66	Fractured rock
"	0.66	29.1	Fractured rock
"	29.1		Moderately fractured
VES168	0	0.71	Top soil
"	0.71	3.65	Fractured rock
"	3.65	45.84	Moderately fractured
"	45.84		Basement rock
VES161	0	2.1	Top soil
"	2.1	10.16	Fractured rock
"	10.16	31.64	Moderately fractured
"	31.64		Moderately fractured
VES157	0	2.49	Top soil
"	2.49	3.43	Fractured rock
"	3.43	5.15	Fractured rock
"	5.15		Basement rock
VES152	0	1.81	Top soil
"	1.81	3.44	Fractured rock
"	3.44		Fractured rock
VES145	0	1.38	Top soil
"	1.38	1.84	Fractured rock
"	1.84	13.22	Fractured rock
"	13.22		Basement rock
VES139	0	0.58	Top soil
"	0.58	4.37	Fractured rock
"	4.37	27.65	Moderately fractured
"	27.65		Basement rock
VES136	0	0.33	Top soil
"	0.33	2.18	Fractured rock
"	2.18	13.53	Fractured rock
"	13.53		Basement rock

LOCATION ID	DEPTH TOP	DEPTH BASE	GEOLOGY CODE
VES130	0	0.78	Top soil
"	0.78	43.51	Fractured rock
"	43.51	70.77	Basement rock
"	70.77		Basement rock
VES192	0	1.04	Top soil
"	1.04	1.36	Fractured rock
"	1.36	37.47	Fractured rock
"	37.47		Basement rock
VES184	0	1.55	Top soil
"	1.55	2.35	Fractured rock
"	2.35	17.08	Fractured rock
"	17.08		Basement rock
VES180	0	0.98	Top soil
"	0.98	1.42	Fractured rock
"	1.42	17.85	Moderately fractured
"	17.85		Basement rock
VES171	0	2.09	Top soil
"	2.09	3.87	Fractured rock
"	3.87	83.26	Moderately fractured
"	83.26		Basement rock
VES169	0	2.42	Top soil
"	2.42	3.73	Moderately fractured
"	3.73	24.04	Moderately fractured
"	24.04		Basement rock
VES160	0	0.8	Top soil
"	0.8	1.18	Fractured rock
"	1.18	2.26	Fractured rock
"	2.26		Basement rock
VES158	0	1.76	Top soil
"	1.76	3.43	Fractured rock
"	3.43	57.14	Fractured rock
"	57.14		Basement rock
VES153	0	0.7	Top soil
"	0.7	0.88	Fractured rock
"	0.88		Basement rock
VES144	0	1.05	Top soil
"	1.05	3.29	Fractured rock

LOCATION ID	DEPTH TOP	DEPTH BASE	GEOLOGY CODE
"	3.29	19.2	Fractured rock
"	19.2		Basement rock
VES141	0	1.3	Top soil
"	1.3	1.88	Fractured rock
"	1.88	17.6	Fractured rock
"	17.6		Basement rock
VES132	0	2.34	Top soil
"	2.34	3.4	Fractured rock
"	3.4	31.85	Moderately fractured
"	31.85		Basement rock
VES131	0	0.55	Top soil
"	0.55	7.05	Fractured rock
"	7.05	59.15	Moderately fractured
"	59.15		Basement rock
VES183	0	2.27	Top soil
"	2.27	5.01	Fractured rock
"	5.01	17.66	Moderately fractured
"	17.66		Basement rock
VES181	0	0.77	Top soil
"	0.77	1.19	Fractured rock
"	1.19	24.01	Moderately fractured
"	24.01		Basement rock
VES170	0	2.09	Top soil
"	2.09	2.86	Fractured rock
"	2.86	13.79	Fractured rock
"	13.79		Basement rock
VES159	0	0.53	Top soil
"	0.53	2.95	Moderately fractured
"			
"	2.95	50.32	Moderately fractured
"	50.32		Basement rock
VES143	0	1.05	Top soil
"	1.05	1.89	Fractured rock
"	1.89		Basement rock
VES142	0	2.55	Top soil
"	2.55	4.06	Fractured rock
"	4.06		Basement rock
VES182	0	0.6	Top soil

LOCATION ID	DEPTH TOP	DEPTH BASE	GEOLOGY CODE
"	0.6	5.32	Fractured rock
"	5.32	38.06	Moderately fracture
"	38.06		Basement rock
VES39	0	0.23	Top soil
"	0.23	1.2	Moderately fractured
"	1.2	2.58	Fractured rock
"	2.58		Basement rock
VES103	0	0.51	Top soil
"	0.51	1.5	Fractured rock
"	1.5	2.11	Fractured rock
"	2.11		Basement rock
VES80	0	0.88	Top soil
"	0.88	1.82	Fractured rock
"	1.82	1.93	Fractured rock
"	1.93		Basement rock
VES1	0	1.46	Top soil
"	1.46	2.29	Moderately fractured
"	2.29		Basement rock
VES126	0	1.46	Top soil
"	1.46	1.6	Fractured rock
"	1.6	18.98	Fractured rock
"	18.98		Basement rock
VES115	0	0.95	Top soil
"	0.95	14.01	Moderately fractured
"	14.01	19.8	Fractured rock
"	19.8		Basement rock
VES109	0	2.09	Top soil
"	2.09	2.89	Fractured rock
"	2.89	45.34	Fractured rock
"	45.34		Basement rock
VES97	0	45.34	Top soil
"	45.34	2.81	Fractured rock
"	2.81	2.81	Fractured rock
"	2.81		Basement rock
VES79	0	0.38	Top soil
"	0.38	0.6	Fractured rock
"	0.6	60.27	Fractured rock

LOCATION ID	DEPTH TOP	DEPTH BASE	GEOLOGY CODE
"	60.27		Basement rock
VES58	0	0.28	Top soil
"	0.28	1.64	Fractured rock
"	1.64	1.86	Fractured rock
"	1.86	22.99	Fractured rock
"	22.99		Basement rock

Appendix IV.

4.1. Pictures captured during data collection.



